THESIS
2
2007

This is to certify that the
dissertation entitled

FLOW-INDUCED ALIGNMENT AND MIGRATION OF
PARTICELS IN SUSPENSIONS

presented by

LIPING JIA

has been accepted towards fulfillment
of the requirements for the

Ph.D degree in Mechanical Engineering

André Bénard
Major Professor's Signature

Aug. 7, 2006
Date

MSU is an Affirmative Action/Equal Opportunity Institution

LIBRARY
Michigan State
University

PLACE IN RETURN BOX to remove this checkout from your record.
TO AVOID FINES return on or before date due.
MAY BE RECALLED with earlier due date if requested.

DATE DUE	DATE DUE	DATE DUE

6/07 p:/CIRC/DateDue.indd-p.1

FLOW-INDUCED ALIGNMENT AND MIGRATION OF PARTICLES IN SUSPENSIONS

By

Liping Jia

A DISSERTATION

Submitted to
Michigan State University
in partial fulfillment of the requirements
for the degree of

DOCTOR OF PHILOSOPHY

Department of Mechanical Engineering

2006

ABSTRACT

FLOW-INDUCED ALIGNMENT AND MIGRATION OF PARTICLES IN SUSPENSIONS

By

Liping Jia

The alignment and migration of suspensions are important for industrial processes associated with composite processing, the fabrication of microelectronics devices, the manufacturing of products with micro- and nano-scale suspensions, the environment (pollutants migration, particulates, and microbes), and the petroleum industry. In this work, problems associated with the motion of a single particle are solved and models needed to describe the orientation and migration of a large number of particles are developed.

The hydrodynamics of a single ellipsoid suspended in an unbounded homogeneous flow was first investigated by Jeffery in 1922 [1]. Jeffery's work deals with the problem of incompressible Newtonian fluid with constant viscosity, no-slip on the interface of solid/fluid, and linear shear flow. Based on Brenner's asymptotic method [2] analytical solutions are developed to study the influence of other conditions on the motion of a single particle, i. g. slip boundary conditions on the interface, other flow fields (a quadratic flow and cubic flow), and viscosity. The results are partially validated by comparing with existing solutions for some limiting cases of no-slip, perfect slip, sphere, and constant viscosity. Equations describing the motion of a single particle under different conditions are derived. A different method is used to study the influence of inertia forces on the motion of a single particle, which is based on Burgess' general solutions [3] of a viscous Oseen flow. Differ-

ent velocity fields of the fluid are found for the cases of translation motion of a sphere and a deformed sphere with slip and no-slip boundary condition.

Equations describing the motion of ensembles of rigid particles of complex shapes are studied next. Each particle is assumed to be non-axisymmetric, and its orientation is described with three Euler angles. The geometry of such particles (e.g. ellipsoids) and their interactions with the surrounding fluid are described by a third order tensor instead of the single parameter often used for axisymmetric particles (spheroids). To compute the flow-induced alignment of these particles, one must solve an evolution equation for the orientation distribution function but such computations are costly. Instead, an evolution equation for the second moment of the distribution function, which forms a fourth order tensor, is used in order to obtain the average orientation of the particles in homogeneous flows. A closure model is introduced for the unclosed eighth-order tensor which satisfies six-fold symmetry and six-fold projection properties.

In the last part of this work, models describing solid-liquid two-phase flows are developed using a continuum approach. A so-called Eulerian-Eulerian technique is adopted to deal with the motion of the non-spherical particles and Newtonian fluid. Based on the moments of the distribution function, the evolution of the second moment of the orientation tensor is used to govern the orientation of particles statistically. The concept of control volume/control surface method is used to develop closure models for the stresses and interfacial force. The fully symmetric quadratic model (developed for axisymmetric particles) is applied to close the problem associated with computing the orientation tensor. A finite element code is developed to simulate the alignment and migration of dilute suspensions of spheroids in a flowing liquid.

Dedicate this work to my parents and my husband.

ACKNOWLEDGMENTS

I must first thank my dissertation advisor Dr. André Bénard, who was never tired and always with his kindly leading causes to find the way in my dissertation.

I am grateful for Dr. Charles Petty, who not only gave me advices, but also kept tracking with all the detail of my research work.

I would like to thank to Dr. Alejandro Diaz, who helped me to join in my research group and spent lots of time in reviewing my dissertation.

I want to acknowledge Dr. Peter Bates' help for his serving my dissertation defense committee, when he was extremely busy.

I would like thank my husband, Zhijian Huang, who accompanied me all the way through this journey. Without him, I would not be able to finish the research on time.

I want to thank all my instructors at Michigan State University, who taught and encouraged me to reach this point. I would like to thank department staffs for their secretarial support on my study and life at Michigan State University.

Also I want to acknowledge all my friends and family members who gave me support through my years of study, enabling me to accomplish the work.

I gratefully acknowledge partial financial support of this work by the National Science Foundation through the following education and research programs at Michigan State University: NSF/CTS 0083229, NSF/EEC-0331977, and Dissertation Completion Fellowship.

TABLE OF CONTENTS

LIST OF TABLES

LIST OF FIGURES

CHAPTER 1

Introduction

1.1 Background on alignment and migration of particles

Alignment and migration of suspension of solids or droplets in a continuous medium at low Reynolds numbers are important phenomena to various fields in associated with material processing (composites), the fabrication of microelectronics devices, the manufacturing of products with suspensions (micro- and nano-scale particulates), the environment (pollutants dispersion, particulates, microbes), and the petroleum industry [4, 5]. Short-fiber composites are widely used in automobile bodies, business machines, and customer parts. When a short-fiber reinforced polymer is molded, the mold filling flow changes the orientation of the fibers. The fiber orientation in turn affects the physical properties of the composite, including stiffness, strength, thermal expansion, and electrical conductivity. For example, the composite is stiffer and stronger in the direction of greatest orientation, and weaker and more compliant in the direction of least orientation. The most common types of fibers used are glass, carbon, and aramid. Injection molding, extrusion and compression molding are common manufacturing methods for polymer matrices.

1.2 Dilute suspension theory

The basic assumptions employed in almost all dilute suspension models are

(1) The volume fraction, ϕ of fibers is so small that hydrodynamics interaction between fibres or between a fiber and a flow boundary may be ignored.

(2) The particle size is small compared with the macroscopic characteristic length.

(3) The aspect ratio a_p of the fiber is uniform.

(4) The suspending liquid is incompressible and Newtonian.

(5) The effects of inertia and external body force may be neglected

(6) Nonslip boundary condition is applied on the interface of the particle and the fluids.

1.2.1 Hydrodynamics of a single particle

A single particle motion and hydrodynamic forces acting on the particle are fundamentally important in the nature. Comprehensive information about the interaction between the particle and the fluid in low-Reynolds-number flow is required for many practical systems and industrial processes. Much is known at present about a single particle or two particles in a creeping flow. Lamb's classic treatise [6] on hydrodynamics contains much historical and technical information on the development of solutions for creeping flows. Happel and

Brenner [4] developed the theoretical calculations of the Stokes resistance of a particle to translational and rotational motions in an unbounded fluid. The motion of a rigid ellipsoid in a uniform simple shear flow at a low Reynolds number is solved completely by Jeffery [1] and verified accurately by the experiments of Trevelyan and Mason [7]. By using Jeffery's method [1], Bretherton [8] investigated theoretically on the orbit of a particle of a more general shape in a non-uniform shear flow. The motion of non-neutrally buoyant spheroidal particles is investigated with considering the effect of inertia by Broday and his coworkers [9]. The resistance functions for two unequal spheres are derived by Jeffery [10] and extended by Keh [11] to the slip problem on the interface of the particle and fluids. Wetzel [12] set up an analytical model for the deformation of an ellipsoidal Newtonian droplet, suspended in another Newtonian fluid with different viscosity and zero interfacial tension. Transient wake flow patterns and dynamics forces acting on a rotating spherical particle with non-uniform surface blowing are studied by Niazmand [13] for moderate Reynolds numbers.

Hydrodynamics of a single particle include the relations between the hydrodynamic force $\mathbf{F}$, the torque $\mathbf{T}$, and the stresslet $\boldsymbol{\tau}$ exerted by the fluid on the particle. Two kinds of problems are classified in this area. One is from the viewpoint of mathematical boundary value problems. The velocities of the particle and the surrounding flow field are fixed, which supply for the suitable boundary conditions. Then calculate the force $\mathbf{F}$, the torque $\mathbf{T}$, and the stresslet $\boldsymbol{\tau}$. This kind of problem is called resistance problem defined by Brenner [14,15]. The other problem is inverse to the first one, which is defined by Batchelor [16,17] as the mobility problem. For this problem, the force $\mathbf{F}$, and the torque $\mathbf{T}$ are given and the relative motion of the particle through the fluid is to be determined.

1.2.2 Fundamental equations of creeping flows

Introduced in [14], the particle Reynolds number is defined as $\frac{\rho\, d\, |\mathbf{U}|}{\mu}$ in the case of translating bodies or streaming flows, and $\frac{\rho\, d^2\, |\boldsymbol{\omega}|}{\mu}$, in the case of rotating bodies; $\mathbf{U}$ being the translation velocity of the particle; d a characteristic particle dimension and $\boldsymbol{\omega}$ the angular velocity. At small particle Reynolds number, the convective term $\rho \mathbf{v} \cdot \nabla \mathbf{v}$ in the Navier-Stokes equation is very smaller in comparison with the viscous terms, $\mu \nabla^2 \mathbf{v}$. Neglecting the influence of the convective terms in the Navier-Stokes equation, the dynamic and kinematic equations of motion of a viscous, incompressible fluid can be written as

$$\rho \frac{\partial \mathbf{v}}{\partial t} + \nabla p = \mu \nabla^2 \mathbf{v} \tag{1.1}$$

and

$$\nabla \cdot \mathbf{v} = 0 \tag{1.2}$$

where $\mathbf{v}$, ρ, p, μ, and t are respectively the local fluid velocity, the fluid density, the pressure, the viscosity, and the time.

The *local* acceleration terms $\rho \frac{\partial \mathbf{v}}{\partial t}$ in the equation of motion is equal to zero for steady problems. However, this term can also be ignored at a small particle Reynolds number even for unsteady problems. The dynamic equations of motion of the fluid are therefore simplified as

$$\mu \nabla^2 \mathbf{v} = \nabla p \tag{1.3}$$

Consider a rigid particle immersed in an unbounded quiescent flow. The undisturbed ambient flow field is composed of the uniform streaming velocity $\mathbf{U}^{\infty}$ and the linear field (constant velocity gradient), described by

$$\mathbf{v} = \mathbf{U}^{\infty} + \mathbf{\Omega}^{\infty} \times \mathbf{x} + \mathbf{S}^{\infty} \cdot \mathbf{x}. \tag{1.4}$$

where $\mathbf{x}$ is the position vector of a point relative to the origin at O, $\mathbf{\Omega}^{\infty}$ is the rotation of the flow field, and $\mathbf{S}^{\infty}$ the rate-of-strain of the flow fluid. The motion of the particle induced by the fluid has translational velocity $\mathbf{U}$ at a point O, which is regarded as the origin of this particle, and angular velocity $\boldsymbol{\omega}$. If no-slip is applied at the interface of the particle and the fluid, the instantaneous velocity of the fluid at the particle surface is

$$\mathbf{v}(\mathbf{x}) = \mathbf{U} - \mathbf{U}^{\infty} + (\boldsymbol{\omega} - \mathbf{\Omega}^{\infty}) \times \mathbf{x} - \mathbf{S}^{\infty} \cdot \mathbf{x}, \qquad \mathbf{x} \in S_p \tag{1.5}$$

in which S_p is the surface of the particle.

The force, torque and stresslet exerted by the fluid on the particle about the origin of the particle are $\mathbf{F}$, $\mathbf{T}$, and $\boldsymbol{\tau}$ respectively. The relations between the quantities $\mathbf{F}$, $\mathbf{T}$, and $\boldsymbol{\tau}$ with $\mathbf{U} - \mathbf{U}^{\infty}$, $\boldsymbol{\omega} - \mathbf{\Omega}^{\infty}$, and $\mathbf{S}^{\infty}$ are to be determined.

1.2.3 Particle material tensor

The resistance tensor

When the specified quantities are the velocities of the particles and of the prescribed flow, the linearity of the Stokes equations (1.3) permits the expression of the forces, the torques and stresslets [5] in the form

$$\begin{pmatrix} \mathbf{F} \\ \mathbf{T} \\ \boldsymbol{\tau} \end{pmatrix} = \mu \begin{pmatrix} \mathbf{A} & \widetilde{\mathbf{B}} & \widetilde{\mathbf{G}} \\ \mathbf{B} & \mathbf{C} & \widetilde{\mathbf{H}} \\ \mathbf{G} & \mathbf{H} & \mathbf{M} \end{pmatrix} \begin{pmatrix} \mathbf{U}^{\infty} - \mathbf{U} \\ \mathbf{\Omega}^{\infty} - \boldsymbol{\omega} \\ \mathbf{S}^{\infty} \end{pmatrix} \tag{1.6}$$

The square matrix in the above equation is called the *resistance matrix*, in which **A**, **B**, and **C** are second-order tensors, **G** and **H** are third-order tensors, and **M** a fourth-order tensor. According to the reciprocal theorem of Lorentz [4], the resistance matrix is symmetric, i.e.,

$$A_{ij} = A_{ji}, \quad C_{ij} = C_{ji}, \quad M_{ijkl} = M_{klij},$$
$$B_{ij} = \widetilde{B}_{ji}, \quad G_{ijk} = \widetilde{G}_{kij}, \quad H_{ijk} = \widetilde{H}_{kij} \tag{1.7}$$

The mobility tensor

When the particle forces and torques are prescribed in a known ambient flow, the so-called *mobility problem* [5] satisfies the following relation

$$\begin{pmatrix} \mathbf{U}^{\infty} - \mathbf{U} \\ \mathbf{\Omega}^{\infty} - \boldsymbol{\omega} \\ \frac{1}{\mu}\boldsymbol{\tau} \end{pmatrix} = \begin{pmatrix} \mathbf{a} & \widetilde{\mathbf{b}} & \widetilde{\mathbf{g}} \\ \mathbf{b} & \mathbf{c} & \widetilde{\mathbf{h}} \\ \mathbf{g} & \mathbf{h} & \mathbf{m} \end{pmatrix} \begin{pmatrix} \frac{1}{\mu}\mathbf{F} \\ \frac{1}{\mu}\mathbf{T} \\ \mathbf{S}^{\infty} \end{pmatrix} \tag{1.8}$$

in which the square matrix is the *mobility matrix*. Similarly, the **a**, **b**, and **c** are second-order tensor, **g** and **h** third-order tensor, and **m** the fourth-order tensor. The mobility matrix is also symmetric as the consequence of the Lorentz reciprocal theorem:

$$a_{ij} = a_{ji}, \quad c_{ij} = c_{ji}, \quad m_{ijkl} = m_{klij},$$
$$b_{ij} = \widetilde{b}_{ji}, \quad g_{ijk} = \widetilde{g}_{kij}, \quad h_{ijk} = \widetilde{h}_{kij} \tag{1.9}$$

The resistance problem and mobility problem are inverse to each other physically. So the resistance matrix defined by (1.6) and the mobility matrix defined by (1.8) are inverse to each other. The transformation matrix between them can be found in [18].

1.2.4 Jeffery's solution of the motion of an axisymmetric particle in a linear field

In 1922, Jeffery [1] investigated the flow induced motion of an ellipsoid in an unbounded flow field. Some assumptions are made in Jeffery's model: (i) the particle is rigid, neutrally buoyant, and large enough to neglect Brownian motion, (ii) the ambient fluid is Newtonian, (iii) the inertia forces of the particle and the fluid are negligible and the motion of the fluid is governed by Stokes' equations, (iv) the particle is immersed in a homogeneous flow, which means the velocity gradient of the flow field is constant, (v) no-slip boundary conditions are applied on the interface of the particle and the fluid. Under these assumptions, the time evolution of a spheroid orientation is expressed in the form as [1, 19]

$$\dot{\mathbf{p}} = \mathbf{\Omega}^{\infty} \times \mathbf{p} + \lambda\,[\mathbf{S}^{\infty} \cdot \mathbf{p}(\mathbf{p} \cdot \mathbf{p}) - \mathbf{S}^{\infty} : \mathbf{ppp}] \tag{1.10}$$

in which $\mathbf{p}$ is a unit vector representing the orientation of the particle. $\mathbf{p}$ can be characterized with the angles θ and ϕ as shown in Figure 1.1

$$\mathbf{p} = \begin{pmatrix} \sin\theta\cos\phi \\ \sin\theta\sin\phi \\ \cos\phi \end{pmatrix} \tag{1.11}$$

λ is a function of of the particle aspect ratio, $a_p = \dfrac{\text{length}}{\text{diameter}}$, and is expressed as

$$\lambda = \frac{a_p^2 - 1}{a_p^2 + 1} \tag{1.12}$$

$\lambda > 0$ represents a prolate particle, $\lambda = 0$ a sphere, and $\lambda < 0$ an oblate.

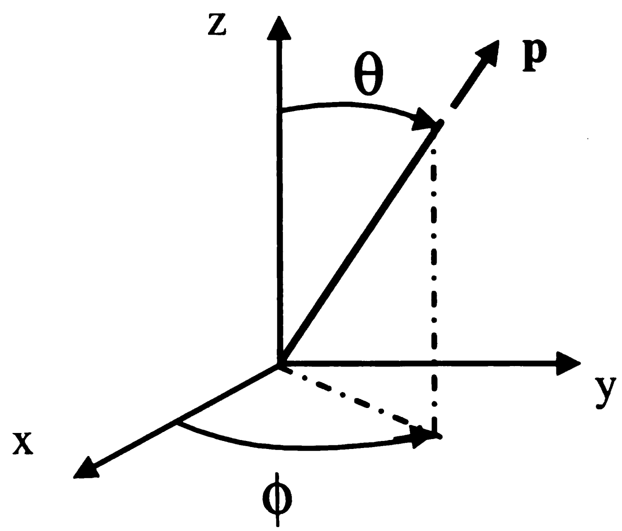

Figure 1.1. Schematic of the coordinate system used to represent the orientation of a particle.

For a special case of a neutrally buoyant torque-free axisymmetric particle in the shear field $\mathbf{v}^{\infty} = \dot{\gamma}\, y\, \mathbf{e}_x$ shown in Figure 1.2. The ambient rotation and rate-of-strain can be given by

$$\boldsymbol{\Omega}^{\infty} = -\frac{1}{2}\dot{\gamma}\,\mathbf{e}_z, \qquad \mathbf{S}^{\infty} = \frac{\dot{\gamma}}{2}\begin{pmatrix} 0 & 1 & 0 \\ 1 & 0 & 0 \\ 0 & 0 & 0 \end{pmatrix} \tag{1.13}$$

Substituting (1.11) and (1.13) into (1.10), the orientation of the particle is governed by the coupled differential equations

$$\dot{\theta} = -\left(\frac{a_p^2 - 1}{a_p^2 + 1}\right)\frac{\dot{\gamma}}{4}\sin 2\theta \sin 2\phi \tag{1.14}$$

$$\dot{\phi} = -\frac{\dot{\gamma}}{a_p^2 + 1}\left(a_p^2 \cos^2\phi + \sin^2\phi\right) \tag{1.15}$$

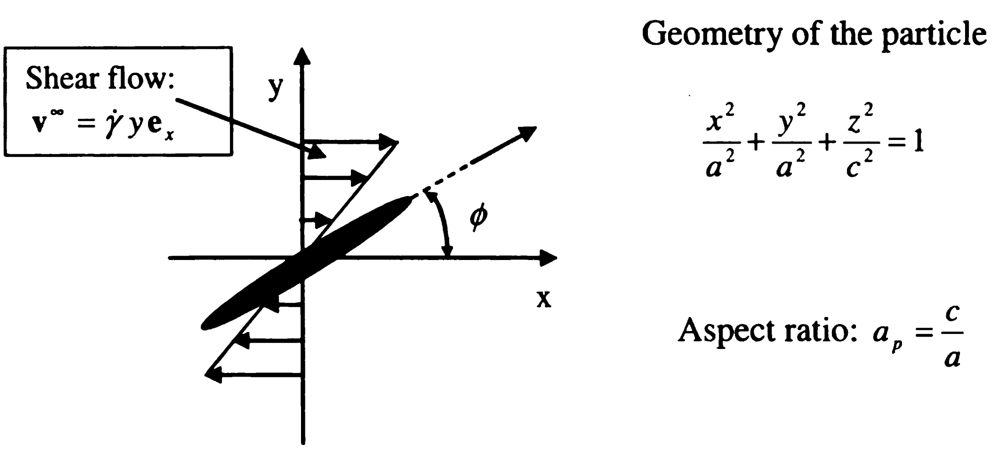

Figure 1.2. An axisymmetric particle, i.g. a spheroid suspended in a simple shear flow. The geometry of the particle is a spheroid and the aspect ratio of the particle is $a_p = \frac{c}{a}$.

The above equations can be solved exactly and yield periodic trajectories known as the *Jeffery orbits* [5],

$$\begin{aligned} \tan\theta &= \frac{Ca_p}{(a_p^2 \cos^2\phi + \sin^2\phi)^{1/2}} \\ \tan\phi &= -a_p \tan\left(\frac{\dot{\gamma}t}{a_p + a_p^{-1}}\right) \end{aligned} \tag{1.16}$$

From these equations it can be seen that the motion of the particle is periodic. The period $T = 2\pi(a_p + a_p^{-1})/\dot{\gamma}$ is proportion to the $\dot{\gamma}^{-1}$ and becomes longer with increasing particle nonsphericity. The constant C is known as the *orbital constant* determined by the initial angle of the particle. The exact shape of the orbit can be determined by the the particle aspect ratio via the Bretherton constant **B** [8]. Jeffery orbits are shown in the Figure 1.3 for different shapes of particles suspended in different shear flows. In these cases, the initial

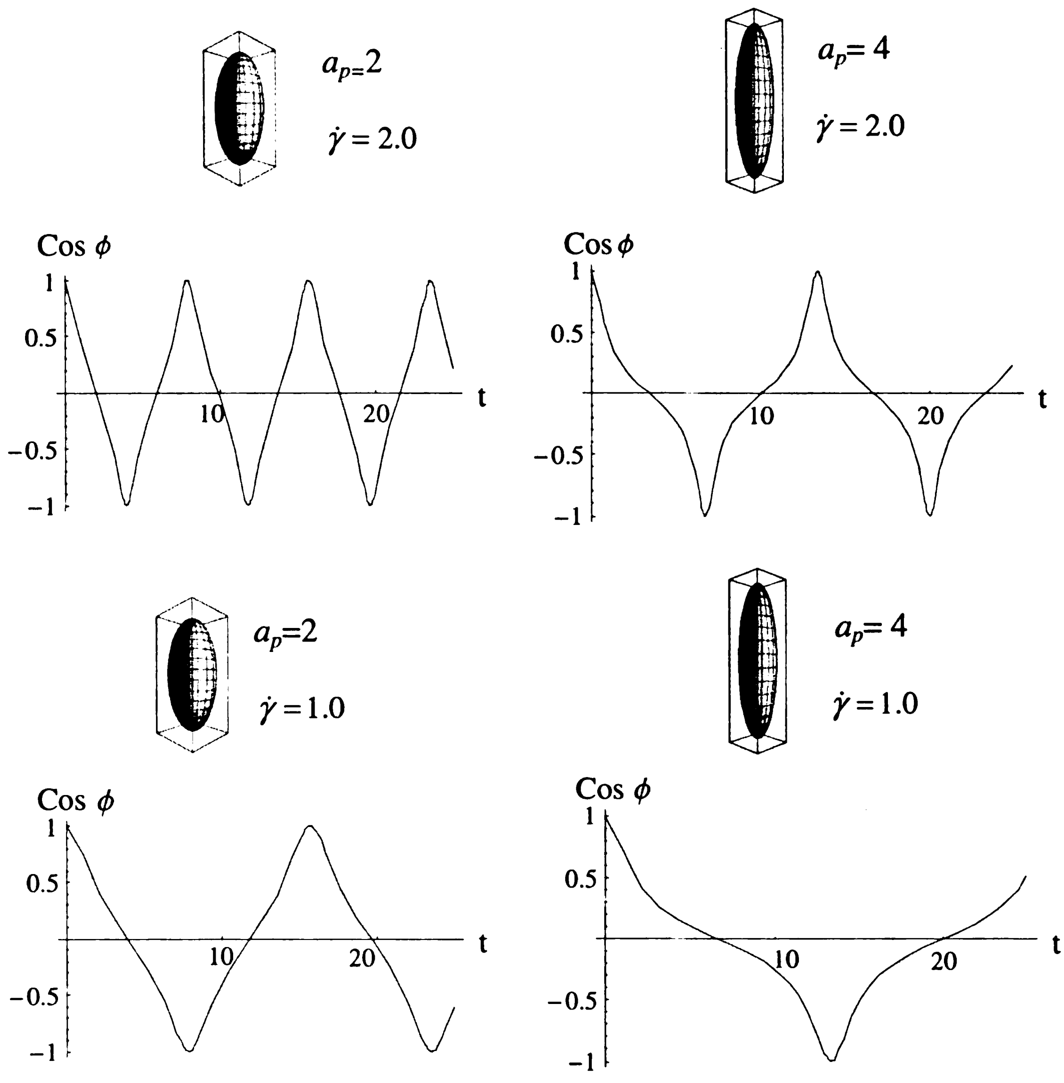

Figure 1.3. Jeffery orbits are shown for spheroidal particles at different aspect ratios a_p and different flow fields $\mathbf{v}_\infty = \dot{\gamma}\ y\mathbf{e}_x$. The motions of the spheroidal particle suspended in a simple shear flow are periodic and the periods depend on the shape of the particle and the constant $\dot{\gamma}$ of the flow field.

angles of the particle are $\phi = 0$, and $\theta = 0$. Suspended in the simple shear flow $\mathbf{v}_\infty = \dot{\gamma} y \, \mathbf{e}_x$, the axisymmetric particle rotates along the z axis. It can be seen the period of the motion of the particle with the aspect ratio of $a_p = 4$ is longer than that of the particle with aspect ratio of $a_p = 2$ when the constants $\dot{\gamma}$ are same for the two cases, and the period of a same particle increases with decreasing the constant $\dot{\gamma}$.

1.3 Non-Dilute Suspensions

Let ν be the number of particles per volume. Solutions for rod-like suspensions, length L and diameter b are distinguished by [20]

$$\begin{cases} \nu < \dfrac{1}{L^3} & \text{dilute} \\[2ex] \dfrac{1}{L^3} \ll \nu \ll \dfrac{1}{dL^2} & \text{Semi - dilute} \\[2ex] \nu = O\left(\dfrac{1}{dL^2}\right) & \text{Concentrated} \end{cases} \tag{1.17}$$

Work has been done theoretically and experimentally on dilute suspensions [21–23]. With the development of new materials, it is necessary to model fiber-fiber interactions and describe quantitatively the effect of the interaction to properties of the suspensions and the final products.

The rheological features of nondilute fiber suspension have been observed experimentally. A summery of the previous experimental studies on the nondilute suspension can be found in [24]. Interesting results stated in those experiments include Blakeney [25], who found that the effective viscosity of a steady-state suspension was approximately equal to the viscosity of the solvent; Maschmeyer [26] showed a Power Law dependence of viscosity on shear rate; Miles's experiment illustrated that the viscosity was dependent on the volume fraction of fibers but independent on the shear rate and the length of fibers for glass-fiber suspensions [27]; The shear-induced corrugation of free interfaces in concentrated suspensions was observed by Loimer [28], in which it was shown that the roughness of the surface disturbances depended on the particle size, the particle concentration and the fluid surface tension.

To model the interactions between suspended fibers, Batchelor [29] treated the semi-dilute regime by using a cell model in the case of aligned particles in Newtonian fluids. This model was applied to the non-Newtonian fluids for aligned fibers in extensional flows [30]. In Batchelor's work, the interaction among randomly oriented dispersed fibers was modelled as a Newtonian drag, which was exerted on a fiber segment in motions relative to the bulk suspension [24]. Similar ideas to model suspensions of non-Newtonian matrices were used later in [31].

1.4 Objectives of this work

Hydrodynamics of a single ellipsoid suspended in an unbounded homogeneous flow was investigated by Jeffery in 1922 and the flow induced motion of the ellipsoid was applied later on to the analysis of dilute suspensions. Jeffery's work dealt with the problem of incompressible Newtonian fluid with constant viscosity, no-slip on the interface of solid/fluid, and linear shear flow. Recent advances in materials processing make it relevant to understand the influence of a slip boundary condition, other flow fields, viscosities, inertia forces on the drag force and rotary motion of a single particle as well as the dynamics of ensemble particles.

The objectives of this work are:

(1) Determine the influence of the slip boundary conditions, flow field, viscosity, and inertia force on the drag force and rotary motion of a single particle suspended in an unbounded flow field.

No-slip on the interface of the fluid/solid is an idealization in the transport process. The slippage phenomena on the solid/fluid interface has been confirmed both experimentally and theoretically. Unfortunately no equations describing the flow-induced motion of an ellipsoid with slip are available so far. Some results are available for a deformed sphere with the slip [32, 33]. These results are limited on the special case of a fixed particle in the space. With the successful application of the motion of a single particle to the analysis of dilute ensemble particles, it is an important step to get the dynamic motion of an ellipsoid with slip to fully understand the microstructure of dilute and concentrated suspensions. A translating or rotating non-spherical particle suspended in a slip flow is one of the main topics in this dissertation. Both of the creeping flow and the Oseen flow are investigated to determine the influence of physical parameters, e.g. geometry parameters of particles, fluid viscosities, and the interfacial slip coefficient, on the drag, torque, and rotary motion of a deformed sphere in an unbounded homogeneous shear flow.

(2) Develop a new closure model for Non-Axisymmetric particles required in the moment equation.

The shape of particles is another factor to the microstructure of suspension systems.

Previous studies of the orientation of particles have restricted attentions on the axisymmetric particles. The current orientation of a nonaxisymmetric particle is specified by a rotation matrix from the reference configuration to its present orientation. Closure approximation is needed in the governing equation of the second moment orientation equation of nonaxisymmetric. This dissertation is also devoted to study the microstructure of non-axisymmetric particles suspensions.

(3) Predict the flow-induced alignments coupled with the migration of multiparticles.

Orientations of particles can affect the rheology properties of a suspension system, and mechanical properties of composite materials. In order to treat the microstructural kinematics of a suspension system, lots of research has been done to predict the orientation of ensemble particles statistically. For the suspension of axisymmetric particles the orientation statistics can conveniently be given in terms of a unit vector $\mathbf{p}$ along the axisymmetric axis and a second-order tensor $\mathbf{a} =< \mathbf{pp} >$ is often used to describe the orientation state of particles. In the previous research, uniform suspension of particles is assumed. It is known that nonuniform suspension, shear force and inertia force will cause particle migration. The influence of flow field parameters on the orientation and fiber stress is studied for a specific two-dimensional problem using finite element calculations. Therefore, to study particles orientations coupled with the migration is another goal in this dissertation.

CHAPTER 2

MOTION OF A DEFORMED SPHERE WITH SLIP

2.1 Introduction

With the evolution of micro- and nanoscale systems, there has been a recent wave of interest in challenging the idea of a "no-slip" boundary condition on liquid/gas flows. Slip has been confirmed experimentally and theoretically by using sensitive force measurements [34,35], visual techniques [36] and molecular dynamics simulation data [37–41]. Situations for which slip may occur can be encountered in solid particles suspended in rarefied gases, and can also be encountered in liquid/solid systems such as polymer melts or water flowing in thin hydrophobic capillaries [42–45]. Contrary to macroscopic flows, a small amount of slip can strongly influence the transport phenomena and serious consequences may occur for miocro- and nanoscale flows. On the design of nanoscale flow devices it is necessary to understand the fundamental aspects of interfacial phenomena and particularly accurate

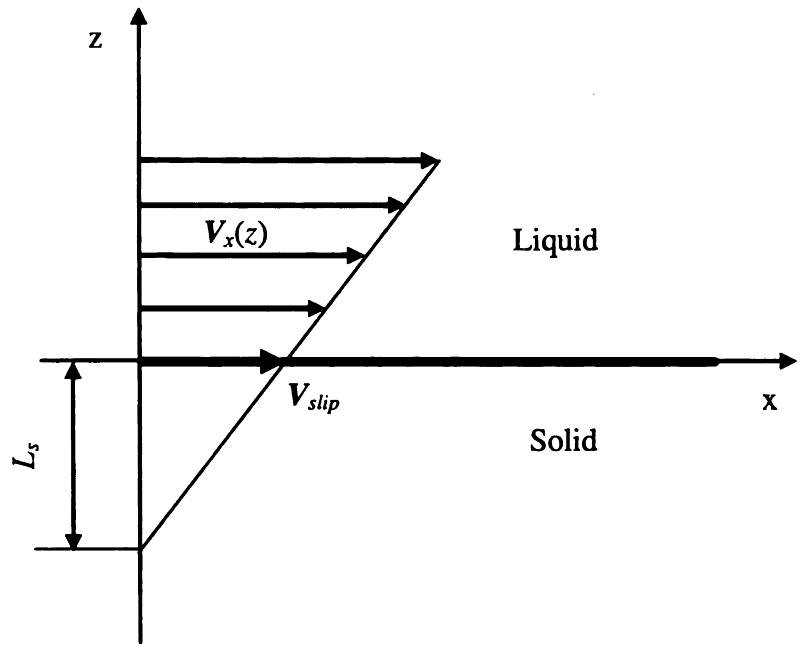

Figure 2.1. The slip length L_S is defined for a simple shear flow in the presence of slip boundary conditions at the interface of solids and liquids.

prediction of the fluid transport through tiny structures [46,47].

The degree of slip is normally characterized by an extrapolated slip length L_S defined as the distance from the surface within the solid phase to where the flow velocity vanishes. The definition of the slip length L_S is explained in Figure 2.1. For most practical situations, with simple fluids (composed of small molecules with a diameter d), small slip lengths $d \sim L_S$ are generally expected. There are many factors that can affect the slip length including the degree of hydrophobicity [48,49], the substrate topography and surface roughness [50–57], the presence of interstitial lubricating layers [56, 58, 59], the polymer molecular weight [60–62], and the applied shear rate [63–68]. Three levels of slip corresponding to the slip length can be distinguished by no slip, finite slip, and perfect slip (infinite slip) as shown in Figure 2.2. The relation between the slip length and the surface slip coefficient can be

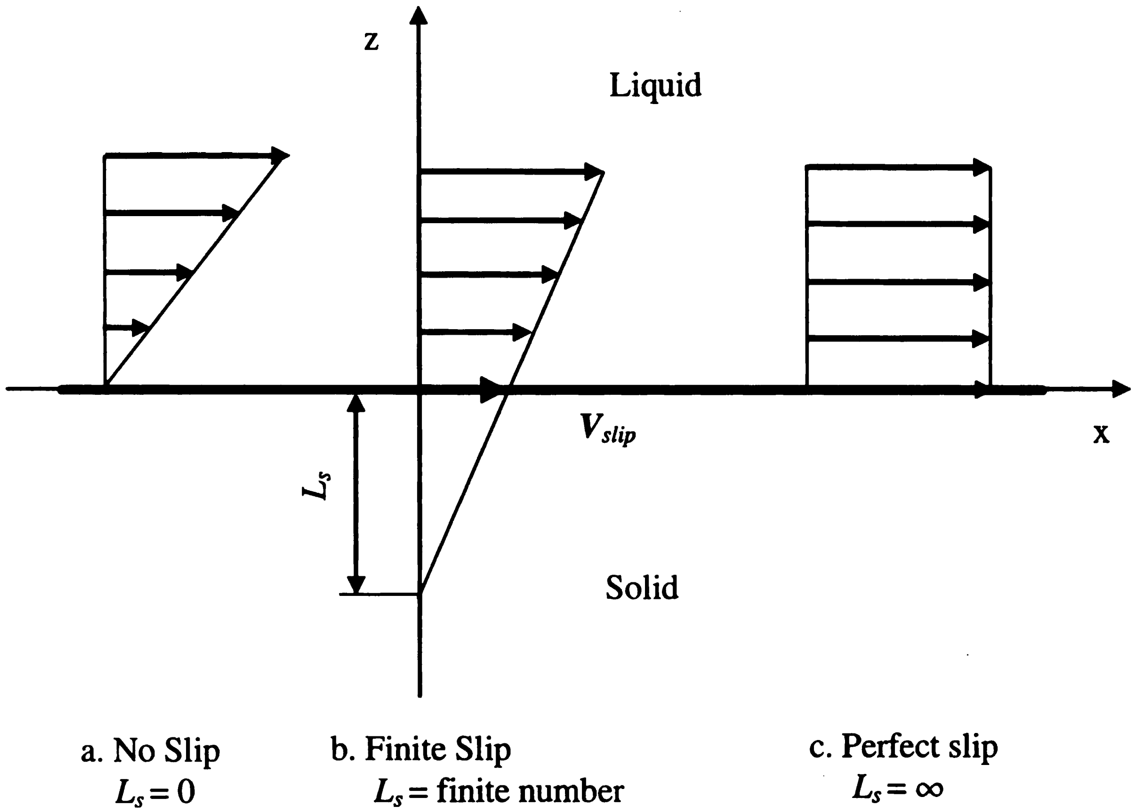

Figure 2.2. Illustration of lengths L_S used to describe different slip cases. When $L_S = 0$, no slip occurs on the interface; when L_S = finitenumber, finite slip occurs on the interface; when L_S = Infinity, perfect slip occurs on the interface.

obtained by [37]

$$L_S = \frac{\mu}{\beta} \tag{2.1}$$

in which μ is the viscosity of the fluid and β is the slip coefficient on the interface.

Analytical solutions for Stokes flow past non-spherical particles with slip on the solid-fluid interface are limited to flows around spheroids fixed in space [32,33] by using a stream function formalism. In this approach, the slip boundary condition can only be satisfied on the surface of a sphere particle even though solutions for flow around a slightly deformed sphere are given in those previous work. Equations describing the motion of spheroidal particles in creeping flows with slip are not available, unlike the case of ellipsoidal particles with no-slip surfaces. The latter equations are available in the classical work of Jeffery [1]. In his paper, the behavior of an ellipsoid suspended in a uniform shear flow field is analyzed based on Stokes' equations of motions. Jeffery's work is extended by Bretherton [8] to investigate the orbit of a particle of a more general shape in a non-uniform shear flow. A series of research papers on the intrinsic hydrodynamic resistance of particles of arbitrary shape based on the application of singular perturbation techniques are studied by Brenner [2, 69–71] presented. Jeffery's equation has been applied to the analysis of dilute suspension problems [19, 21, 39, 72, 73]. Corresponding equations for the induced motion of an ellipsoid with slip boundary conditions are however not available.

2.2 Basic formulations

The slow motion of a slightly deformed sphere in an unbounded Newtonian and incompressible flow is considered. Apart from the disturbance produced in the immediate neighborhood of the particle, the motion of the fluid is assumed to be quasi-steady, and variable in space on a scale which is large compared with the dimensions of the particle. The fluid is allowed to slip over the surface of the particle. At small translational and/or angular Reynolds numbers, $\frac{r_0|\mathbf{U}|}{\nu}$ and $\frac{r_0^2|\omega|}{\nu}$, respectively, the fluid motion is governed by Stokes equations,

$$\mu\nabla^2\mathbf{v} = \nabla p, \nabla\cdot\mathbf{v} = 0 \tag{2.2}$$

Representation of the general solution for the Stokes equations in terms of solid spherical harmonics and surface spherical harmonics is given by Lamb as [6]

$$\mathbf{v} = \sum_{n=-\infty}^{\infty}\left[\nabla\times(\mathbf{r}\chi_n) + \nabla\phi_n + \frac{(n+3)}{2(n+1)(2n+3)\mu}r^2\nabla p_n - \mathbf{r}\frac{n}{(n+1)(2n+3)\mu p_n}\right] \tag{2.3}$$

$$p = \sum_{n=-\infty}^{\infty} p_n \tag{2.4}$$

where χ_n, ϕ_n, and p_n are solid spherical harmonics of degree n and can be determined by suitable boundary conditions. Lamb's general solution to the Stokes equations assumes the velocity field vanishes as $r\to\infty$. In the event that the velocity field is required to be prescribed at $\mathbf{v}_\infty$, the specified velocity $\mathbf{v}_\infty$ and corresponding pressure p_∞ are added to the right side of (2.3). Naturally $\mathbf{v}_\infty$ must itself satisfy Stokes equations.

The surface of a deformed sphere is assumed to be described by an equation of the form

$$r = r_0(1+\varepsilon f(\theta,\phi)) \tag{2.5}$$

in which (r,θ,ϕ) are spherical coordinates and the origin is located at the center of an undeformed sphere with a radios of $r = r_0$; $|\ \varepsilon|$ is a small dimensionless parameter, and $f(\theta,\phi)$ is an arbitrary function which can be approximated by a series of surface spherical harmonics, $f_k(\theta,\phi)$. Hence, the surface of the deformed sphere can be written as

$$r = r_0\left(1+\varepsilon\sum_{k=0}^{\infty}f_k(\theta,\phi)\right) \tag{2.6}$$

The slip boundary condition at the solid-fluid interface is modeled as [6, 11]

$$\mathbf{u} = \mathbf{v} - \frac{1}{\beta}\boldsymbol{\sigma}_{rt} \tag{2.7}$$

where $\mathbf{u}$ and $\mathbf{v}$ are the velocities of the particle and the fluid on the interface respectively, β the slip coefficient. $\boldsymbol{\sigma}_{rt}$ is the tangential traction on the surface of the particle. The traction on the particle can be decomposed by two parts

$$\begin{aligned} \boldsymbol{\sigma}_r &= \boldsymbol{\sigma} \cdot \frac{\mathbf{r}}{r} \\ &= \underbrace{\frac{\mathbf{rr}}{r^2} \cdot \boldsymbol{\sigma}_r}_{\sigma_{rr}} + \underbrace{(\mathbf{I} - \frac{\mathbf{rr}}{r^2}) \cdot \boldsymbol{\sigma}_r}_{\boldsymbol{\sigma}_{rt}} \end{aligned} \tag{2.8}$$

in which $\boldsymbol{\sigma}_{rr}$ is the normal traction and $\boldsymbol{\sigma}_{rt}$ the tangential traction. The motion of the particle on the surface can be expressed as

$$\mathbf{u} = \mathbf{U} + \boldsymbol{\omega} \times \mathbf{r} \qquad \text{on } S_d \tag{2.9}$$

in which $\mathbf{U}$ is the translation at the center of the particle, $\boldsymbol{\omega}$ is the angular velocity of the particle around its axes. S_d represents the surface of the deformed sphere. The boundary condition at infinity is described by

$$\mathbf{v} = \mathbf{v}_\infty(\mathbf{x}) \qquad\qquad \text{as } r \to \infty \tag{2.10}$$

where $\mathbf{v}_\infty$ is an arbitrary flow field.

For the problem of slip flows pasting a deformed sphere, solutions are sought by assuming that the velocity and pressure can be expanded in powers of ε in the form

$$\mathbf{v} = \sum_{i=0}^{\infty} \varepsilon^i \mathbf{v}^{(i)} \tag{2.11}$$

$$p = \sum_{i=0}^{\infty} \varepsilon^i p^{(i)} \tag{2.12}$$

$$\boldsymbol{\sigma}_{rt} = \sum_{i=0}^{\infty} \varepsilon^i \boldsymbol{\sigma}_{rt}^{(i)} \tag{2.13}$$

$$\mathbf{v}_\infty = \sum_{i=0}^{\infty} \varepsilon^i \mathbf{v}_\infty^{(i)} \tag{2.14}$$

$$\mathbf{u} = \sum_{i=0}^{\infty} \varepsilon^i \mathbf{u}^{(i)} \tag{2.15}$$

Due to the linearity of the Stokes equations both of the individual perturbations $\mathbf{v}^{(i)}$ and $p^{(i)}$ still satisfy Stokes equations.

$$\mu \nabla^2 \mathbf{v}^{(i)} = \nabla p^{(i)}, \nabla \cdot \mathbf{v}^{(i)} = 0 \tag{2.16}$$

Substituting (2.11) into the boundary conditions (2.7) and (2.10), and equating terms involving the orders of ε, it can result:

$$\mathbf{u}^{(i)} - \mathbf{v}_\infty = \mathbf{v}^{(i)} - \frac{1}{\beta}\boldsymbol{\sigma}_{rt}^{(i)} \qquad \text{on } S_d \tag{2.17}$$

$$\mathbf{v}^{(i)} = \mathbf{v}_\infty^{(i)} \qquad \text{at } r = \infty \tag{2.18}$$

Approximating $\mathbf{v}^{(i)}$ and $\boldsymbol{\sigma}_{rt}^{(i)}$ using Taylor series expansion about $r = r_0$, boundary conditions on the interface can be written as:

$$\sum_{i=0}^{\infty} \varepsilon^i \mathbf{u}^{(i)} = \sum_{i=0}^{\infty} \varepsilon^i \left\{ \left[\left(\mathbf{v}^{(i)}\right)_{r=r_0} - \frac{1}{\beta}\left(\boldsymbol{\sigma}_{rt}^{(i)}\right)_{r=r_0} \right] + \sum_{j=1}^{i} \frac{1}{j!}\varepsilon^j r_0^j f^j(\theta,\phi) \left[\left(\frac{\partial^{(j)} \mathbf{v}^{(i-j)}}{\partial r^{(j)}}\right)_{r=r_0} - \frac{1}{\beta}\left(\frac{\partial^{(j)} \boldsymbol{\sigma}_{rt}^{(i-j)}}{\partial r^{(j)}}\right)_{r=r_0} \right] \right\} \quad \text{at } r = r_0 \tag{2.19}$$

It is difficult to obtain solid spherical harmonics χ_n, p_n, and ϕ_n by directly substituting the boundary conditions (2.17-2.18)into (2.3). Three identities are instead introduced to the slip boundary conditions for the each power of ε [2]:

$$\frac{\mathbf{r}}{r} \cdot \left[\mathbf{u}^{(0)} - \mathbf{v}_\infty^{(0)}\right]_{r=r_0} = \frac{\mathbf{r}}{r} \cdot \left[\mathbf{v}^{(0)} - \frac{1}{\beta}\boldsymbol{\sigma}_{rt}^{(0)}\right]_{r=r_0} \tag{2.20}$$

$$-r\,\nabla\cdot\left[\mathbf{u}^{(0)}-\mathbf{v}_{\infty}^{(0)}\right]_{r=r_0} = -r\,\nabla\cdot\left[\mathbf{v}^{(0)}-\frac{1}{\beta}\boldsymbol{\sigma}_{rt}^{(0)}\right]_{r=r_0} \tag{2.21}$$

$$\mathbf{r}\cdot\nabla\times\left[\mathbf{u}^{(0)}-\mathbf{v}_{\infty}^{(0)}\right]_{r=r_0} = \mathbf{r}\cdot\nabla\times\left[\mathbf{v}^{(0)}-\frac{1}{\beta}\boldsymbol{\sigma}_{rt}^{(0)}\right]_{r=r_0} \tag{2.22}$$

and

$$\frac{\mathbf{r}}{r}\cdot\left\{(\mathbf{u}^{(1)})-\mathbf{v}_{\infty}^{(1)}(r,\theta,\phi)\left[\left(\frac{\partial v^{(0)}}{\partial r}\right)-\frac{1}{\beta}\left(\frac{\sigma_{rt}^{(0)}}{\partial r(j)}\right)\right]\right\}_{r=r_0} = \frac{\mathbf{r}}{r}\cdot\left[\mathbf{v}^{(1)}-\frac{1}{\beta}\boldsymbol{\sigma}_{rt}^{(1)}\right]_{r=r_0} \tag{2.23}$$

$$-r\,\nabla\cdot\left\{(\mathbf{u}^{(1)})-\mathbf{v}_{\infty}^{(1)}(r,\theta,\phi)\left[\left(\frac{\partial v^{(0)}}{\partial r}\right)-\frac{1}{\beta}\left(\frac{\sigma_{rt}^{(0)}}{\partial r(j)}\right)\right]\right\}_{r=r_0} = -r\,\nabla\cdot\left[\mathbf{v}^{(1)}-\frac{1}{\beta}\boldsymbol{\sigma}_{rt}^{(1)}\right]_{r=r_0} \tag{2.24}$$

$$\mathbf{r}\cdot\nabla\times\left\{(\mathbf{u}^{(1)})-\mathbf{v}_{\infty}^{(1)}(r,\theta,\phi)\left[\left(\frac{\partial v^{(0)}}{\partial r}\right)-\frac{1}{\beta}\left(\frac{\sigma_{rt}^{(0)}}{\partial r(j)}\right)\right]\right\}_{r=r_0} = \mathbf{r}\cdot\nabla\times\left[\mathbf{v}^{(1)}-\frac{1}{\beta}\boldsymbol{\sigma}_{rt}^{(1)}\right]_{r=r_0} \tag{2.25}$$

$$\vdots$$

$$\vdots$$

2.3 Relation between p_n, ϕ_n, and χ_n with X_n, Y_n and Z_n

Substituting (2.3) into right hands of the three scalar identities (2.20-2.22), it yields,

$$\frac{\mathbf{r}}{r}\cdot\left[\mathbf{v}^{(i)}-\frac{1}{\beta}\boldsymbol{\sigma}_{rt}^{(i)}\right]_{r=r_0} = \sum_{n=-\infty}^{\infty}\left[\frac{nr_0}{2(2n+3)\mu}\left(\frac{r_0}{r}\right)^n p_n^{(i)}+\frac{n}{r_0}\left(\frac{r_0}{r}\right)^n\phi_n^{(i)}\right] \tag{2.26}$$

$$\begin{aligned}-r\nabla\cdot\left[\mathbf{v}^{(i)}-\frac{1}{\beta}\boldsymbol{\sigma}_{rt}^{(i)}\right]_{r=r_0} &= \sum_{n=-\infty}^{\infty}\left[\frac{n(n+1)r_0}{2(2n+3)\mu}\left(\frac{r_0}{r}\right)^n p_n^{(i)}+\frac{n(n-1)}{r_0}\left(\frac{r_0}{r}\right)^n\phi_n^{(i)}\right] \\ &+\frac{1}{\beta}\sum_{n=-\infty}^{\infty}\left[\frac{2n(1-n^2)\mu}{r_0^2}\left(\frac{r_0}{r}\right)^n\phi_n^{(i)}-\frac{n^2(n+2)}{2n+3}\left(\frac{r_0}{r}\right)^n p_n^{(i)}\right]\end{aligned} \tag{2.27}$$

$$\mathbf{r}\cdot\nabla\times\left[\mathbf{v}^{(i)}-\frac{1}{\beta}\boldsymbol{\sigma}_{rt}^{(1)}\right]_{r=r_0}=\sum_{n=-\infty}^{\infty}\left[n(n+1)\left(\frac{r_0}{r}\right)^n\chi_n^{(i)}-\frac{1}{\beta}\frac{\mu(n^2-1)n}{r_0}\left(\frac{r_0}{r}\right)^n\chi_n^{(i)}\right] \quad (2.28)$$

When the velocity field is prescribed at the surface of the particle, the left hand sides of (2.20)-(2.25) can be represented by surface spherical harmonics

$$\frac{\mathbf{r}}{r}\cdot\left[\mathbf{u}^{(0)}-\mathbf{v}_\infty^{(0)}\right]_{r=r_0} = \sum_{n=1}^{\infty}X_n^{(0)} \quad (2.29)$$

$$-r\,\nabla\cdot[\mathbf{u}^{(0)}-\mathbf{v}_\infty^{(0)}(r_0,\theta,\phi)]_{r=r_0} = \sum_{n=1}^{\infty}Y_n^{(0)} \quad (2.30)$$

$$\mathbf{r}\cdot\nabla\times[\mathbf{u}^{(0)}-\mathbf{v}_\infty^{(0)}(r_0,\theta,\phi)]_{r=r_0} = \sum_{n=1}^{\infty}Z_n^{(0)} \quad (2.31)$$

and

$$\frac{\mathbf{r}}{r}\cdot\left\{(\mathbf{u}^{(1)})-\mathbf{v}_\infty^{(1)}(r,\theta,\phi)\left[\left(\frac{\partial\mathbf{v}^{(0)}}{\partial r}\right)-\frac{1}{\beta}\left(\frac{\boldsymbol{\sigma}_{rt}^{(0)}}{\partial r^{(j)}}\right)\right]\right\}_{r=r_0} = \sum_{n=1}^{\infty}X_n^{(1)} \quad (2.32)$$

$$-r\,\nabla\cdot\left\{(\mathbf{u}^{(1)})-\mathbf{v}_\infty^{(1)}(r,\theta,\phi)\left[\left(\frac{\partial\mathbf{v}^{(0)}}{\partial r}\right)-\frac{1}{\beta}\left(\frac{\boldsymbol{\sigma}_{rt}^{(0)}}{\partial r^{(j)}}\right)\right]\right\}_{r=r_0} = \sum_{n=1}^{\infty}Y_n^{(1)} \quad (2.33)$$

$$\mathbf{r}\cdot\nabla\times\left\{(\mathbf{u}^{(1)})-\mathbf{v}_\infty^{(1)}(r,\theta,\phi)\left[\left(\frac{\partial\mathbf{v}^{(0)}}{\partial r}\right)-\frac{1}{\beta}\left(\frac{\boldsymbol{\sigma}_{rt}^{(0)}}{\partial r^{(j)}}\right)\right]\right\}_{r=r_0} = \sum_{n=1}^{\infty}Z_n^{(1)} \quad (2.34)$$

By replacing n by $-(n+1)$ in those terms of (2.26)-(2.28) for which n is negative, the sum can be made to extend form $n = 1$ to ∞ rather than $-\infty$ to ∞. Hence the following three relations are obtained

$$\begin{aligned}\sum_{n=1}^{\infty}X_n^{(i)} &= \sum_{n=1}^{\infty}\left[\frac{nr_0}{2(2n+3)\mu}\left(\frac{r_0}{r}\right)^n p_n^{(i)}+\frac{n}{r_0}\left(\frac{r_0}{r}\right)^n\phi_n^{(i)}\right] \\ &+ \sum_{n=1}^{\infty}\left[\frac{-(n+1)r_0}{2(-2n+1)\mu}\left(\frac{r}{r_0}\right)^{-(n+1)}p_{-(n+1)}^{(i)}-\frac{n+1}{r_0}\left(\frac{r}{r_0}\right)^{-(n+1)}p_{-(n+1)}^{(i)}\right]\end{aligned} \quad (2.35)$$

$$\sum_{n=-\infty}^{\infty} Y_n^{(i)} = \sum_{n=1}^{\infty}\left[\frac{n(n+1)r_0}{2(2n+3)\mu}\left(\frac{r_0}{r}\right)^n p_n^{(i)} + \frac{n(n-1)}{r_0}\left(\frac{r_0}{r}\right)^n \phi_n^{(i)}\right] \tag{2.36}$$
$$+\frac{1}{\beta}\sum_{n=1}^{\infty}\left[\frac{2n(1-n^2)\mu}{r_0^2}\left(\frac{r_0}{r}\right)^n \phi_n^{(i)} - \frac{n^2(n+2)}{2n+3}\left(\frac{r_0}{r}\right)^n p_n^{(i)}\right]$$
$$+\sum_{n=1}^{\infty}\left[\frac{-n(n+1)r_0}{2(2n-1)\mu}\left(\frac{r}{r_0}\right)^{-(n+1)} p_{-(n+1)}^{(i)} + \frac{(n+1)(n+2)}{r_0}\left(\frac{r}{r_0}\right)^{-(n+1)} \phi_{-(n+1)}^{(i)}\right]$$
$$+\frac{1}{\beta}\sum_{n=1}^{\infty}\left[\frac{2(n+1)(n^2+2n)\mu}{r_0^2}\left(\frac{r}{r_0}\right)^{-(n+1)} \phi_{-(n+1)}^{(i)} - \frac{(n+1)^2(n-1)}{2n-1}\left(\frac{r}{r_0}\right)^{-(n+1)} p_{-(n+1)}^{(i)}\right]$$

$$\sum_{n=1}^{\infty} Z_n^{(i)} = \sum_{n=1}^{\infty}\left[n(n+1)\left(\frac{r_0}{r}\right)^n \chi_n^{(i)} - \frac{1}{\beta}\frac{\mu(n^2-1)n}{r_0}\left(\frac{r_0}{r}\right)^n \chi_n^{(i)}\right] \tag{2.37}$$
$$+ \sum_{n=1}^{\infty}\left[n(n+1)\left(\frac{r}{r_0}\right)^{-(n+1)} \chi_{-(n+1)}^{(i)} - \frac{1}{\beta}\frac{\mu n(n+1)(n+2)}{r_0}\left(\frac{r}{r_0}\right)^{-(n+1)} \chi_{-(n+1)}^{(i)}\right]$$

For an exterior problems, conditions that the fluid should be at rest at infinity require that

$$p_n^{(i)} = \phi_n^{(i)} = \chi_n^{(i)} = 0 \qquad \text{for} \quad n \geq 0, \tag{2.38}$$

so only the negative harmonic functions survive in (2.35)-(2.37). Due to the orthogonality of surface harmonics of different orders, the left- and right-sides of the resulting equations are equated term-by-term under the summation signs. The resulting equations may then be solved simultaneously for the three harmonic functions. When $n \geq 0$, it is found that

$$p_{-(n+1)}^{(i)} = \frac{(2n-1)r_0^n\mu(2r_0\beta X_n^{(i)} + r_0 n\beta X_n^{(i)} + r_0\beta Y_n^{(i)} + 4n\mu X_n^{(i)} + 2n^2\mu X_n^{(i)})}{(n+1)r^{(n+1)}(r_0\beta + \mu + 2n\mu)} \tag{2.39}$$

$$\Phi_{-(n+1)}^{(i)} = \frac{r_0^{(n+2)}\mu(2r_0\beta X_n^{(i)} + r_0\beta Y_n^{(i)} - 2\mu X_n^{(i)} + 2n^2\mu X_n^{(i)})}{2(n+1)r^{(n+1)}(r_0\beta + \mu + 2n\mu)} \tag{2.40}$$

$$\chi_{-(n+1)}^{(i)} = \frac{r_0^{(n+2)}\beta Z_n^{(i)}}{n(n+1)r^{(n+1)}(r_0\beta + \mu + 2n\mu)} \tag{2.41}$$

Substituting these relations into Lamb's solution (2.3), the velocity and pressure field can be written in the form

$$\mathbf{v}^{(i)} = \sum_{n=1}^{\infty}\left[\nabla\times(\mathbf{r}\chi^{(i)}_{-(n+1)}) + \nabla\phi^{(i)}_{-(n+1)} - \frac{(n-2)}{2n(2n-1)\mu}r^2\nabla p^{(i)}_{-(n+1)} + \mathbf{r}\frac{(n+1)}{n(2n-1)\mu}p^{(i)}_{-(n+1)}\right] \tag{2.42}$$

and

$$p^{(i)} = \sum_{n=1}^{\infty} p^{(i)}_{-(n+1)} \tag{2.43}$$

The hydrodynamic force and torque exerted by the fluid on the deformed sphere can be written as [2]

$$\mathbf{F} = \sum_{i=0}^{\infty}\varepsilon^i\mathbf{F}^{(i)} = \mathbf{F}^{(0)} + \varepsilon\mathbf{F}^{(1)} + 0(\varepsilon^2) \tag{2.44}$$

$$\mathbf{T} = \sum_{i=0}^{\infty}\varepsilon^i\mathbf{T}^{(i)} = \mathbf{T}^{(0)} + \varepsilon\mathbf{T}^{(1)} + 0(\varepsilon^2) \tag{2.45}$$

in which

$$\mathbf{F}^{(i)} = -4\pi\nabla(r^3 p^{(i)}_{-2}) \tag{2.46}$$

and

$$\mathbf{T}^{(i)} = -8\pi\mu\nabla(r^3\chi^{(i)}_{-2}) \tag{2.47}$$

2.4 Stokes' resistance of a spheroid

2.4.1 Functions to describe the shape of a deformed sphere

The flow past a spheroid is considered here and the hydrodynamic force and torque exerted by the fluid on the surface of the spheroid are determined. The shape of the spheroid can be described by

$$\frac{x^2+y^2}{r_0^2}+\frac{z^2}{r_0^2(1-\varepsilon)^2}=1 \qquad \begin{cases} \text{Prolate spheroid when } \varepsilon<0 \\ \text{Oblate spheroid when } \varepsilon>0 \end{cases} \tag{2.48}$$

To the first order in the deformation parameter ε, (2.48) can be written in a polar form as in [74]

$$r=r_0\left(1-\varepsilon\left[\left\{\frac{1}{3}p_0(\cos\theta)+\frac{2}{3}p_2(\cos\theta)\right\}\right]\right)+0(\varepsilon^2) \tag{2.49}$$

Comparing (2.49) with (2.5) results in

$$f(\theta)=-\left\{\frac{1}{3}p_0(\cos\theta)+\frac{2}{3}p_2(\cos\theta)\right\} \tag{2.50}$$

where $\cos\theta=\frac{z}{r}$. $p_0(\cos\theta)$ and $p_2(\cos\theta)$ are Legendre functions given by

$$p_0(\cos\theta)=1, \qquad p_2(\cos\theta)=\frac{1}{2}(3cos^2\theta-1) \tag{2.51}$$

2.4.2 Uniform streaming flow past a stationary deformed sphere

The undisturbed uniform streaming flows past a stationary spheroid with velocity $\mathbf{v}_\infty = U\mathbf{e}_x+V\mathbf{e}_y+W\mathbf{e}_z$ is considered in this section. The expansion of $\mathbf{u}$ and $\mathbf{v}_\infty$ can be expressed as

$$\mathbf{u}^{(i)}=\mathbf{0} \qquad i\geq 0 \tag{2.52}$$

$$\mathbf{v}_\infty^{(0)}=U\mathbf{e}_x+V\mathbf{e}_y+W\mathbf{e}_z \qquad \mathbf{v}_\infty^{(i)}=0 \qquad i\geq 1 \tag{2.53}$$

The hydrodynamic force and torque acting on the surface of the spheroid as a whole are therefore

$$
\begin{aligned}
\mathbf{F} &= 6\pi r_0 \mu U \left(\frac{\gamma+2}{\gamma+3} - \frac{\varepsilon(2\gamma^2 + 11\gamma + 6)}{5(\gamma+3)^2} \right) \mathbf{e}_x \\
&+ 6\pi r_0 \mu V \left(\frac{\gamma+2}{\gamma+3} - \frac{\varepsilon(2\gamma^2 + 11\gamma + 6)}{5(\gamma+3)^2} \right) \mathbf{e}_y \\
&+ 6\pi r_0 \mu W \left(\frac{\gamma+2}{\gamma+3} - \frac{\varepsilon(\gamma^2 + 8\gamma + 18)}{5(\gamma+3)^2} \right) \mathbf{e}_z
\end{aligned}
\tag{2.54}
$$

and

$$
\mathbf{T} = 0 \tag{2.55}
$$

in which $\gamma = \dfrac{r_0 \beta}{\mu}$ is a dimensionless parameter.

For a streaming flow parallel to the spheroid axis with velocity $\mathbf{v} = v_\infty \mathbf{e}_z$, the hydrodynamic force and torque exerted on the spheroid by the fluid can be obtained as

$$
\mathbf{F} = -\frac{6\pi r_0 v_\infty \mu \left(\gamma^2(-5+\varepsilon) + \gamma(-25+8\varepsilon)\mu + 6(-5+3\varepsilon)\mu^2 \right)}{5(\gamma+3)^2} \mathbf{e}_z \tag{2.56}
$$

and

$$
\mathbf{T} = 0 \tag{2.57}
$$

For the limiting cases of the perfect slip and non-slip boundary conditions, the hydrodynamic forces are found to be

$$
\mathbf{F} = \begin{cases} 4\pi\, r_0\, v_\infty\, \mu \left(1 - \dfrac{3\varepsilon}{5}\right) \mathbf{e}_z & \text{when} \quad \beta \to 0 \\[2ex] 6\pi\, r_0\, v_\infty\, \mu \left(1 - \dfrac{\varepsilon}{5}\right) \mathbf{e}_z & \text{when} \quad \beta \to \infty \end{cases} \tag{2.58}
$$

For an undeformed sphere, for which $\varepsilon = 0$, the hydrodynamic force with slip is

$$
\mathbf{F} = 6\pi r_0 v_\infty \mu \left(1 - \frac{\mu}{\gamma+3}\right) \mathbf{e}_z \tag{2.59}
$$

which is exactly same as Basset's solution [75].

The comparable results for streaming flow perpendicular to the spheroid axis, $\mathbf{v}_\infty = v_\infty \mathbf{e}_x$, are

$$\mathbf{F} = \frac{6\pi r_0 v_\infty \mu \left[\gamma^2\left(1 - \frac{2\varepsilon}{5}\right) + \gamma\left(5 - \frac{11\varepsilon}{5}\right) + 6\mu^2\left(1 - \frac{\varepsilon}{5}\right)\right]}{(\gamma+3)^2}\mathbf{e}_x \tag{2.60}$$

and

$$\mathbf{T} = 0 \tag{2.61}$$

For special cases of perfect slip and non-slip boundary conditions, the forces can be obtained as

$$\mathbf{F} = \begin{cases} 4\pi r_0 v_\infty \mu \left(1 - \frac{\varepsilon}{5}\right)\mathbf{e}_x & \text{when} \quad \beta \to 0 \\ \\ 6\pi r_0 v_\infty \mu \left(1 - \frac{2\varepsilon}{5}\right)\mathbf{e}_x & \text{when} \quad \beta \to \infty \end{cases} \tag{2.62}$$

Equations (2.58) and (2.62) for the hydrodynamic forces of non-slip boundary condition are exactly same as Brenner's expression [2].

2.5 Uniform streaming flow past a rotating deformed sphere

Let the spheroid rotate in a uniform streaming flow about its axis by $\boldsymbol{\omega}$, which can be decomposed as

$$\boldsymbol{\omega} = \omega_x \mathbf{e}_x + \omega_y \mathbf{e}_y + \omega_z \mathbf{e}_z \tag{2.63}$$

in which ω_i is the angular velocity component along the i direction. Boundary conditions appropriate to the rotation of a spheroid are given by

$$\mathbf{u} = \boldsymbol{\omega} \times \frac{\mathbf{r}}{r} r \quad \text{on } S_d \tag{2.64}$$

On the surface of the particle, each of the perturbation of the spheroid velocity can be written as

$$\mathbf{u}^{(0)} = \boldsymbol{\omega} \times \frac{\mathbf{r}}{r} r_0 \tag{2.65}$$

$$\mathbf{u}^{(1)} = \boldsymbol{\omega} \times \frac{\mathbf{r}}{r} r_0 f(\theta, \phi) \tag{2.66}$$

$$\mathbf{u}^{(i)} = 0 \quad i \geq 2 \tag{2.67}$$

The undisturbed motion of the fluid in the neighborhood of the spheroid is given as

$$\mathbf{v}_\infty = U\mathbf{e}_x + V\mathbf{e}_y + W\mathbf{e}_z \tag{2.68}$$

The hydrodynamic force and torque can be obtained as

$$\begin{aligned} \mathbf{F} &= 6\pi r_0 \mu U \left(\frac{\gamma+2}{\gamma+3} - \frac{\varepsilon(2\gamma^2 + 11\gamma + 6)}{5(\gamma+3)^2} \right) \mathbf{e}_x \\ &+ 6\pi r_0 \mu V \left(\frac{\gamma+2}{\gamma+3} - \frac{\varepsilon(2\gamma^2 + 11\gamma + 6)}{5(\gamma+3)^2} \right) \mathbf{e}_y \\ &+ 6\pi r_0 \mu W \left(\frac{\gamma+2}{\gamma+3} - \frac{\varepsilon(2\gamma^2 + 8\gamma + 18)}{5(\gamma+3)^2} \right) \mathbf{e}_z \end{aligned} \tag{2.69}$$

and

$$\begin{aligned} \mathbf{T} &= \pi r_0^4 \beta \mu \omega_x \left(-\frac{8}{r_0\beta + 3\mu} + \frac{48\varepsilon(r_0\beta + 4\mu)}{5(r_0\beta + 3\mu)^2} \right) \mathbf{e}_x \\ &+ \pi r_0^4 \beta \mu \omega_y \left(-\frac{8}{r_0\beta + 3\mu} + \frac{48\varepsilon(r_0\beta + 4\mu)}{5(r_0\beta + 3\mu)^2} \right) \mathbf{e}_y \\ &+ \pi r_0^4 \beta \mu \omega_z \left(-\frac{8}{r_0\beta + 3\mu} + \frac{24\varepsilon(r_0\beta + 4\mu)}{5(r_0\beta + 3\mu)^2} \right) \mathbf{e}_z \end{aligned} \tag{2.70}$$

At the first order of ε, it can be seen that the translational motion of the fluid relative to the spheroid determines the hydrodynamic force, while the rotation motion of the particle determines the torque on the spheroid.

For a spheroid rotating about the symmetry axis in a quiescent flow, $\boldsymbol{\omega} = \omega_z \mathbf{e}_z$, the hydrodynamic force and torque exerted by the fluid on the spheroid can be written as

$$\mathbf{F} = 0 \tag{2.71}$$

$$\mathbf{T} = \frac{8\pi r_0^4 \beta\mu[\gamma(-5+3\varepsilon)+3(-5+4\varepsilon)\mu]\omega_z}{5(\gamma+3)^2}\mathbf{e}_z \tag{2.72}$$

of which the limiting cases are

$$\mathbf{T} = \begin{cases} \mathbf{0} & \text{when} \quad \beta = 0 \\ \frac{8}{5}\pi r_0^3(-5+3\varepsilon)\mu\omega_z\mathbf{e}_z & \text{when} \quad \beta \to \infty \end{cases} \tag{2.73}$$

Analogous results for rotation about the equatorial diameter $\boldsymbol{\omega} = \omega_x \mathbf{e}_x$ in a quiescent flow are

$$\mathbf{F} = 0 \tag{2.74}$$

and

$$\mathbf{T} = \frac{8\pi r_0^4 \beta\mu[\gamma(-5+6\varepsilon)+3(-5+8\varepsilon)\mu]\omega_x}{5(r_0\beta+3\mu)^2}\mathbf{e}_x \tag{2.75}$$

For the limiting cases of the perfect slip and non-slip, the torques are

$$\mathbf{T} = \begin{cases} \mathbf{0} & \text{when} \quad \beta = 0 \\ \frac{8}{5}\pi r_0^3(-5+6\varepsilon)\mu\omega_x\mathbf{e}_x & \text{when} \quad \beta \to \infty \end{cases} \tag{2.76}$$

For the non-slip case, the torque on the deformed sphere is same as Brenner's solution [2]. For a sphere rotating in a quiescent flow with slip the torque is given by

$$\mathbf{T} = -\frac{8\pi r_0^4 \beta\omega_x\mathbf{e}_x}{\gamma+3} \qquad \text{when} \quad \varepsilon = 0 \tag{2.77}$$

2.6 Flow-induced motion of a spheroidal particle with slip

A rigid deformed sphere is considered in this problem to be suspended in a homogeneous flow. The problem is expressed in two coordinate systems. The first system rotates with

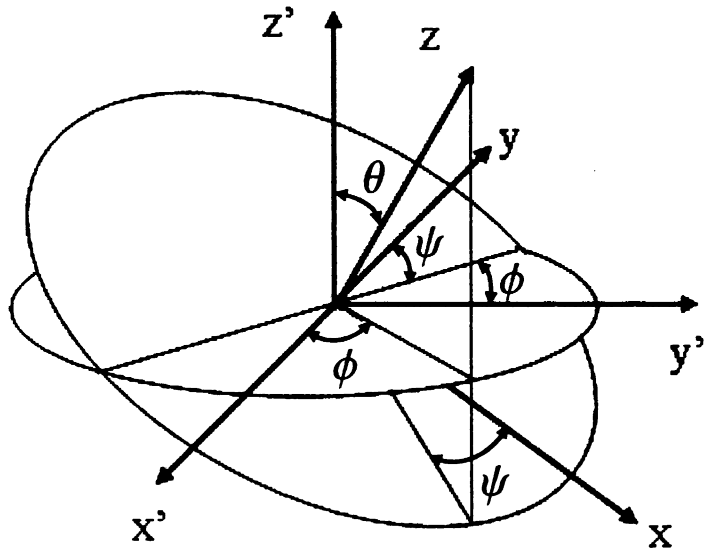

Figure 2.3. Illustration of three Euler angles $\phi, \theta,$ and ψ used to describe the coordinate systems of a particle. x', y' and z' are the reference coordinate system and x, y and z are the rotating coordinated system.

the particle and is denoted by x, y and z. The second coordinate system is fixed in space and denoted by x', y' and z'. The position of the rotating coordinate system with respect to the fixed system can be described in terms of three Euler angles shown in Figure 2.3.The angle θ is simply the angle between the z axes of both coordinate systems. The angle ϕ is the angle between the x axis of the reference coordinate system and the projection of z into the x', y' plane. Finally, ψ is the angle between the y axis and the line of nodes. These two systems are connected through the transformation

$$\begin{pmatrix} x \\ y \\ z \end{pmatrix} = \begin{pmatrix} \cos\psi\cos\phi - \cos\theta\sin\phi\sin\psi & \cos\psi\sin\phi + \cos\theta\cos\phi\sin\psi & \sin\theta\sin\psi \\ -\sin\psi\cos\phi - \cos\theta\sin\phi\cos\psi & -\sin\psi\sin\phi + \cos\theta\cos\phi\cos\psi & \cos\psi\sin\theta \\ \sin\theta\sin\phi & -\sin\theta\cos\phi & \cos\theta \end{pmatrix} \begin{pmatrix} x' \\ y' \\ z' \end{pmatrix} \tag{2.78}$$

Rotations of the particle around the body axes may be described by

$$\begin{aligned}\boldsymbol{\omega} &= \begin{pmatrix} \omega_x & \omega_y & \omega_z \end{pmatrix} \\ &= \begin{pmatrix} \sin\psi\sin\phi\dot{\theta} + \cos\psi\dot{\phi} & \cos\psi\sin\phi\dot{\theta} - \sin\psi\dot{\phi} & \cos\phi\dot{\theta} + \dot{\psi} \end{pmatrix}\end{aligned} \tag{2.79}$$

A homogeneous flow field far from the particle can be defined in the rotating coordinate system as

$$\mathbf{v}_\infty = \left[\begin{pmatrix} a & h & g \\ h & b & f \\ g & f & c \end{pmatrix} + \begin{pmatrix} 0 & -\zeta & \eta \\ \zeta & 0 & -\xi \\ -\eta & \xi & 0 \end{pmatrix}\right]\begin{pmatrix} x \\ y \\ z \end{pmatrix} \tag{2.80}$$

in which $\mathbf{S} = \begin{pmatrix} a & h & g \\ h & b & f \\ g & f & c \end{pmatrix}$ is the distortion of the fluid and $\mathbf{W} = \begin{pmatrix} 0 & -\zeta & \eta \\ \zeta & 0 & -\xi \\ -\eta & \xi & 0 \end{pmatrix}$ is the rotation of the fluid. The parameters are constant in space, but can be a function of the time, since the particle will rotate under the influence of the flow field. Let

$$\mathbf{G} = \mathbf{S} + \mathbf{W} \tag{2.81}$$

The velocity field at infinity of the fluid can be written into a tensor form as

$$\mathbf{v}_\infty = \mathbf{G} \cdot \mathbf{r} \tag{2.82}$$

and

$$\mathbf{v}_\infty^{(0)} = \mathbf{G} \cdot \frac{\mathbf{r}}{r} r_0 \tag{2.83}$$

$$\mathbf{v}_\infty^{(1)} = \mathbf{G} \cdot \frac{\mathbf{r}}{r} r_0 f(\theta) \tag{2.84}$$

$$\mathbf{v}_\infty^{(i)} = \mathbf{0} \quad \text{when} \quad i \geq 2 \tag{2.85}$$

The hydrodynamic force and torque applying on the surface of the spheroid are

$$\mathbf{F} = \mathbf{0} \tag{2.86}$$

and

$$\mathbf{T} = T_x \mathbf{e}_x + T_y \mathbf{e}_y + T_z \mathbf{e}_z \tag{2.87}$$

in which

$$T_x = \frac{8\pi r_0^3 \mu \left\{ f\varepsilon(3+\gamma)(32+38\gamma+5\gamma^2) - \gamma(\gamma+5)[-5(\gamma+3)+6\varepsilon(\gamma+4)](\xi-\omega_x) \right\}}{5(\gamma+3)^2(\gamma+5)} \tag{2.88}$$

$$T_y = -\frac{8\pi r_0^3 \mu \left\{ g\varepsilon(3+\gamma)(32+38\gamma+5\gamma^2) - \gamma(\gamma+5)[-5(\gamma+3)+6\varepsilon(\gamma+4)](\eta-\omega_y) \right\}}{5(\gamma+3)^2(\gamma+5)} \tag{2.89}$$

$$T_z = -\frac{8\pi r_0^3 \mu [\gamma(-5+3\varepsilon)+3(-5+4\varepsilon)](\zeta-\omega_z)}{5(\gamma+3)^2} \tag{2.90}$$

If a particle is subjected to no external forces except those exerted by the fluid upon its surface, then the resultant torque on the particle will be vanished at each instant. Let the three components of the resultant torque equal to zeros. The angular velocities of the particle can be solved to be

$$\omega_x = -f\lambda + \xi, \quad \omega_y = g\lambda + \eta, \quad \omega_z = \zeta, \tag{2.91}$$

where

$$\lambda = \frac{(3+\gamma)(32+38\gamma+5\gamma^2)\varepsilon}{\gamma(5+\gamma)[-5(3+\gamma)+6\varepsilon(4+\gamma)]} \tag{2.92}$$

and the dimensionless parameter $\gamma = \frac{r_0 \beta}{\mu}$ is introduced. If $\gamma \to \infty$, the no-slip boundary condition is satisfied on the interface, and (2.92) can be simplified to

$$\begin{aligned} \lambda &= \frac{5\varepsilon}{-5+6\varepsilon} \\ &= -\varepsilon - \frac{6}{5}\varepsilon^2 + 0(\varepsilon^3) \end{aligned} \tag{2.93}$$

Actually λ can be decomposed into two parts as

$$\lambda = \frac{5\varepsilon}{-5+6\varepsilon} + \frac{\varepsilon(-480-355\gamma-65\gamma^2)+\varepsilon^2(576+276\gamma+48\gamma^2)}{\gamma(5+\gamma)(-5+6\varepsilon)[-5(3+\gamma)+6\varepsilon(4+\gamma)]} \tag{2.94}$$

In equation(2.94), the first term of λ is the no-slip part and the second term is the additional part due to slip on the interface.

The evolution of the orientation of a spheroidal particle can be described with [76]

$$\dot{\mathbf{p}} = -\mathbf{W}\cdot\mathbf{p} + \lambda(\mathbf{S}\cdot\mathbf{p} - \mathbf{S}:\mathbf{ppp}) \tag{2.95}$$

in which $\mathbf{p}$ is the orientation of the particle which is a unit vector along the long axis. This equation is identical to Jeffery's equation for the orientation of the particle with exception of the definition of parameter λ. With consideration of the slip on the particle surface, it is convenient to group λ into parameters related to the geometry of the particle, the slip coefficient, and the viscosity. In Jeffery's solution [1], $\lambda_J = \dfrac{a_p^2-1}{a_p^2+1}$ is only related to the geometry of the spheroid, i.e. the aspect ratio the ellipsoid a_p (length/diameter), and the range λ_J is $[-1,1]$. $\lambda_J = 1$ represents for long fiber with infinite aspect ratio, $\lambda_J = 0$ indicates for sphere, whereas $\lambda_J = -1$ corresponds to a disk. The relation of λ with the dimensionless variable γ when $\varepsilon = \pm 0.1$ and $\varepsilon = \pm 0.2$ are shown in the Figure 2.4. It can be seen that λ is always positive when $\varepsilon < 0$ and negative when $\varepsilon > 0$. For the case of $\varepsilon = -0.1$ only one positive root $\gamma = 0.1239$ exist to let $\lambda = 1$ shown by the dash line in the Figure 2.4. Jeffery [1] found the equations describing the motion of an ellipsoid in an unbounded fluid with nonslip boundary conditions. When simplified to a slightly deformed sphere, it is found that

$$\omega_{Jx} = -f\lambda_J + \xi, \quad \omega_{Jy} = g\lambda_j + \eta, \quad \omega_{Jz} = \zeta, \tag{2.96}$$

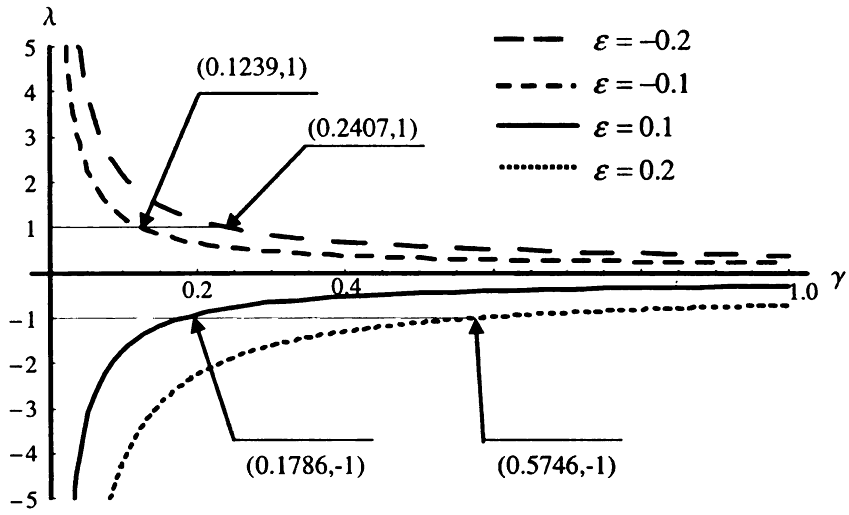

Figure 2.4. Influence of the slip coefficient β and the particle aspect ratio ε on the fluid/particle coupling coefficient λ. λ is always positive when $\varepsilon < 0$ and negative when $\varepsilon > 0$.

where

$$\begin{aligned} \lambda_J &= \frac{\varepsilon(\varepsilon - 2)}{\varepsilon^2 - 2\varepsilon + 2} \\ &= -\varepsilon - \frac{1}{2}\varepsilon^2 + O(\varepsilon^3) \end{aligned} \tag{2.97}$$

By the present approach, for the limiting case of nonslip boundary condition, the error of the present approach is $O(\varepsilon^2)$, and this is also observed after comparing (2.91) and (2.93) with Jeffery's solution [1], i.e. (2.96) and (2.97).

The case of a simple shear flow imposed far from the particle is considered next and described with $\mathbf{v}'_\infty = \begin{pmatrix} 0 & 0 & Ky' \end{pmatrix}$ where K is a constant. The velocity field at infinity is shown in Figure 2.5. From (2.78) the distortion and rotation of the undisturbed fluid in the

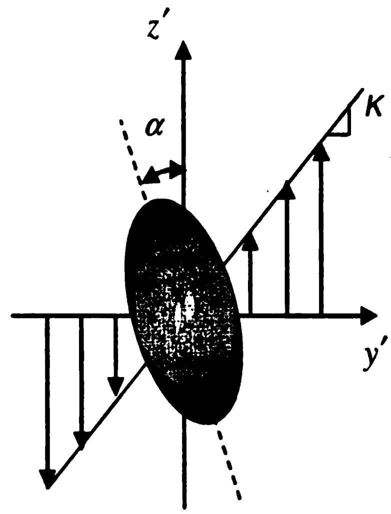

$\mathbf{v}'_\infty = [0 \quad 0 \quad Ky']$

Figure 2.5. Illustration of a simple shear flow surrounding a deformed sphere.

rotating coordinate system are found to be

$$\mathbf{S} = \begin{pmatrix} 0 & 0 & 0 \\ 0 & K\cos\alpha\sin\alpha & \frac{1}{2}K\cos 2\alpha \\ 0 & \frac{1}{2}K\cos 2\alpha & -K\cos\alpha\sin\alpha \end{pmatrix} \tag{2.98}$$

$$\mathbf{W} = \begin{pmatrix} 0 & 0 & 0 \\ 0 & 0 & \frac{K}{2} \\ 0 & -\frac{K}{2} & 0 \end{pmatrix} \tag{2.99}$$

The motion of spheroid can be described with

$$\omega_x = \dot{\alpha}, \quad \omega_y = 0, \quad \omega_z = 0 \tag{2.100}$$

Using (2.91) the rotation of the particle is

$$\omega_x = \dot{\alpha} = -\frac{K}{2}(\lambda\cos 2\alpha + 1) \tag{2.101}$$

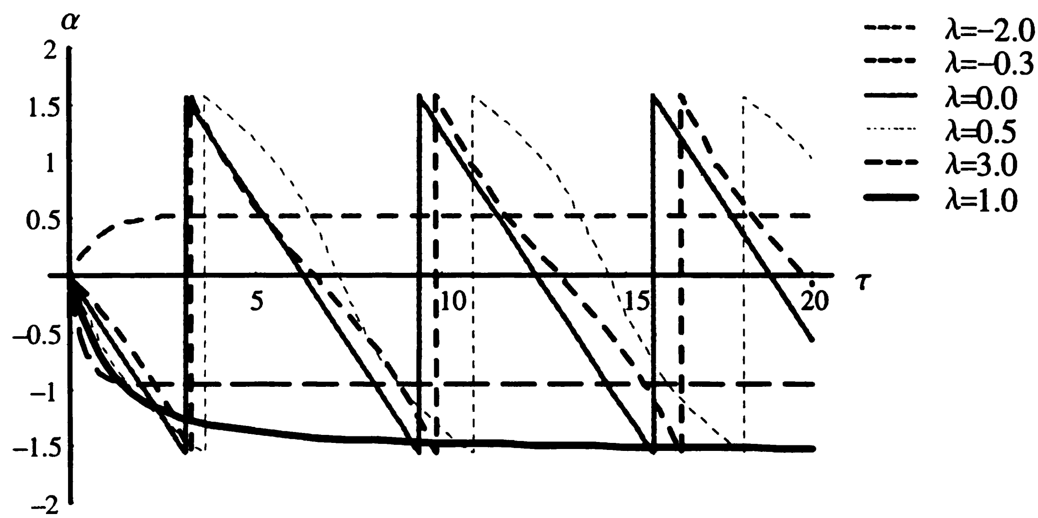

Figure 2.6. The influence of the fluid/particle coupling coefficient λ on the rotation of a spheroid in the flow/shear plane is shown by plotting the cosine of the rotation angle α of a particle for various values of λ. When $|\lambda| < 1$, the induced motion of the particle is periodic; when $|\lambda| \geq 1$, the induced motion of the particle is steady.

Integrating (2.101) over the time domain, the angle α can be expressed in terms of the dimensionless time τ as

$$\alpha = \arctan\left[\frac{\sqrt{\lambda^2 - 1}}{\lambda - 1}\tanh\left(-\frac{\sqrt{\lambda^2 - 1}}{2}\tau\right)\right] \tag{2.102}$$

in which $\tau = Kt$. The evolution of angle α is shown in Figure 2.6. It can be seen that when $|\lambda| < 1$, the motions of the particle are periodic; when $|\lambda| \geq 1$, the particle rotates to a fixed angle and then reaches a steady state. The period increases with the absolute value of λ. In Figure 2.4, the horizontal lines $\lambda = \pm 1$ separate the steady motion and periodic motion of the particle. Between these two lines, the motion of the particle induced by the simple shear flow is periodic. For the cases of $|\lambda| \geq 1$, the steady state of the particle means that the orientation of the particle does not change with time. Taking the time derivative of the orientation α equal to zero, the orientation of the particle reaching a steady state can be obtained as

$$\alpha_{ss} = \begin{cases} \arccos\sqrt{\dfrac{\lambda - 1}{2\lambda}} & \lambda < -1 \\ \\ -\arccos\sqrt{\dfrac{\lambda - 1}{2\lambda}} & \lambda \geq 1 \end{cases} \tag{2.103}$$

From Figure 2.6 it can be seen that when $\lambda < -1$, the angle α_{ss} is positive, and when $\lambda > 1$, the angle α_{ss} is negative.

The phenomenon of a periodic motion or a steady state of a force-free particle inside a simple shear flow can also be explained physically. Eq. (2.95) stems from a balance of angular momentum. The underlying assumption in the Jeffery analysis is that there is no external torque acting directly on the particle. Therefore all the intrinsic couples (torques) between the particle and the fluid must balance and the angular momentum of the particle is constant. As a consequence, the angular velocity must satisfy (2.95), which requires the orientation of the particle to change continuously if $|\lambda| < 1$ (i.e. , periodic behavior). Eq. (2.95) shows that the angular velocity is caused by two processes: 1) a coupling of the particle with the vorticity of the imposed flow field; and, 2) a coupling of the particle with the strain rate of the imposed flow field. A vector produced by a pure rotation of the orientation vector represents the first effect: $-\mathbf{W} \cdot \mathbf{p}$. This vector is always orthogonal to the orientation vector. If the external flow field has vorticity and if $\lambda = 0$ (sphere), then the sphere must rotate continuously to balance the torque induced by the external hydrodynamic field. For a neutrally buoyant system (i.e., density of the fluid and particle are equal), the sphere translates with the local velocity and a drag force is exerted on the particle, which is countered by the external force needed to sustain the flow field

Table 2.1. Predicted periods of the particle motion induced by a simple shear flow. The periods of the motion of the particle increase with the increasing of the deformation of the particle and decrease with the increasing of the parameter γ.

period	$\gamma = 0.2$	$\gamma = 1.0$	$\gamma \to \infty$	Jeffery
$\varepsilon = 0.1$	30.2	14.1	13.3	13.3
$\varepsilon = 0.2$	steady	17.4	13.2	13.1
$\varepsilon = 0.3$	steady	steady	14.5	12.7
$\varepsilon = -0.1$	16.5	13.2	12.5	12.5
$\varepsilon = -0.2$	steady	14.3	13.1	13.2
$\varepsilon = -0.3$	steady	15.6	13.4	13.5

and the particle velocity. If $\lambda \neq 0$, then the particle can also couple with the strain rate of the external flow to produce a torque. (2.95) shows that the resulting angular velocity is proportional to the coupling coefficient λ and a vector produced by a rotation-stretch-projection operation on the instantaneous orientation vector: $\lambda(\mathbf{S} \cdot \mathbf{p} - \mathbf{S} : \mathbf{ppp})$. This vector is also orthogonal to the orientation vector. If $|\lambda| < 1$, then the torque produced by the strain rate is too weak to balance the torque produced by the vorticity field. Consequently, in order to satisfy the torque balance, the particle must rotate (Jeffery orbits). If $|\lambda| > 1$, the torque on the particle due to the coupling with the strain rate is now large enough to balance the torque due the vorticity field in the absence of tumbling! Most significantly, the particle is not aligned with the flow field. This surprising and interesting result is due to the slip phenomena.

To illustrate with a simple problem, the parameters affecting the motion are selected to be $r_0 = 0.01, \mu = 0.02$, and $K = 0.5$. ε and γ are changed to study the influence of

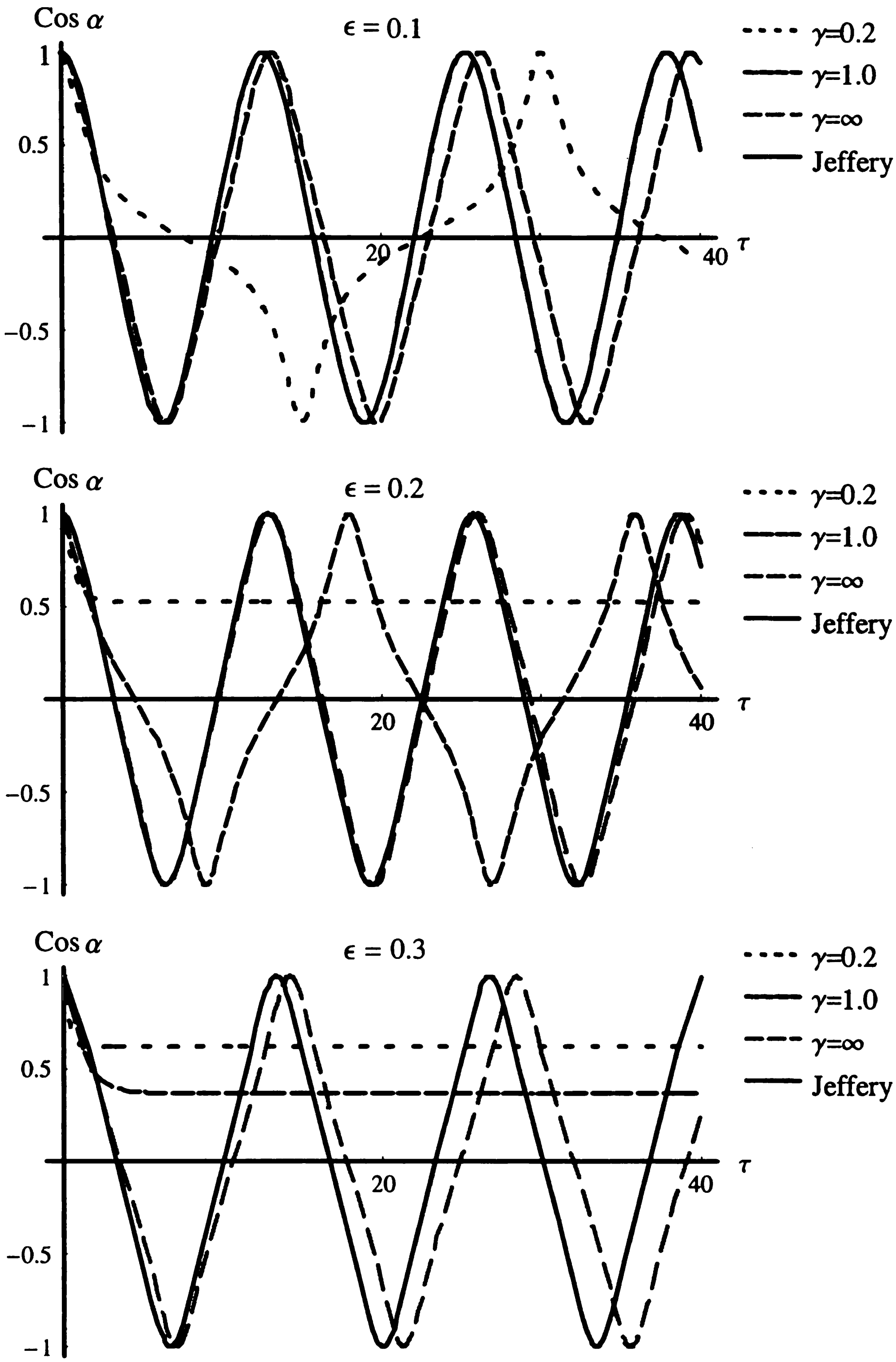

Figure 2.7. The figure shows the influence of the fluid/particle coupling coefficient λ and the particle aspect ratio ε on the temporal response of a spheroid to a steady simple shear flow at positive values of εs.

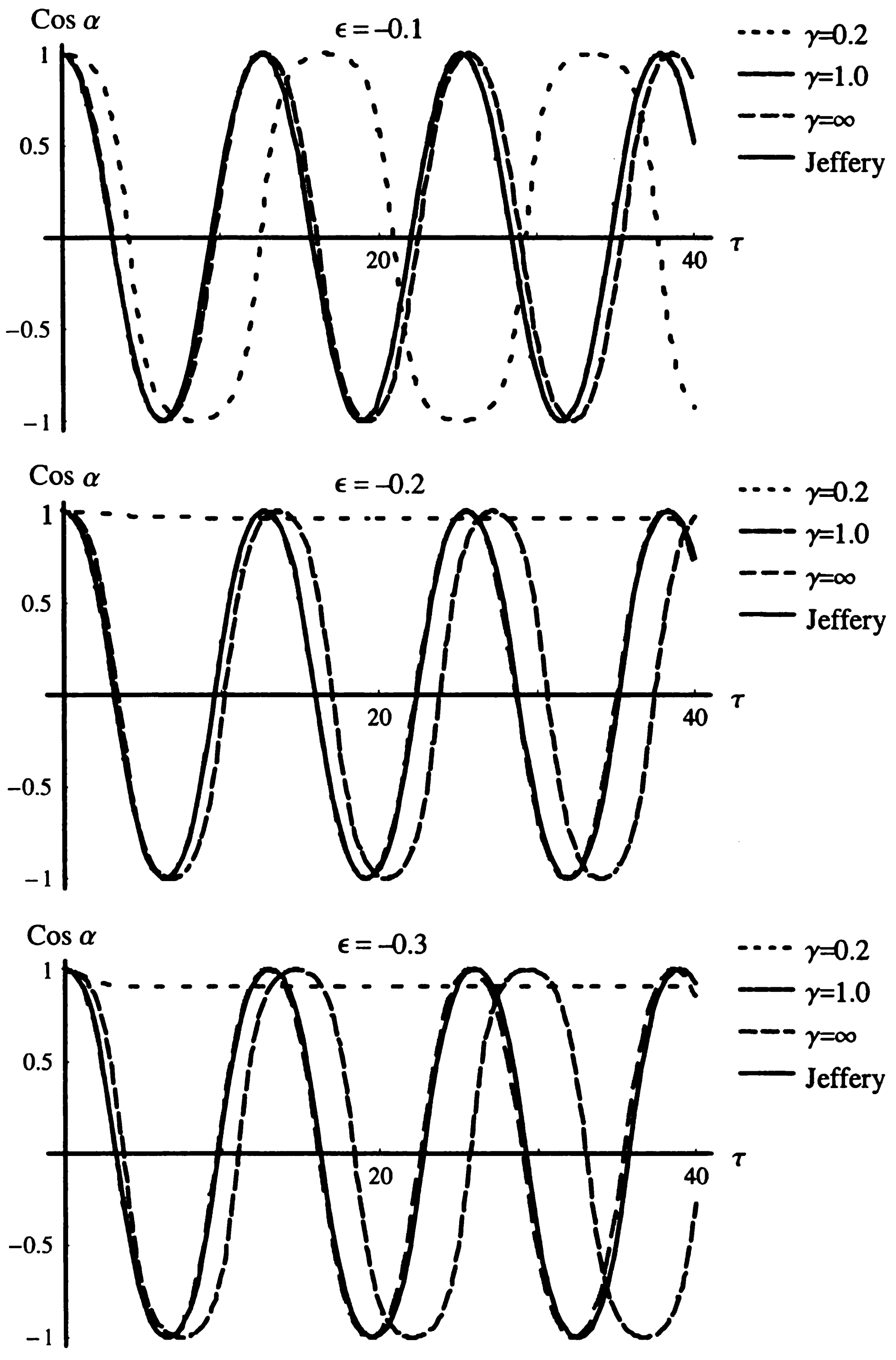

Figure 2.8. The above figure shows the influence of the fluid/particle coupling coefficient and the particle aspect ratio on the temporal response of a spheroid to a steady simple shear flow at negative values of εs.

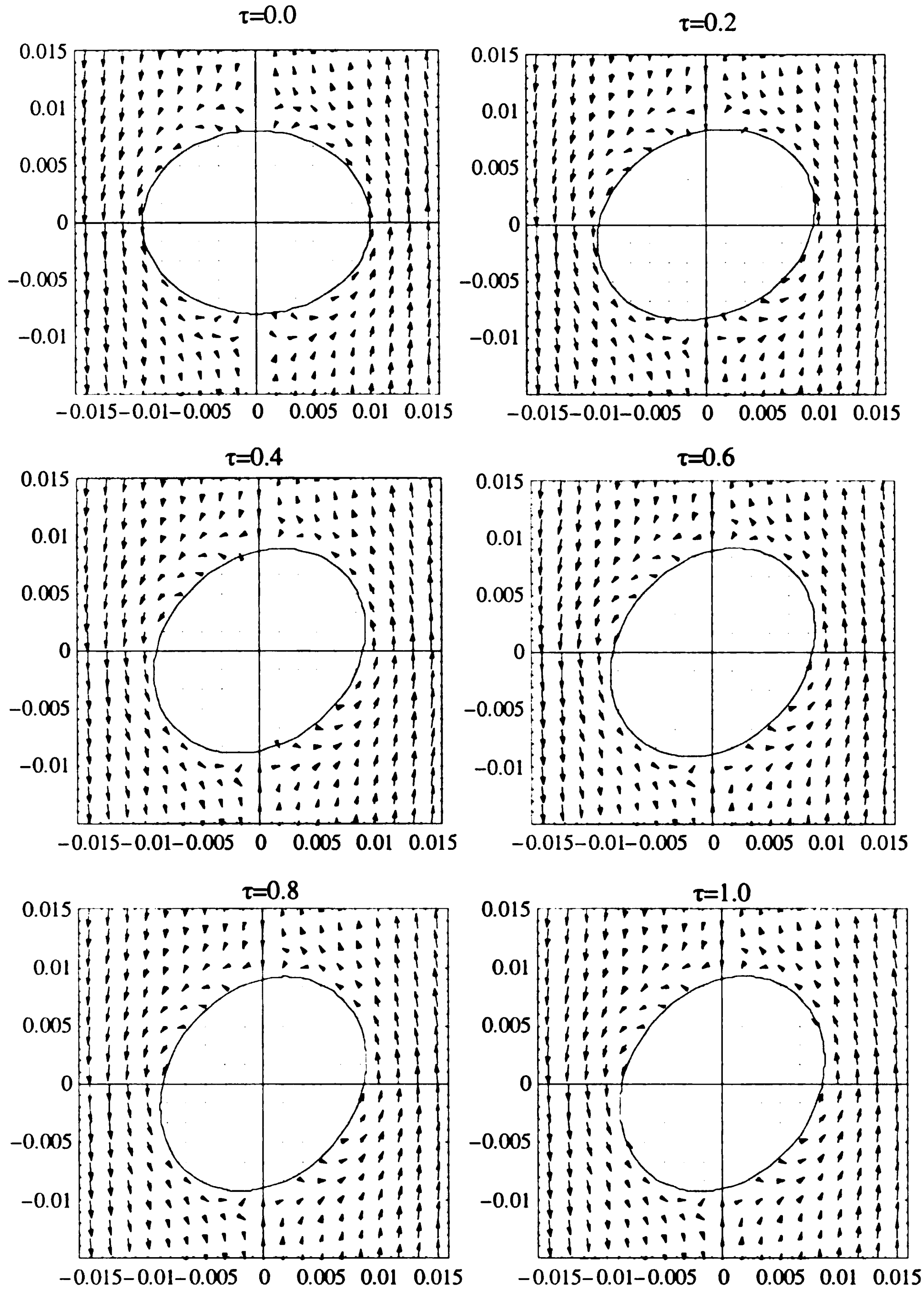

Figure 2.9. These graphs show the velocity field around of a spheroid with steady motion. The particle reaches a special orientation after some time and then keep this orientation inside the flow field.

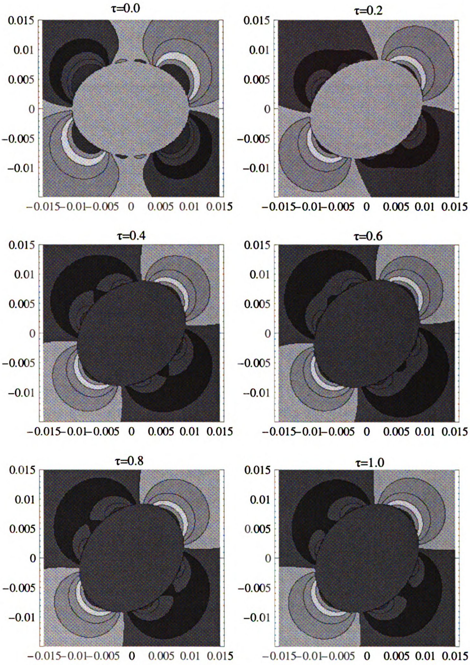

Figure 2.10. These graphs show the pressure field around of a spheroid with steady motion.

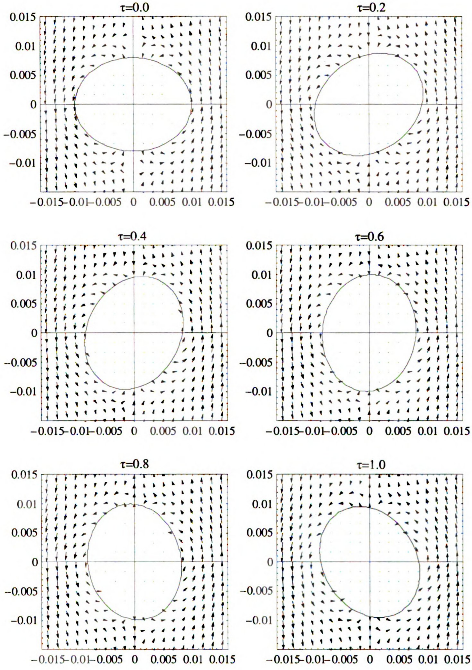

Figure 2.11. These graphs show the velocity field around of a spheroid with periodic motion.

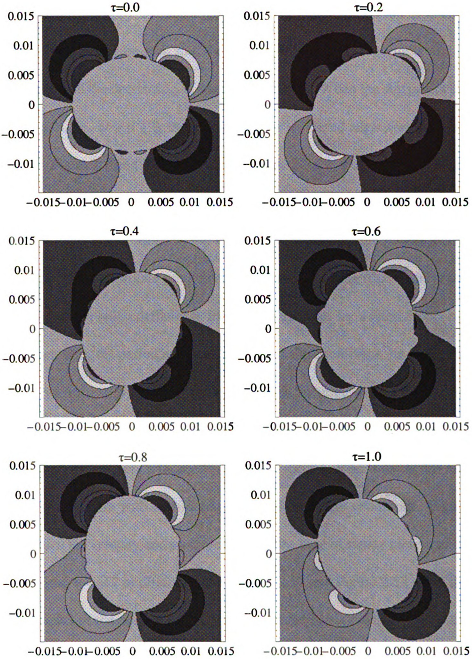

Figure 2.12. These graphs show the pressure field around of a spheroid with periodic motion.

slip coefficient and the geometry to the motion of the particle. Different motions of the particle are shown in Figure 2.7 and Figure 2.8. The predicted period of each motion is shown in Table2.1. It can be seen that the motion of a particle is periodic and the period becomes longer with the decreasing of the slip coefficient. When the slip coefficient goes to sufficiently small, i.e., at $\gamma = 1.0$, the particle rotates to a fixed angle and achieves a steady state shown in Figure2.7 and Figure2.8 by fine dashed lines. For oblate spheroids($\varepsilon > 0$), as the sliding friction decreases relative to the viscous friction (slip coefficient), the period increases for a fixed aspect ratio; as the aspect ratio increases, the period increases for a fixed slip coefficient. For prolate spheroids ($\varepsilon < 0$), as the sliding friction decreases relative to the viscous friction (slip coefficient), the period increases for a fixed aspect ratio; as the aspect ratio increases, the period increases for a fixed slip coefficient. As mentioned before, the solutions with the slip by the present method is accurate to $O(\varepsilon^2)$. For the slightly deformed sphere the motion of the particle for when $\gamma \to \infty$, shown in Figure 2.7 by dashed lines, agrees well with Jeffery's [1]no-slip solutions. So the present method is effective for slightly deformed sphere with consideration of slip boundary conditions. Figure 2.9 and Figure 2.10 show the velocity and pressure fields of the case of steady motion of the particle when $\gamma = 2.5$ and $\varepsilon = 0.2$ at different time. Figure 2.11 and Figure 2.12 show the velocity and pressure fields of the case of periodic motion of the particle when $\gamma \to \infty$ and $\varepsilon = 0.2$ at different time.

2.7 Summary

A perturbation method is used to solve for the motion of a fluid influenced by the presence of a deformed sphere. Slip is assumed at the surface of the particle.The hydrodynamic force and torque exerted by the fluid on the deformed sphere are expressed explicitly for a fixed and rotating particle in a uniform streaming flow. Solutions to the limiting cases of non-slip and perfect slip are identical to the existing solutions. The motion and orientation evolution of a spheroid induced by a homogeneous flow are derived. Errors in the angular velocity calculated by this method are of the order of $O(\varepsilon^2)$. The period of rotation of the spheroid is found to be longer as a dimensionless parameter that incorporates the slip coefficient becomes small. When the slip coefficient becomes sufficiently low, the deformed sphere rotates to a fixed angle and reaches to a quasi-steady state in the flow.

CHAPTER 3

MOTION OF AN ELLIPSOID IN QUADRATIC AND CUBIC FLOWS

The influence of the physical parameters, such as the geometry of the particle, the viscosity of the surrounding fluid, the slip coefficient, to the drag force and the motion of a deformed sphere suspending in homogeneous shear flow has been studied in Chapter 2 and Chapter 3. The influence of the velocity field to the drag force and the motion of the particle will be studied in this chapter.

3.1 Motion of an ellipsoid in a quadratic flow field

First, quadratic flow field is considered and the hydrodynamic force and torque exerted on the surface of the spheroid by the surrounding fluid are determined. The same particle is studied as that in the chapter 2 and chapter 3. The surface of the particle can be described by the same function in the polar form as

$$r = r_0[1 + \varepsilon f(\theta)] + 0(\varepsilon^2) \tag{3.1}$$

in which

$$f(\theta) = -\left\{\frac{1}{3}p_0(\cos\theta) + \frac{2}{3}p_2(\cos\theta)\right\} \tag{3.2}$$

The velocity of the particle can be decomposed by two parts, the translation velocity and the rotation velocity.

$$\begin{aligned} \mathbf{u} &= \mathbf{u}_0 + \boldsymbol{\omega} \times \mathbf{r} \\ &= \begin{pmatrix} u_{x0} \\ u_{y0} \\ u_{z0} \end{pmatrix} + \begin{pmatrix} \omega_x z - \omega_z y \\ \omega_z x - \omega_x z \\ \omega_x y - \omega_y x \end{pmatrix} \end{aligned} \tag{3.3}$$

in which $\mathbf{u}_0$ is the translation velocity of the center of the particle, and $\boldsymbol{\omega}$ is the angular velocity. The velocity field of the fluid far away from the particle is defined as

$$\mathbf{v}_\infty = \begin{pmatrix} v_{x0} \\ v_{y0} \\ v_{z0} \end{pmatrix} + \begin{pmatrix} G_{11} & G_{12} & G_{13} \\ G_{21} & G_{22} & G_{23} \\ G_{31} & G_{32} & G_{33} \end{pmatrix} \begin{pmatrix} x \\ y \\ z \end{pmatrix} + \begin{pmatrix} A_{111} & A_{112} & A_{113} & A_{123} & A_{122} & A_{133} \\ A_{211} & A_{212} & A_{213} & A_{223} & A_{222} & A_{233} \\ A_{311} & A_{312} & A_{313} & A_{323} & A_{322} & A_{333} \end{pmatrix} \begin{pmatrix} x^2 \\ xy \\ xz \\ yz \\ y^2 \\ z^2 \end{pmatrix} \tag{3.4}$$

In spherical coordinates, denoted as (r, θ, ϕ), the position vector shown in (3.1), is expressed as

$$\mathbf{r} = r\sin\theta\cos\phi\mathbf{e}_x + r\sin\theta\sin\phi\mathbf{e}_y + r\cos\theta\mathbf{e}_z \tag{3.5}$$

Using the following definitions

$$x_{(0)} = r_0\sin\theta\cos\phi \tag{3.6}$$

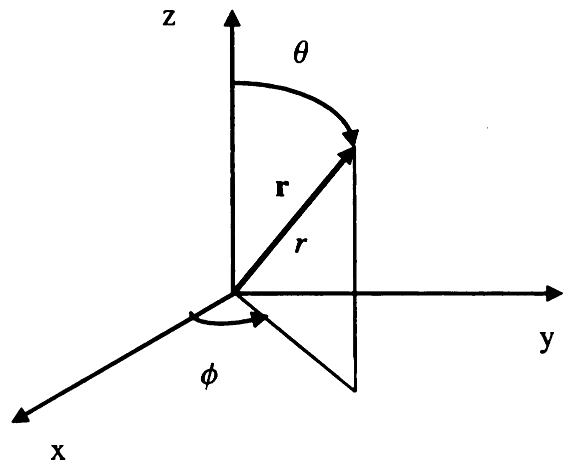

Figure 3.1. This figure shows a spherical coordinate system.

$$y_{(0)} = r_0 \sin\theta \sin\phi \tag{3.7}$$

$$z_{(0)} = r_0 \cos\theta \tag{3.8}$$

and substituting (3.6-3.8) and (3.1) into (3.4), the velocity field can be decomposed as

$$\mathbf{v}_\infty^{(0)} = \begin{pmatrix} v_{x0} \\ v_{y0} \\ v_{z0} \end{pmatrix} + \begin{pmatrix} G_{11} & G_{12} & G_{13} \\ G_{21} & G_{22} & G_{23} \\ G_{31} & G_{32} & G_{33} \end{pmatrix} \begin{pmatrix} x_{(0)} \\ y_{(0)} \\ z_{(0)} \end{pmatrix} + \begin{pmatrix} A_{111} & A_{112} & A_{113} & A_{123} & A_{122} & A_{133} \\ A_{211} & A_{212} & A_{213} & A_{223} & A_{222} & A_{233} \\ A_{311} & A_{312} & A_{313} & A_{323} & A_{322} & A_{333} \end{pmatrix} \begin{pmatrix} x_{(0)}^2 \\ x_{(0)}y_{(0)} \\ x_{(0)}z_{(0)} \\ y_{(0)}z_{(0)} \\ y_{(0)}^2 \\ z_{(0)}^2 \end{pmatrix} \tag{3.9}$$

and

$$\mathbf{v}_\infty^{(1)} = f(\theta)\begin{pmatrix} G_{11} & G_{12} & G_{13} \\ G_{21} & G_{22} & G_{23} \\ G_{31} & G_{32} & G_{33} \end{pmatrix}\begin{pmatrix} x_{(0)} \\ y_{(0)} \\ z_{(0)} \end{pmatrix} \tag{3.10}$$

$$+2f(\theta)\begin{pmatrix} A_{111} & A_{112} & A_{113} & A_{123} & A_{122} & A_{133} \\ A_{211} & A_{212} & A_{213} & A_{223} & A_{222} & A_{233} \\ A_{311} & A_{312} & A_{313} & A_{323} & A_{322} & A_{333} \end{pmatrix}\begin{pmatrix} x_{(0)}^2 \\ x_{(0)}y_{(0)} \\ x_{(0)}z_{(0)} \\ y_{(0)}z_{(0)} \\ y_{(0)}^2 \\ z_{(0)}^2 \end{pmatrix}$$

and

$$\mathbf{v}_\infty^{(i)} = 0 \quad \text{when } i \geq 2 \tag{3.11}$$

To satisfy the continuity equation of the fluid, it is required that

$$\mathrm{Tr}(\nabla \mathbf{v}) = 0 \tag{3.12}$$

The following relations can then be obtained

$$G_{11} + G_{22} + G_{22} = 0 \tag{3.13}$$

$$(2A_{111} + A_{212} + A_{313})x = 0 \tag{3.14}$$

$$(A_{112} + 2A_{222} + A_{323})x = 0 \tag{3.15}$$

$$(A_{113} + A_{223} + 2A_{333})x = 0 \tag{3.16}$$

In (3.13-3.16), x, y, and z can be any arbitrary number. Hence the coefficient of x, y, and z should satisfy the following conditions

$$G_{33} = -(G_{11} + G_{22}) \tag{3.17}$$

$$A_{111} = -\frac{A_{212} + A_{313}}{2} \tag{3.18}$$

$$A_{222} = -\frac{A_{112} + A_{323}}{2} \tag{3.19}$$

$$A_{333} = -\frac{A_{113} + A_{223}}{2} \tag{3.20}$$

If no-slip is assumed to be satisfied on the interface of the solid/fluid, then the appropriate boundary conditions are

$$\mathbf{v} = \mathbf{u} \quad \text{on} \quad S_d \tag{3.21}$$

and

$$\mathbf{v} = \mathbf{v}_\infty \quad \text{on} \quad r \to \infty \tag{3.22}$$

where S_d denotes the surface of the deformed sphere.

By using a similar method in chapter 2 [2], the three-scalar identities for a sphere with no-slip are

$$\sum_{n=-\infty}^{\infty} \left[\frac{n r_0}{2(2n+3)\mu} \left(\frac{r_0}{r}\right)^n p_n^{(i)} + \frac{n}{r_0} \left(\frac{r_0}{r}\right)^n \phi_n^{(i)} \right] = \frac{\mathbf{r}}{r} \cdot \mathbf{v}^{(i)} \tag{3.23}$$

$$\sum_{n=-\infty}^{\infty} \left[\frac{n(n+1) r_0}{2(2n+3)\mu} \left(\frac{r_0}{r}\right)^n p_n^{(i)} + \frac{n(n-1)}{r_0} \left(\frac{r_0}{r}\right)^n \phi_n^{(i)} \right] = -r\nabla \cdot \mathbf{v}^{(i)} \tag{3.24}$$

$$\sum_{n=-\infty}^{\infty} n(n+1) \left(\frac{r_0}{r}\right)^n \chi_n^{(i)} = \mathbf{r} \cdot \nabla \times \mathbf{v}^{(i)} \tag{3.25}$$

When the velocity field is prescribed at the surface of the sphere, $\mathbf{v}(r_0, \theta, \phi)$ is a given function and each of the functions appearing on the rightside of (3.23- 3.25) may be expanded in a series of surface harmonics as

$$\frac{\mathbf{r}}{r} \cdot \mathbf{v}(r_0, \theta, \phi) = \sum_{n=1}^{\infty} X_n(\theta, \phi) \tag{3.26}$$

$$-r\nabla \cdot \mathbf{v}(r_0, \theta, \phi) = \sum_{n=1}^{\infty} Y_n(\theta, \phi) \tag{3.27}$$

$$\mathbf{r} \cdot \nabla \times \mathbf{v}(r_0, \theta, \phi) = \sum_{n=1}^{\infty} Z_n(\theta, \phi) \tag{3.28}$$

For exterior problems, the following relations can be obtained for $n \geq 0$

$$p_{-(n+1)} = \frac{2n-1}{\mu}(n+1)r_0 \frac{r_0}{r}^{n+1} [(n+2)X_n + Y_n] \tag{3.29}$$

$$\phi_{-(n+1)} = \frac{r_0}{2(n+1)} \frac{r_0}{r}^{n+1} [nX_n + Y_n] \tag{3.30}$$

$$\chi_{-(n+1)} = \frac{1}{n(n+1)} \frac{r_0}{r}^{n+1} Z_n \tag{3.31}$$

Substituting (3.29)-(3.31) into Lamb's general solution for Stoke's equation (2.3), the velocity field of the fluids surrounding the particle may be written in the form

$$\mathbf{v} = \sum_{n=1}^{\infty} \left[\nabla \times (\mathbf{r}\chi_{-(n+1)}) + \nabla\phi_{-(n+1)} - \frac{(n-2)}{2n(2n-1)\mu} r^2 \nabla p_{-(n+1)} + \mathbf{r}\frac{(n+1)}{n(2n-1)\mu} p_{-(n+1)} \right] \tag{3.32}$$

and

$$p = \sum_{n=1}^{\infty} p_{-(n+1)} \tag{3.33}$$

By using (2.46) each component of the hydrodynamic force on the particle with consideration of the no-slip on the interface can be obtained as

$$\begin{aligned} F_x = {} & 6\pi r_0 \mu (v_{x0} - u_{x0})(1 - +\tfrac{2}{5}\varepsilon) + \pi r_0^3 \mu (2A_{122} + 2A_{133} - A_{212} - A_{313}) \\ & + \tfrac{1}{35}\pi r_0^3 \mu (-14A_{112} - 122A_{133} + 7A_{212} + 39A_{313})\varepsilon \end{aligned} \tag{3.34}$$

and

$$\begin{aligned} F_y = {} & 6\pi r_0 \mu (v_{y0} - u_{y0})(1 - \tfrac{2}{5}\varepsilon) + \pi r_0^3 \mu (-A_{112} + 2A_{211} + 2A_{233} - A_{323}) \\ & + \tfrac{1}{35}\pi r_0^3 \mu (7A_{112} - 14A_{211} - 122A_{233} + 39A_{323})\varepsilon \end{aligned} \tag{3.35}$$

and

$$F_z = 6\pi r_0\mu(v_{z0} - u_{z0})(1 - \tfrac{1}{5}\varepsilon) + \pi r_0^3\mu(-A_{113} - 2A_{223} + 2A_{311} + 2A_{322})$$

$$+\tfrac{1}{35}\pi r_0^3\mu(-2A_{113} - 2A_{223} + 32A_{311} + 32A_{322})\varepsilon \tag{3.36}$$

The hydrodynamic torque exerted on the particle by the surrounding fluids can be obtained by using (2.47)

$$\mathbf{T}^{\mathrm{T}} = 4\pi r_0^3\mu \begin{pmatrix} \tfrac{1}{5}[(-5G_{23} + 5G_{32} - 10\omega_x) + \varepsilon(11G_{23} - G_{32} + 12\omega_x)] \\ \tfrac{1}{5}[(5G_{13} - 5G_{31} - 10\omega_y) + \varepsilon(-11G_{13} + G_{31} + 12\omega_y)] \\ (-G_{12} + G_{21} - 2\omega_z) + \tfrac{3}{5}\varepsilon(G_{12} - G_{21} + 2\omega_z) \end{pmatrix} \tag{3.37}$$

If the particle is subjected to no external torques except those exerted by the fluid on its surface, the torque will be cancelled out at each instant. From (3.37), the angular velocities can be solved as

$$\omega_x = \frac{5(G_{23} - G_{32}) + (G_{32} - 11G_{23})\varepsilon}{-10 + 12\varepsilon} \tag{3.38}$$

$$\omega_y = \frac{5(G_{31} - G_{13}) + (11G_{13} - G_{31})\varepsilon}{-10 + 12\varepsilon} \tag{3.39}$$

$$\omega_z = \frac{1}{2}(-G_{12} + G_{21}) \tag{3.40}$$

From the equations of force and torque on the particle, it can been seen that the quadratic term and the constant term in the velocity field of the fluids only result in force on the particle while the hydrodynamic force is resulted from the linear term of the velocity field.

Compared with the homogeneous velocity field at infinity of the fluid in the chapter 3, **G** can also be decomposed by the symmetric and antisymmetric part, i.g. **S** and **W**,

$$\begin{pmatrix} G_{11} & G_{12} & G_{13} \\ G_{21} & G_{22} & G_{23} \\ G_{31} & G_{32} & G_{33} \end{pmatrix} = \begin{pmatrix} a & h & g \\ h & b & f \\ g & f & c \end{pmatrix} + \begin{pmatrix} 0 & -\zeta & \eta \\ \zeta & 0 & \xi \\ -\eta & \xi & 0 \end{pmatrix} \tag{3.41}$$

From (3.41), the angular velocity of the particle can be written as

$$\omega_x = -f\lambda + \xi, \quad \omega_y = g\lambda + \xi, \quad \omega_x = \zeta \tag{3.42}$$

in which

$$\lambda = \frac{5\varepsilon}{-5 + 6\varepsilon} \tag{3.43}$$

This equation is exact same as (2.91) for the no-slip problem. The flow-induced rotation motion of a particle suspended in quadratic flows is same as that the particle in homogeneous shear flows (constant gradient of the velocity field of the fluid).

3.2 Motion of an ellipsoid in a cubic flow field

3.2.1 The hydrodynamic resistance

To study the influence of cubic flow on the motion a particle, a cubic flow field far from a deformed sphere is investigated here, i.e.

$$\mathbf{v}_\infty = \begin{pmatrix} A_{1111} & A_{1112} & A_{1113} & A_{1123} & A_{1122} & A_{1133} & A_{1222} & A_{1223} & A_{1233} & A_{1333} \\ A_{2111} & A_{2112} & A_{2113} & A_{2123} & A_{2122} & A_{2133} & A_{2222} & A_{2223} & A_{2233} & A_{2333} \\ A_{3111} & A_{3112} & A_{3113} & A_{3123} & A_{3122} & A_{3133} & A_{3222} & A_{3223} & A_{3233} & A_{3333} \end{pmatrix} \tag{3.44}$$
$$\begin{pmatrix} x^3 & x^2y & x^2z & xyz & xy^2 & xz^2 & y^3 & y^2z & yz^2 & z^3 \end{pmatrix}^{\mathrm{T}}$$

Using (3.6)-(3.8), if $|\varepsilon|$ is a small number, the velocity field can be expanded by

$$\mathbf{v}_\infty^{(0)} = \begin{pmatrix} A_{1111} & A_{1112} & A_{1113} & A_{1123} & A_{1122} & A_{1133} & A_{1222} & A_{1223} & A_{1233} & A_{1333} \\ A_{2111} & A_{2112} & A_{2113} & A_{2123} & A_{2122} & A_{2133} & A_{2222} & A_{2223} & A_{2233} & A_{2333} \\ A_{3111} & A_{3112} & A_{3113} & A_{3123} & A_{3122} & A_{3133} & A_{3222} & A_{3223} & A_{3233} & A_{3333} \end{pmatrix} \tag{3.45}$$
$$\begin{pmatrix} x_{(0)}^3 & x_{(0)}^2 y_{(0)} & x_{(0)}^2 z_{(0)} & x_{(0)} y_{(0)} z_{(0)} & x_{(0)} y_{(0)}^2 & x_{(0)} z_{(0)}^2 & y_{(0)}^3 & y_{(0)}^2 z_{(0)} & y_{(0)} z_{(0)}^2 & z_{(0)}^3 \end{pmatrix}^{\mathrm{T}}$$

$$\mathbf{v}_\infty^{(1)} = 3f(\theta)\begin{pmatrix} A_{1111} & A_{1112} & A_{1113} & A_{1123} & A_{1122} & A_{1133} & A_{1222} & A_{1223} & A_{1233} & A_{1333} \\ A_{2111} & A_{2112} & A_{2113} & A_{2123} & A_{2122} & A_{2133} & A_{2222} & A_{2223} & A_{2233} & A_{2333} \\ A_{3111} & A_{3112} & A_{3113} & A_{3123} & A_{3122} & A_{3133} & A_{3222} & A_{3223} & A_{3233} & A_{3333} \end{pmatrix} \cdot$$

$$\begin{pmatrix} x_{(0)}^3 & x_{(0)}^2 y_{(0)} & x_{(0)}^2 z_{(0)} & x_{(0)} y_{(0)} z_{(0)} & x_{(0)} y_{(0)}^2 & x_{(0)} z_{(0)}^2 & y_{(0)}^3 & y_{(0)}^2 z_{(0)} & y_{(0)} z_{(0)}^2 & z_{(0)}^3 \end{pmatrix}^{\mathrm{T}} \quad (3.46)$$

$$\mathbf{v}_\infty^{(i)} = 0 \quad \text{when } i \geq 2 \quad (3.47)$$

For incompressible flow, to satisfy the continuity equation, it is required that

$$A_{2112} = -(3A_{1111} + A_{3113}) \quad (3.48)$$

$$A_{1122} = -(3A_{2222} + A_{3223}) \quad (3.49)$$

$$A_{2233} = -(3A_{3333} + A_{3113}) \quad (3.50)$$

$$A_{3123} = -2(A_{1112} + A_{2122}) \quad (3.51)$$

$$A_{2123} = -2(A_{1113} + A_{3133}) \quad (3.52)$$

$$A_{1123} = -2(A_{2223} + A_{3233}) \quad (3.53)$$

With a no-slip boundary condition, the hydrodynamic force and torque exerted on the particle are

$$\mathbf{F} = \mathbf{0} \quad (3.54)$$

$$\begin{aligned} T_x &= \frac{4}{25}\pi r_0^5 \mu[(-5 + 11\varepsilon)A_{2113} + (-5 + 11\varepsilon)A_{2223} + (-15 + 63\varepsilon)A_{2333} \\ &+ (5 - \varepsilon)A_{3112} + (15 + 3\varepsilon)A_{3222} + (5 - 11\varepsilon)A_{3233} + (-50 + 60\varepsilon)\frac{\omega_x}{r_0^2}] \end{aligned} \quad (3.55)$$

$$\begin{aligned} T_y &= -\frac{4}{25}\pi r_0^5 \mu[(-5 + 11\varepsilon)A_{1113} + (-5 + 11\varepsilon)A_{1223} + (-15 + 63\varepsilon)A_{1333} \\ &+ (15 - 3\varepsilon)A_{3111} + (5 - \varepsilon)A_{3122} + (5 - 11\varepsilon)A_{3133} + (50 - 60\varepsilon)\frac{\omega_y}{r_0^2}] \end{aligned} \quad (3.56)$$

$$T_z = \frac{4}{25}\pi r_0^5\mu[(-5+3\varepsilon)A_{1112} + (-15+9\varepsilon)A_{1222} + (-5+13\varepsilon)A_{1233} \tag{3.57}$$
$$+ (15-9\varepsilon)A_{2111} + (5-3\varepsilon)A_{2122} + (5-13\varepsilon)A_{2133} + (-50+30\varepsilon)\frac{\omega_z}{r_0^2}]$$

One possible induced angular velocity of the particle if no external torque applying on the particle can be obtained

$$\omega_x = \frac{r_0^2}{50-60\varepsilon}[(-5+11\varepsilon)A_{2113} + (-5+11\varepsilon)A_{2223} + (-15+63\varepsilon)A_{2333} \tag{3.58}$$
$$+(5-\varepsilon)A_{3112} + (15+3\varepsilon)A_{3222} + (5-11\varepsilon)A_{3233}]$$

$$\omega_y = \frac{r_0^2}{-50+60\varepsilon}[(-5+11\varepsilon)A_{1113} + (-5+11\varepsilon)A_{1223} + (-15+63\varepsilon)A_{1333} \tag{3.59}$$
$$+(15-3\varepsilon)A_{3111} + (5-\varepsilon)A_{3122} + (5-11\varepsilon)A_{3133}]$$

$$\omega_z = \frac{r_0^2}{50-30\varepsilon}[(-5+3\varepsilon)A_{1112} + (-15+9\varepsilon)A_{1222} + (-5+13\varepsilon)A_{1233} \tag{3.60}$$
$$+(15-9\varepsilon)A_{2111} + (5-3\varepsilon)A_{2122} + (5-13\varepsilon)A_{2133}]$$

3.2.2 Motion of a deformed sphere in a simple cubic flow

The motion of a deformed sphere in simple cubic flow, shown in Figure 3.2, is investigated. Described in the fixed coordinate system (x', y', z'), the velocity field far from the particle is assumed to be

$$\mathbf{v}'_\infty = \begin{pmatrix} 0 & 0 & Ky'^3 \end{pmatrix} \tag{3.61}$$

Induced by this cubic flow, the deformed sphere rotates around x (x') by angle α. In Figure 3.2, (x', y', z') is the fixed coordinate system and (x, y, z) the rotating coordinate system attached on the axis of the particle. Between these two coordinate systems, the

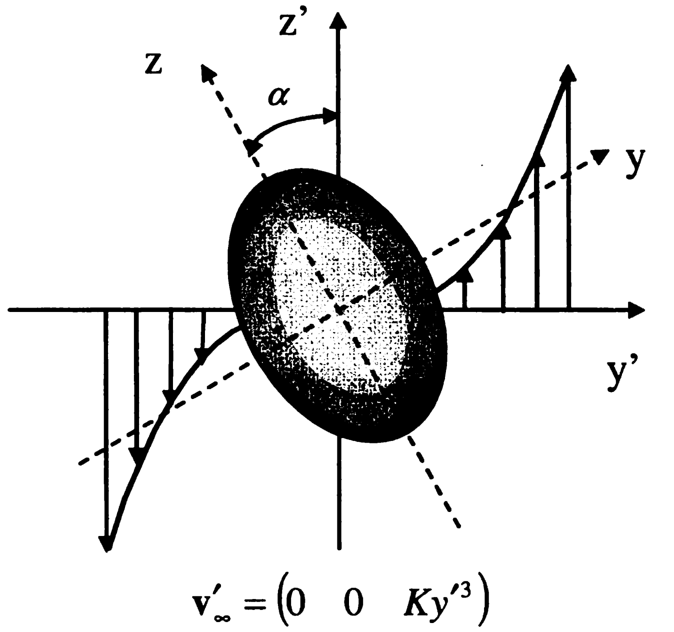

Figure 3.2. Illustration of a cubic flow field surrounding a deformed sphere.

following relation can be satisfied

$$\begin{pmatrix} x' \\ y' \\ z' \end{pmatrix} = \begin{pmatrix} 1 & 0 & 0 \\ 0 & \cos\alpha & -\sin\alpha \\ 0 & \sin\alpha & \cos\alpha \end{pmatrix} \begin{pmatrix} x \\ y \\ z \end{pmatrix} \tag{3.62}$$

According to the (2.78) between these two coordinate systems, i.e., the fixed coordinate system and the rotating coordinate system, the velocity of the surrounding fluid far away from the particle can be described in the rotating coordinate system as

$$\begin{aligned} \mathbf{v}_\infty &= \begin{pmatrix} 1 & 0 & 0 \\ 0 & \cos\alpha & \sin\alpha \\ 0 & -\sin\alpha & \cos\alpha \end{pmatrix} \mathbf{v}'_\infty \\ &= \begin{pmatrix} 1 & 0 & 0 \\ 0 & \cos\alpha & \sin\alpha \\ 0 & -\sin\alpha & \cos\alpha \end{pmatrix} \begin{pmatrix} 0 \\ 0 \\ Ky'^3 \end{pmatrix} \end{aligned} \tag{3.63}$$

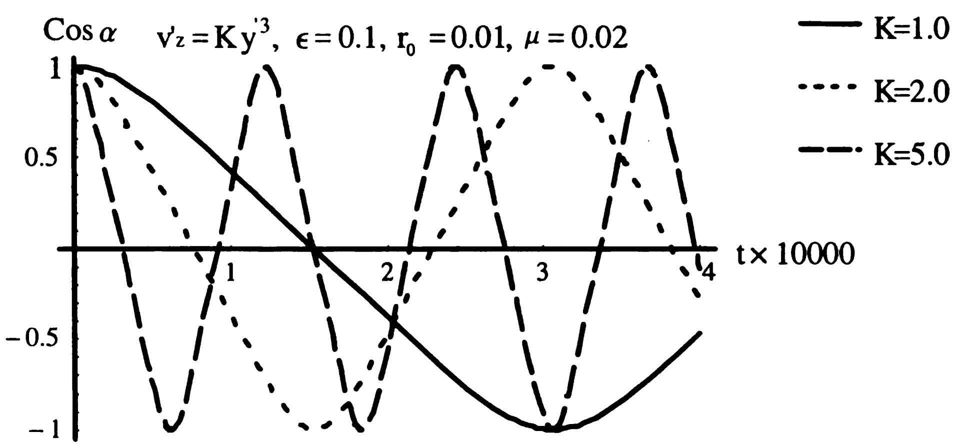

Figure 3.3. Evolution of the cosine of the rotation angle of the particle induced by simple cubic flows at different constant Ks.

From (3.62), then

$$\mathbf{v}_\infty = K\begin{pmatrix} 0 \\ \sin\alpha(\cos^3\alpha y^3 - 3\cos^2\alpha\sin\alpha y^2 z + 3\cos\alpha\sin^2\alpha yz^2 - \sin^3\alpha z^3) \\ \cos\alpha(\cos^3\alpha y^3 - 3\cos^2\alpha\sin\alpha y^2 z + 3\cos\alpha\sin^2\alpha yz^2 - \sin^3\alpha z^3) \end{pmatrix} \tag{3.64}$$

Comparing with (3.46), the following is obtained

$$\mathbf{v}_\infty = K\begin{pmatrix} 0&0&0&0&0&0&0&0&0&0 \\ 0&0&0&0&0&0&\sin\alpha\cos^3\alpha&-3\cos^2\alpha\sin^2\alpha&3\cos\alpha\sin^3\alpha&-\sin^4\alpha \\ 0&0&0&0&0&0&\cos^4\alpha&-3\cos^3\alpha\sin\alpha&3\cos^2\alpha\sin^2\alpha&-\cos\alpha\sin^3\alpha \end{pmatrix}$$
$$\begin{pmatrix} x^3 & x^2y & x^2z & xyz & xy^2 & xz^2 & y^3 & y^2z & yz^2 & z^3 \end{pmatrix}^{\mathrm{T}} \tag{3.65}$$

From (3.58)-(3.60), components of the angular velocity of the particle are

$$\omega_x = \dot{\alpha} = -\frac{3Kr_0^2[5 - \varepsilon(11 - 10\cos 2\alpha)]}{-50 + 60\varepsilon} \tag{3.66}$$

$$\omega_y = 0 \tag{3.67}$$

$$\omega_z = 0 \tag{3.68}$$

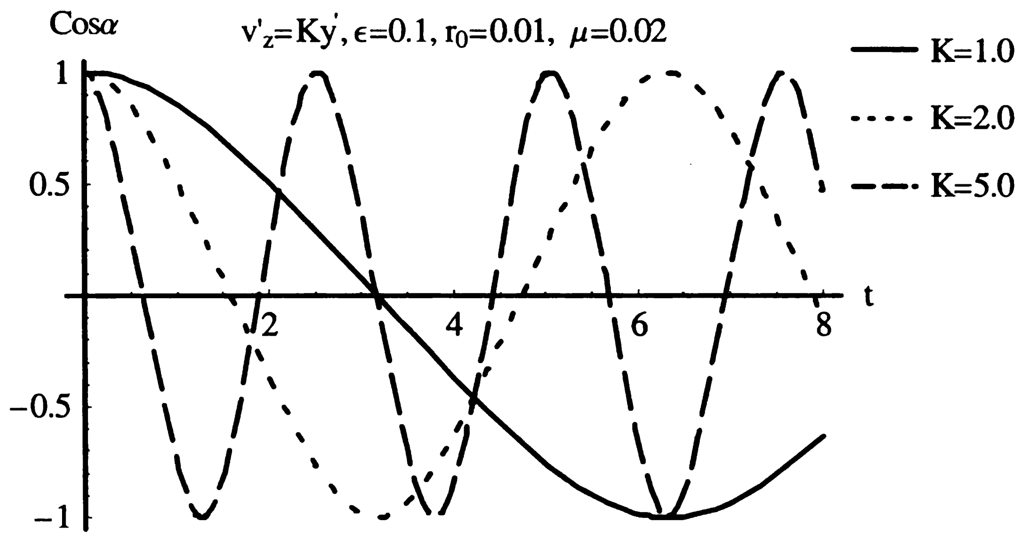

Figure 3.4. Evolution of the cosine of the rotation angle of the particle induced by simple shear flow at different constant Ks.

Integrating (3.66), the angle α is obtained

$$\alpha = \arctan\left[\sqrt{\frac{5-\varepsilon}{-5+21\varepsilon}}\tanh\left(\frac{3Kr_0}{10}\sqrt{\frac{21\varepsilon-5}{-5+\varepsilon}}\right)\right] \tag{3.69}$$

The evolution of cosine of the angle α is shown in Figure 3.3 at different Ks. It can be seen that the induced motions of the particle by a cubic flow is periodic. It is known that the induced motion of a deformed sphere in a homogeneous shear flow field is also periodic. In order to compare the difference of the two motions induced by a cubic flow and a simple

Table 3.1. Predicted periods of the particle motion induced by cubic flows and simple shear flows.

	$v_z' = Ky'^3$			$v_z' = Ky'$		
	K=1.0	K=2.0	K=5.0	K=1.0	K=2.0	K=5.0
period(s)	6000	3100	1250	12.50	6.40	2.56

shear flow, the period of each motion at different Ks are listed in the Table3.1 when other parameters are $\varepsilon = 0.1, r_0 = 0.01$, and $\mu = 0.02$. The periodic motion of the particle induced by the simple shear flow is shown in the Figure 3.4. From the Table 3.1, it can be seen that at the same K, periods of the induced motion by a cubic flow are much longer than those by simple shear flows. For both cases the period is proportional to the inverse of the coefficient K.

CHAPTER 4

POWER-LAW MODEL OF A DEFORMED SPHERE

4.1 Introduction

Newtonian fluids are investigated in the first four chapters, in which the viscosity is assumed to be a constant. In several industrial problems, polymeric liquids are involved and their viscosity is often dependent on the shear rate, temperature, pressure, etc. This chapter is devoted to studying the influence of a non-Newtonian viscosity on the motion of a particle.

4.2 Power-Law model for the Non-Newtonian viscosity

One of the earliest empiricism for Non-Newtonian fluids is based on the modification of Newton's law of the viscosity in which the viscosity is allowed to vary with the shear rate.

For example, for an arbitrary incompressible Newtonian fluid, $\mathbf{v} = \mathbf{v}(x, y, z)$, the constitutive equation is modelled as :

$$\boldsymbol{\tau} = -\mu\dot{\boldsymbol{\gamma}} \tag{4.1}$$

in which μ is a constant for a given temperature, pressure, and composition, $\dot{\boldsymbol{\gamma}}$ the rate-of-strain tensor $\frac{1}{2}[\nabla\mathbf{v} + (\nabla\mathbf{v})^{T}]$. To include the idea of a non-Newtonian viscosity, the constitutive equation is modified by

$$\boldsymbol{\tau} = -\eta\dot{\boldsymbol{\gamma}} \tag{4.2}$$

in which η is a function of the scalar invariants of $\dot{\boldsymbol{\gamma}}$.

There are three invariants for a second order tensor $\dot{\boldsymbol{\gamma}}$ as the following:

$$\mathrm{I} = \sum_i \dot{\gamma}_{ii} \tag{4.3}$$

$$\mathrm{II} = \sum_i \sum_j \dot{\gamma}_{ij}\dot{\gamma}_{ji} \tag{4.4}$$

$$\mathrm{III} = \sum_i \sum_j \sum_k \dot{\gamma}_{ij}\dot{\gamma}_{jk}\dot{\gamma}_{ki} \tag{4.5}$$

For an incompressible fluid $\mathrm{I} = 2(\nabla \cdot \mathbf{v}) = 0$. For shearing flows III turns out to be zero; Because (4.2) should be used only for shearing flows, or at least flows that are very nearly shearing, omitting III from any further consideration is not a serious restriction. Hence η is taken to depend only on II. In practice, $\dot{\gamma}$, the magnitude of the rate-of-strain tensor $\dot{\boldsymbol{\gamma}}$, is often used instead of II, i.e.

$$\dot{\gamma} = \sqrt{\frac{1}{2}\sum_i \sum_j \dot{\gamma}_{ij}\dot{\gamma}_{ji}} = \sqrt{\frac{1}{2}\mathrm{II}} \tag{4.6}$$

Experimentally, a typical viscosity vs shear-rate curve is shown in Figure 4.1. It is composed of two regions, a zero-shear-region and a power-law-region. In the zero-shear-region (low shear rate), the shear stress is proportional to $\dot{\gamma}$, and the viscosity approaches a

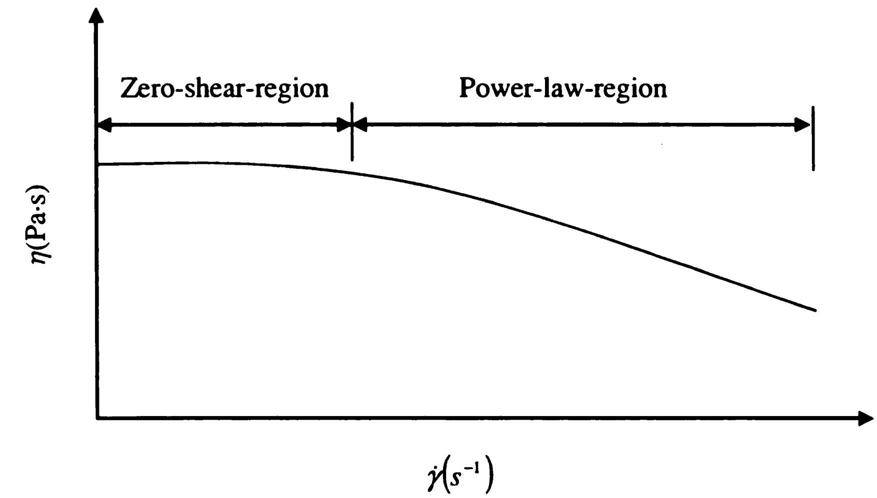

Figure 4.1. Schematic of a typical viscosity variation w.r.t to the shear rate.

constant value η_0, the *zero-shear-rate viscosity*. At the power-law-region (the higher shear rate), the viscosity decreases with increasing shear rates.

Two models for the viscosity $\eta(\dot{\gamma})$ are often used to describe the viscosity in term of shear rate [77]. The first one is the Carreau-Yasuda model. The Carreau-Yasuda model is a five-parameter model, which has sufficient flexibilities to fit a wide variety of experimental $\eta(\dot{\gamma})$ curves. The model is

$$\frac{\eta - \eta_\infty}{\eta_0 - \eta_\infty} = [1 + (\lambda\dot{\gamma})^a]^{(n-1)/a} \tag{4.7}$$

Here η_0 is the zero-shear-rate viscosity, η_∞ is the infinite-shear-rate viscosity, λ is a time constant, n is the "power-law exponent"(since it describes the slope of $\frac{\eta - \eta_\infty}{\eta_0 - \eta_\infty}$ in the "power-law region", and a is a dimensionless parameter that describes the transition region between the zero-shear-rate region and the power-law region. In most industrial problems, the descending linear region (the "power-law-region") shown in Figure 4.1 is more important. The titled straight line can be expressed simply by

$$\eta = m\dot{\gamma}^{n-1} \tag{4.8}$$

which contains two parameters: m (with units of $Pa \cdot s^n$), and n (dimensionless). (4.8) can be regarded as the limiting expression for high shear rates obtained from (4.7) with $\eta_\infty = 0$. When $n = 1$ and $m = \mu$, a Newtonian fluid is recovered. When $n < 1$, the fluid is said to be "pseudoplastic" or "shear thinning". When $n > 1$, the fluid is called "dilatant" or "shear thickening".

4.3 Solution to flow problems using a Power-Law model

Since the viscosity depends on the strain rate of the flow field, the Stokes' equations to govern the motion of the fluid will be nonlinear. It is not feasible to get an analytical solution for such nonlinear equations. Assume that the viscosity of the fluid is locally constant. Solutions obtained from the linear Stokes equations (with constant viscosity) can be used to get the hydrodynamic force and torque on the particle approximately (see Chapter 2 and Chapter 3). The hydrodynamics force on the surface of the sphere is given by

$$\mathbf{F} = \int\int \boldsymbol{\tau} \cdot d\mathbf{S} \tag{4.9}$$

where $\boldsymbol{\tau}$ is the stress dyadic and $d\mathbf{S}$ is a directed element of surface area parallel to the outer normal direction. By using the divergence theorem, the hydrodynamic force exerted by the fluid can be written in the form

$$\mathbf{F} = \int_{S_1} \mathbf{P}_r r^2 d\Omega \tag{4.10}$$

where $\mathbf{P}_r = \boldsymbol{\tau} \cdot \mathbf{r}/r$ is the stress vector acting across the surface, r = constant and $d\Omega = \sin\theta d\theta d\phi$ is an element area on the surface of a sphere of a unit radius, S_1. The hydrodynamic torque applying on the surface of the sphere is

$$\mathbf{T} = \int \mathbf{r} \times \boldsymbol{\tau} \cdot \mathbf{r}/r d\Omega \tag{4.11}$$

Substituting (4.2) and (4.8) into (4.10) and ((4.11), the force and torque will be

$$\mathbf{F} = \int m\dot{\gamma}^{n-1}\dot{\boldsymbol{\gamma}} \cdot \mathbf{r}/r d\Omega \tag{4.12}$$

$$\mathbf{T} = \int \mathbf{r} \times m\dot{\gamma}^{n-1}\dot{\boldsymbol{\gamma}} \cdot \mathbf{r}/r d\Omega \tag{4.13}$$

(1) **A fixed sphere in a uniform stream flow**

A sphere is fixed in a space and a uniform streaming flow passes by the sphere at the velocity $U\mathbf{e}_x$. By using (4.12) and (4.13), the hydrodynamic force and torque on the sphere are

$$\mathbf{F} = \begin{cases} \dfrac{9m\pi U^3}{8r_0} & n = 3 \\ \\ \dfrac{81m\pi U^5}{320r_0^3} & n = 5 \\ \\ \dfrac{2187m\pi U^7}{35840r_0^5} & n = 6 \end{cases} \tag{4.14}$$

and

$$\mathbf{T} = \mathbf{0} \tag{4.15}$$

(2) **A fixed spheroid in a uniform stream flow**

When a spheroid with deformation coefficient ε is fixed in a uniform flow at velocity $U\mathbf{e}_x$. The geometry function of the spheroid is same as (2.49). By using (4.12) and (4.13), the hydrodynamic force and torque can be obtained when $n = 3$

$$\mathbf{F} = \left[\frac{9m\pi U^3}{8r_0} + 13.4181\frac{m\pi U^3}{8r_0}\varepsilon + O(\varepsilon^2)\right]\mathbf{e}_x \tag{4.16}$$

and

$$\mathbf{T} = \mathbf{0} \tag{4.17}$$

If the velocity field of the fluid at the infinity is $W\mathbf{e}_z$, when $n = 3$ the hydrodynamic force and torque are

$$\mathbf{F} = \left[\frac{9m\pi W^3}{8r_0} - 0.9366\frac{m\pi W^3}{8r_0}\varepsilon + O(\varepsilon^2)\right]\mathbf{e}_z \tag{4.18}$$

and

$$\mathbf{T} = \mathbf{0} \tag{4.19}$$

(3) **A free spheroid in a homogeneous shear flow**

The far away velocity field of the fluid is assumed to be simple shear, e.g. $\mathbf{v}' = Ky'\mathbf{e}_z$, which is described in the fixed coordinate system. Suppose that initially the long axis of the particle is parallel to the z' axis [seen Figure 2.5]. Due to the nonlinear property of this problem there may be multiple solutions for the induced motion of the spheroid. In order to make this problem solvable a hypothesis is introduced here, which is that the particle can rotate around the x axis and the other angular velocity $\omega_y = \omega_z = 0$. According to this hypothesis the distortion and the rotation of the fluid described in the rotating coordinate system which is attached on the particle can be written in the form

$$\mathbf{S} = \begin{pmatrix} 0 & 0 & 0 \\ 0 & b & f \\ 0 & f & -b \end{pmatrix} \tag{4.20}$$

and

$$\mathbf{W} = \begin{pmatrix} 0 & 0 & 0 \\ 0 & 0 & -\xi \\ 0 & \xi & 0 \end{pmatrix} \tag{4.21}$$

in which

$$b = \frac{1}{2}K\sin 2\alpha, \ f = \frac{1}{2}K\cos 2\alpha, \ \text{and } \xi = -K/2 \tag{4.22}$$

The hydrodynamic force and torque exerted by the surrounding fluid on the spheroid can be obtained as

$$F_x = \frac{m\pi r_0^2\varepsilon}{18018}[(292328K^3+569868K^2\omega_x+1287K(253\omega_x^2-149\omega_y^2)+34749\omega_x(\omega_x^2+\omega_y^2)] \tag{4.23}$$

$$\begin{aligned} F_y = \quad & \frac{m\pi r_0^2}{14}[388K^2\varepsilon\omega_y + 3(\omega_x^2+\omega_y^2)(9\varepsilon\omega_y + 14\omega_x\log 2) \\ & +K(402\varepsilon\omega_x\omega_y + 56(\omega_x^2+\omega_y^2)\log 2] \end{aligned} \tag{4.24}$$

$$\begin{aligned} F_z = \quad & \frac{-m\pi r_0^2\varepsilon\omega_y}{441548800}\{+8316[(7897088+214865\pi)\omega_x^2 - 102400\omega_y^2]\omega_x \\ & +K^2(158195474432+5729848905\pi) \\ & +924K(222636032+7061595\pi)\} \end{aligned} \tag{4.25}$$

and

$$\begin{aligned} T_x \ = \ & \left[-bm\pi r_0^3\varepsilon(33938801875b^2 + 3(14079425275f^2- \right. \\ & \left. -7702408035f(\xi-\omega_x)) + 3976823046(\xi-\omega_x)^2)\right]/386260875 \end{aligned} \tag{4.26}$$

$$T_y = 0 \tag{4.27}$$

$$T_z = 0 \tag{4.28}$$

If there is no external torque applying on the spheroid, two possible induced motions of the spheroid are

$$\omega_x = -0.9684f \pm 1.6132\sqrt{(-1.0930b^2 - f^2)} + \xi \tag{4.29}$$

$$\omega_y = 0 \tag{4.30}$$

$$\omega_z = 0 \tag{4.31}$$

Substituting (4.22) into (4.29), it can be obtained

$$\omega_x = -0.9684f \pm 0.8066\sqrt{(-1 - 0.093\sin^2 2\alpha)} - K/2 \tag{4.32}$$

From above equation it can be seen that the induced angular velocity of the particle is a complex number. The reasons to result in a complex angular velocity may be from two hypophyses: one hypophysis is that the local viscosity is assumed to be constant when solving the Stokes' equation by Brenner's method; and another one supposes that the particle just rotates along the axis x. Due to the complexity of this problem, some other model to describe the property of Non-Newtonian flow will be sought in the future work.

CHAPTER 5

MOTION OF A SPHEROID IN AN OSEEN FLOW

5.1 Introduction

It is well-know by the Stokes' law, that a force of $6\pi\mu Wa$ is required to maintain a uniform velocity W of a sphere of radius a moving through a liquid with viscosity μ. However, this result can not apply to the cases which arise in practice to deal with, for example, the motion of ships. A mathematical incompleteness of the solution is because the advective terms are not negligible compared to the viscous terms at large distances. From Chapter 2, the large viscous term is of the order

$$\text{viscous force} \;=\text{stess gradient} \;\sim \frac{\mu Ua}{r^3} \quad \text{as } r \to \infty \tag{5.1}$$

while the largest inertia force is

$$\text{inertia force} \;\sim \rho u_r \frac{\partial u_\theta}{\partial r} \sim \frac{\rho U^2 a}{r^2} \quad \text{as } r \to \infty \tag{5.2}$$

Therefore

$$\frac{\text{inertia force}}{\text{viscous force}} \sim \frac{\rho U a}{\mu}\frac{r}{a} = Re\frac{r}{a} \quad \text{as } r \to \infty \tag{5.3}$$

It can be seen that the inertia forces are not negligible for distances larger than $r/a \sim 1/Re$. The neglected terms become arbitrarily large at sufficiently large distances, on matter how small Re may be [78].

Several attempts have been made to correct this error. In 1893, Rayleigh introduced some additional forces to improve the accuracy of the Stokes' solution. In 1911, Oseen proposed a modified system of equations, in which the inertia terms are partly taken into account, and obtained the solution for flow past a fixed sphere using these equations. Oseen's solution is satisfied at infinity; it also gives good approximation near the sphere if the velocity or the radius of the sphere is small. Lamb [6], used a different method to present Oseen's solution, but it still can not overcome the restriction of Oseen's. Burgess [3] used a simpler method than that of either Oseen or Lamb. The solution from Burgess method can satisfy the boundary conditions at infinity and the boundary conditions on the sphere can be satisfied to any desired degree of approximation. Afterwards, solutions of Oseen's equation have been extended to the spinning sphere [79], circular cylinder [80–83], circular and elliptic cylinders [84–86] and flat plate [84, 87].

5.2 Analytical structure of the Oseen flow

Derived by Burgess [3], the motion equation of a viscous flow in the cylinder coordinate system is

$$(-W\frac{\partial}{\partial z} - \nu \mathrm{D})\mathrm{D}\psi = 0 \tag{5.4}$$

in which W is the velocity of the particle $\nu = \mu/\rho$ is the kinetic viscosity of the fluid, and $\mathrm{D} \equiv \frac{\partial^2}{\partial r^2} - \frac{1}{r}\frac{\partial}{\partial r} + \frac{\partial^2}{\partial z^2}$.

Due to the commutativity of this equation, a solution can be given as

$$\psi = \psi' + \psi'' \tag{5.5}$$

where

$$\mathrm{D}\psi' = 0 \tag{5.6}$$

and

$$(\nu\mathrm{D} + W\frac{\partial}{\partial z})\psi'' = 0 \tag{5.7}$$

Solving above partial differential equations by using a perturbation method, the stream function of the Oseen flow is obtained by Burgess as

$$\begin{aligned}\psi = \quad & e^{-k\rho(1+\cos\theta)}\left[C + D\cos\theta + b_1\sin^2\theta(k+\frac{1}{\rho}) + b_2\sin^2\theta\cos\theta(k^2+\frac{3k}{\rho}+\frac{3}{\rho^2}) + \cdots\right] \\ & L\cos\theta + \frac{M\sin^2\theta}{\rho} + \frac{N\sin^2\theta\cos\theta}{\rho^2} + \frac{P\sin^2\theta}{\rho^3}(5\cos^2\theta - 1) + \cdots\end{aligned} \tag{5.8}$$

in which $\rho = \sqrt{r^2+z^2}$ and $\theta = \cos^{-1}\frac{z}{r^2+z^2} = \sin^{-1}\frac{r}{\sqrt{r^2+z^2}}$. Constants in the stream function can be fixed by suitable boundary conditions. From the stream function the radial velocity and tangential velocity of the fluid can be easily obtained as

$$v_\rho = \frac{1}{\rho^2\sin\theta}\frac{\partial\psi}{\partial\theta} \tag{5.9}$$

and

$$v_\theta = -\frac{1}{\rho\sin\theta}\frac{\partial\psi}{\partial\rho} \tag{5.10}$$

The normal and shear stress in the fluid are

$$\sigma_{\rho\rho} = 2\mu\frac{\partial v_\rho}{\partial\rho} \tag{5.11}$$

$$\sigma_{\theta\theta} = 2\mu\left(\frac{1}{\rho}\frac{\partial v_\theta}{\partial \theta} + \frac{v_\rho}{\rho}\right) \tag{5.12}$$

$$\sigma_{\phi\phi} = 2\mu\left(\frac{1}{\rho\sin\theta}\frac{\partial v_\phi}{\partial \phi} + \frac{v_\rho}{\rho} + \frac{v_\theta\cot\theta}{\rho}\right) \tag{5.13}$$

$$\tau_{\rho\theta} = 2\mu\left(\rho\frac{\partial}{\partial \rho}(\frac{v_\theta}{\rho}) + \frac{1}{\rho}\frac{\partial v_\rho}{\partial \theta}\right) \tag{5.14}$$

Two kinds of boundary conditions can be applied on the interface of the particle and fluids.

(1) No-slip Boundary conditions on the particle

$v_\rho = 0, v_\theta = 0$ at Infinity

$v_\rho = 0, v_\theta = 0$ on the surface of the particle

(2) Slip Boundary conditions on a symmetric particle

$v_\rho = 0, v_\theta = 0$ at Infinity

$v_\rho = u_\rho$ and $v_\theta - u_\theta = \frac{1}{\beta}\tau_{\rho\theta}$ on the surface of the of the particle

5.3 Applications of Burgess's solution

A simple form of stream functions of Oseen flows is used as

$$\psi = e^{-k\rho(1+\cos\theta)}b - 0(1-\cos\theta) + L\cos\theta + \frac{M\sin^2\theta}{\rho} \tag{5.15}$$

A symmetric particle moves in a quiescent fluid with a velocity W in the z direction with different boundary conditions and different shapes of the particle. Described in Figure 5.1 the radial and tangential velocity velocities on the surface of the particle are

$$u_\rho = W\cos\theta, u_\theta = -W\sin\theta \tag{5.16}$$

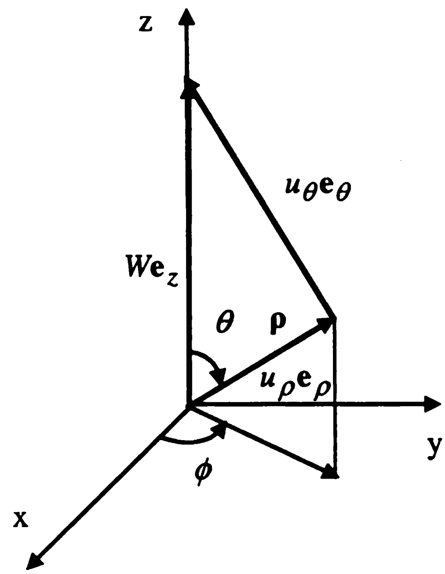

Figure 5.1. Description of the surface velocity of the particle.

Applying slip and nonslip boundary conditions and taking account of different shapes of the particle, several solutions are obtained as the following:

Case I Uniform motion of a sphere in Oseen flow with nonslip boundary condition

Solutions of this case have been already given by Burgess as [3]

$$L = b_0 = -\frac{3aW}{4k}, M = \frac{Wa^3}{4} \tag{5.17}$$

in which a is the radius of the sphere, $k = 2\mu/\rho$. The velocity field of the fluid around the sphere with no-slip boundary conditions is shown in the Figure 5.2(a).

Case II Uniform motion of a sphere in Oseen flows with slip boundary conditions

If the production of ak is a small number, i.e. a is small or/and k is small, the term $e^{-ak(1+\cos\theta)}$ can be expanded by series with neglecting the higher order terms of ak as

$$e^{-ak(1+\cos\theta)} \approx 1 - ak(1 + \cos\theta) \tag{5.18}$$

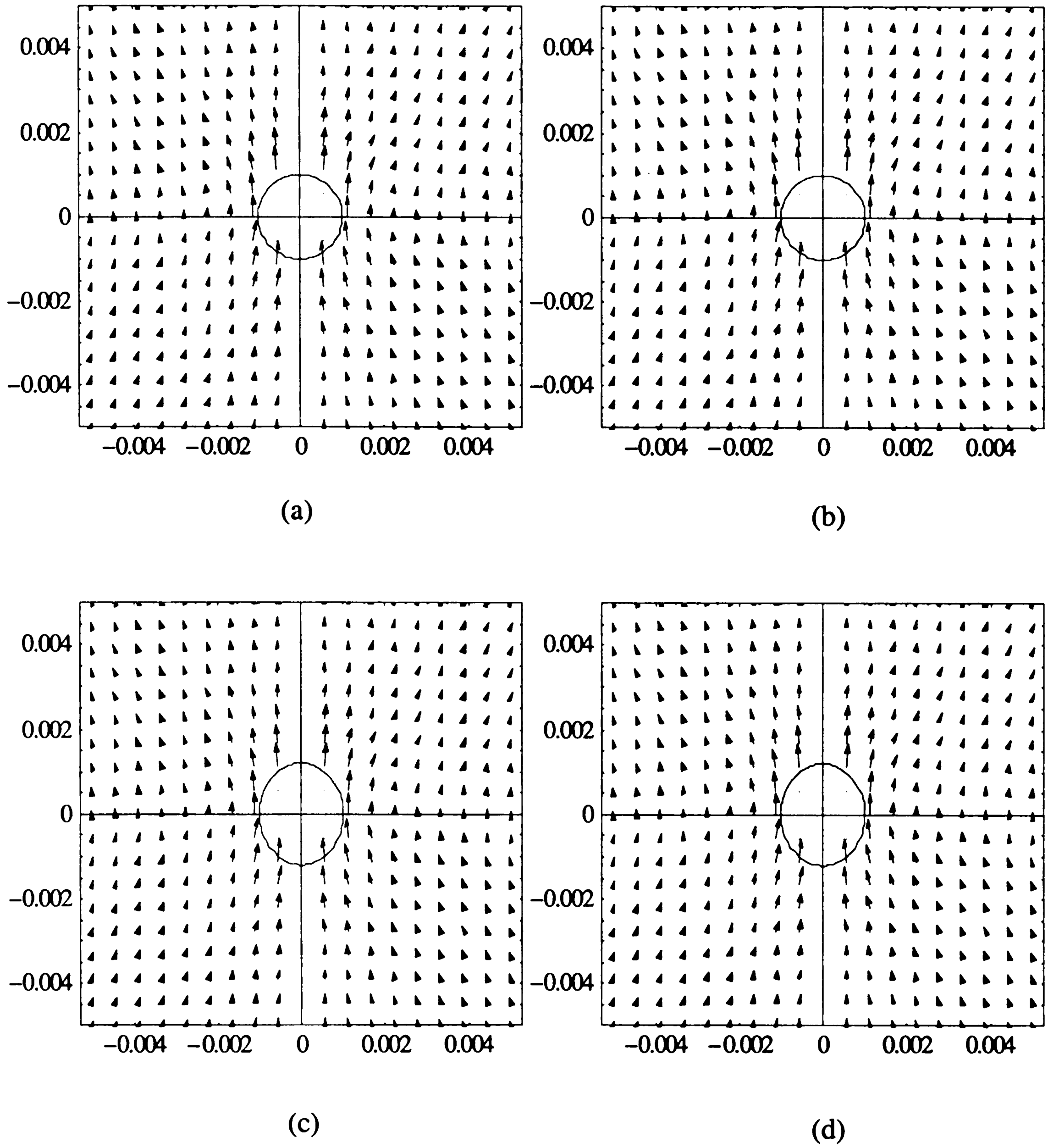

Figure 5.2. Velocity vectors of the surrounding fluids with different boundary condition on the surface of a particle. (a) no-slip boundary condition applying on a sphere; (b) slip boundary condition applying on a sphere($\beta = 0.1$); (c) no-slip boundary condition applying on a deformed sphere($\varepsilon = 0.2$); (d) slip boundary condition applying on a deformed sphere($\varepsilon = 0.2, \beta = 0.1$).

Substituting (5.15) into (5.9), (5.10), and (5.14), the radial and tangential velocities, and the shear stress of the fluid on the surface of the particle with neglecting the higher order terms of ak can be written as

$$v_\rho\big|_{\rho=a} \approx -\frac{L}{a^2} + \frac{2M\cos\theta}{a^3} + \frac{b_0}{a^2}(1 - 2ak\cos\theta) \tag{5.19}$$

$$v_\theta\big|_{\rho=a} \approx \frac{M\sin\theta}{a^3} + \frac{b_0 k\sin\theta}{a} \tag{5.20}$$

$$\tau_{\rho\,\theta}\big|_{\rho=a} \approx -\frac{6\mu M\sin\theta}{a^4} \tag{5.21}$$

Applying the slip boundary conditions on the sphere to determined the constants in the stream function, the following relations can be obtained

$$W\cos\theta = -\frac{L}{a^2} + \frac{b_0}{a^2} + (\frac{2M}{a^3} - \frac{2b_0 k}{a})\cos\theta \tag{5.22}$$

$$\frac{M\sin\theta}{a^3} + \frac{b_0 k\sin\theta}{a} + W\sin\theta = -\frac{6\mu M\sin\theta}{\beta a^4} \tag{5.23}$$

Equate the constant terms and the coefficients of $\cos\theta$ and $\sin\theta$ and each side of (5.22) and (5.23), then

$$\begin{cases} \dfrac{M}{a^3} + \dfrac{b_0 k}{a} + W = -\dfrac{6\mu\beta M}{a^4} \\[2ex] L = b_0 \\[2ex] \dfrac{2M}{a^3} - \dfrac{2b_0 k}{a} = W \end{cases} \tag{5.24}$$

Solving the above equations, the constants of the stream function are

$$L = b_0 = -\frac{3(a^2 W\beta + 2aW\mu)}{4k(a\beta + 3\mu)}, M = -\frac{a^4 W\beta}{4(a\beta + 3\mu)} \tag{5.25}$$

When $\beta \to \infty$, slip boundary conditions change into the nonslip boundary conditions. From the solution above letting $\beta \to \infty$ will result in the following constants

$$L = b_0 = -\frac{3aW}{4k}, M = \frac{Wa^3}{4} \tag{5.26}$$

These constants are exactly same as those solved by using nonslip boundary conditions. The velocity field of the fluid around the sphere with slip boundary condition is shown in the Figure 5.2(b).

Case III Uniform motion of a slightly deformed sphere with no slip on the interface

A spheroid, regarded as a deformed sphere, moves in a viscous fluid with the velocity W in the z direction. The shape function of a spheroid is

$$\frac{x^2+y^2}{a^2}+\frac{z^2}{a^2(1-\varepsilon)^2}=1 \tag{5.27}$$

If ε is a small number, the shape of the spheroid can be described in a polar form with neglecting the terms of $O(\varepsilon^2)$ as

$$\rho = a(1-\varepsilon\cos^2\theta) \tag{5.28}$$

For the nonslip boundary conditions by using Burgess's solution, it can be obtained

$$L = b_0 = -\frac{3Wa(1-\varepsilon)}{4(1-2\varepsilon)k} \tag{5.29}$$

and

$$M = -\frac{a^3W(1+\varepsilon)}{4(1-2\varepsilon)} \tag{5.30}$$

Expanding these constants by series of ε, the constants can be expressed as

$$L = b_0 = -\frac{3aW}{4k}-\frac{3aW\varepsilon}{4k}-\frac{3aW\varepsilon^2}{2k}+O(\varepsilon^3) \tag{5.31}$$

and

$$M = -\frac{a^3W}{4}-\frac{3a^3W\varepsilon}{4}-\frac{3a^3W\varepsilon^2}{2}+O(\varepsilon^3) \tag{5.32}$$

From (5.31, 5.32) it can be seen that when $\varepsilon \to 0$, the constants solved for this case are exactly same as the constants solved for the nonslip sphere problem (Case I). The velocity field of the fluid around a deformed sphere with no-slip boundary condition is shown in the Figure 5.2(c).

Case IV Uniform motion of a deformed sphere with slip on the interface

Applying the slip boundary conditions on the interface of the spheroid, the constants can be obtained

$$L = b_0 = \frac{3W(a^2\beta + 2a\mu)}{2k(-2a\beta + a\varepsilon\beta - 6\mu + 4\varepsilon\mu)}, \tag{5.33}$$

and

$$M = \frac{a^3W(a\beta + a\varepsilon\beta + 4\varepsilon\mu)}{2(-2a\beta + a\varepsilon\beta - 6\mu + 4\varepsilon\mu)} \tag{5.34}$$

When $\beta \to \infty$,

$$L = b_0 = -\frac{3aW}{2k(2+\varepsilon)} = -\frac{3aW}{4k} - \frac{3aW\varepsilon}{8k} - \frac{3aW\varepsilon^2}{16k} + O(\varepsilon^3) \tag{5.35}$$

and

$$M = \frac{a^3W(1+\varepsilon)}{2(-2+\varepsilon)} = -\frac{a^3W}{4} - \frac{3a^3W\varepsilon}{8} - \frac{3a^3W\varepsilon^2}{16} + O(\varepsilon^3) \tag{5.36}$$

Because both ak and ε are small numbers, the errors between these solutions and the solutions for case III are negligible.

Let $\beta \to \infty$ and $\varepsilon = 0$. The constants will be

$$L = b_0 = -\frac{3aW}{4k}, M = \frac{Wa^3}{4} \tag{5.37}$$

which are the same constants for the first case. The velocity field of the fluid around a deformed sphere with slip boundary conditions is shown in the Figure 5.2(d). It can be seen that the difference of the velocity field around the particle with considering slip and no-slip boundary conditions is small.

5.4 Summary

Uniform motions of a particle through a viscous flow are solved analytically by using Burgess' general solution for the Oseen flow. Nonslip and slip boundary conditions are considered on the interface of the particle and the fluid respectively. Two kinds of geometry of the particle, e.g. a sphere and a slightly deformed sphere, are studied. Four cases are calculated respectively according to different boundary conditions on the interface and the shape of the particle, e.g. (1) the motion of a sphere with nonslip, (2) the motion of a sphere with slip, (3) the motion of a deformed sphere with noslip, and (4) the motion of a deformed sphere with slip. Both of the solution of the case (2) and case (3) can recover the solution of case (1) when letting the slip coefficient β and deformation coefficient ε equal to zeros correspondingly. The error between the solution of case (4) when the slip coefficient goes to ∞ and that of case (3) is negligible if when the velocity and the diameter of the particle are small. The boundary condition at the infinity are satisfied well and the boundary condition at the interface can be approximated satisfied if the length dimension of the particle or the velocity of the particle is small.

CHAPTER 6

THE FLOW-INDUCED ORIENTATION OF RIGID PARTICLES IN DILUTE SUSPENSIONS

6.1 Introduction

The prediction of the flow and orientation of suspensions during the processing of composite materials is important to understand how the processing conditions influence the mechanical properties of the final part. A variety of models and algorithms have been made to derive the relationships between processing conditions and orientation of fibers [39, 73, 88–97]. If the particle is axisymmetric and the diameter is much less than the length of the particle, a unit vector $\mathbf{p}$, collinear with the long axis of the particle, can be used to represent the orientation of the particle. Only two Euler angles are related with this vector $\mathbf{p}$ by

$$\mathbf{p} = (\sin\theta\cos\phi \quad \sin\theta\sin\phi \quad \cos\theta)^{\mathrm{T}}. \tag{6.1}$$

Two methodologies are often used to describe the flow-induced alignments of particles. One is based on an orientation distribution function N, which is a function of Euler angles and time, and the other one uses an ensemble average orientation tensor $<\mathbf{pp}>$ or $<\mathbf{RR}>$. For spheroids, the orientation distribution function N can be defined over a state space of orientation vectors $\mathbf{p}$ and N is also related to the aspect ratio of the particle, i. c. $\frac{c}{a}$. For ellipsoids, N can be defined over a state space of rotation operators $\mathbf{R}$, and N depends on two aspect ratios $\frac{c}{a}$ and $\frac{b}{a}$ as well. Comparing with the distribution function method, the averaged orientation tensor method is often preferred but a closure problem arises due to the averaging procedure [98, 98–103].

Efforts have also been focused on the motion of non-axisymmetric particles suspended in a slow viscous flow. The classic work pertaining to the motion of a particle, e.g. an ellipsoid, in a uniform shear flow can be tracked back to the work of Jeffery's [1]. In his paper, the behavior of an ellipsoid suspending in uniform shear flow field is analyzed on basic of Stokes' equations of motions. Some previous authors [8, 69–71, 104] extended Jeffery's work to a more general shape particle.

The orientation distribution function for rigid ellipsoidal particles in a simple shear flow was given by Workman and Hollingsworth [105] in terms of a series of spherical harmonics by expressing the coefficients in these series in the Feenberg perturbation form.

In both Brenner [71] and Workman's (1969) work [105], Euler angles are used to represent the orientation of the particle. Rallison [106] proposed a rotation matrix to represent the orientation of the particles instead of using the Euler-angle representation. Considering the influence of Brownian motions, Rallison [106] derived the time evolution of the orientation probability distribution on the basic of Fokker-Planck equation and obtained the form of the orientation probability distribution for small departures from an isotropy state. The second-order moment of the probability distribution was also developed in Rallison's paper [106].

In this chapter, a new closure model is developed for the motion of rigid particles of complex shapes. Each particle is non-axisymmetric and its orientation is described with a second order tensor $< \mathbf{R} >$. An evolution equation for the second moment of the distribution function, which forms a fourth order tensor $< \mathbf{RR} >$, is used in order to obtain the average orientation of the particles in homogeneous flows.

6.2 Prediction of orientation of axisymmetric particles

Due to large amount fibers encountered in many applications, an approach based on a distribution function is preferred to predict fiber orientation. The distribution function is $\psi(\mathbf{p}, t)$ where $\mathbf{p}$ is a unit vector along the axis of each fiber to represent its orientation. The governing equation for $\psi(\mathbf{p}, t)$ depends on the conservation of fiber orientations. In homogenous flows with neglecting Brownian motions, it is given by [95]

$$\frac{D\psi}{Dt} = -\frac{\partial}{\partial \mathbf{p}} \cdot (\dot{\mathbf{p}}\psi) \tag{6.2}$$

The flow-induced motion of a single spheroid in the uniform shear flow is derived by

Jeffery [1] as

$$\dot{\mathbf{p}}_J = -\mathbf{W}\cdot\mathbf{p} + \lambda(\mathbf{S}\cdot\mathbf{p} - \mathbf{S}:\mathbf{ppp}) \tag{6.3}$$

where $\mathbf{W}$ is the vorticity tensor and $\mathbf{S}$ the strain rate of the flow fields. With considering the rotary diffusion due to the particle-particle interaction, the following hypothesis is used [77,95,107]

$$(\dot{\mathbf{p}} - \dot{\mathbf{p}}_J)\psi = -D_R\frac{\partial\psi}{\partial\mathbf{p}} \tag{6.4}$$

in which D_R is the rotary diffusion coefficient. Combining (6.2) - (6.4), the evolution equation for the distribution function can be derived as

$$\frac{D\psi}{Dt} = -\frac{\partial}{\partial\mathbf{p}}\cdot[\mathbf{W}\cdot\mathbf{p} + \lambda(\mathbf{S}\cdot\mathbf{p} - \mathbf{S}:\mathbf{ppp})] + \frac{\partial}{\partial\mathbf{p}}\cdot D_R\frac{\partial\psi}{\partial\mathbf{p}} \tag{6.5}$$

This approach can represent the exact and full solution for fiber orientations [108, 109]. However, this partial-differential-equation is not analytically solvable for a general problem. Furthermore, using numerical calculations this method is still too complex when solving three-dimensional fiber orientational in complex geometries.

An alternative approach is to use a more compact description of the distribution function. A second-order tensor $\mathbf{a}$ is often used to represent the fiber orientation state at any point in the material. This tensor is defined as

$$\mathbf{a} = \int \mathbf{pp}\psi(\mathbf{p})d\mathbf{p} \tag{6.6}$$

where the integral is taken over all possible directions of $\mathbf{p}$. A fourth-order tensor can be defined in the same way as

$$\mathbf{A} = \int \mathbf{pppp}\psi(\mathbf{p})d\mathbf{p} \tag{6.7}$$

The second-order orientation tensor is symmetric ($a_{ij} = a_{ji}$), and it has a unit trace ($a_{ii} = 1$). Applying the similar symmetry conditions to the fourth-order tensor **A**, it is shown that

$$A_{ijkl} = A_{jikl} = A_{kijl} = A_{lijk} = A_{klij}, \text{ etc} \tag{6.8}$$

The fourth-order-tensor provides complete information about the second-order-tensor because

$$a_{ij} = A_{ijkk} \tag{6.9}$$

Combining (6.6) and (6.5) gives the evolution equation for the orientation tensor,

$$\frac{\mathrm{D}\mathbf{a}}{\mathrm{D}t} = -\mathbf{W}\cdot\mathbf{a} - \mathbf{a}\cdot\mathbf{W}^{\mathrm{T}} + \lambda(\mathbf{S}\cdot\mathbf{a} + \mathbf{a}\cdot\mathbf{S} - 2\mathbf{S} : \mathbf{A}) + 2\mathrm{D_R}(\boldsymbol{\delta} - 3\mathbf{a}) \tag{6.10}$$

The advantages of using a tensorial approach [73] are that **a** is independent of the coordinate systems and easily transforms between coordinate systems; it can be measured by direct experiments; the tensor representation is extremely compact, and computational efficiency. However, a disadvantage of this approach is that an unknown fourth-order orientation tensor is introduced in the momentum equation since only the second-order tensor is used to represent the orientation state. Closure approximations must be used to describe the fourth-order orientation tensor.

One simple approach is to approximate the fourth-order tensor in terms of the second-order tensor. Several closure models have been developed to predict the orientation of ensemble particles, such as the quadratic model [98], the linear model of Hand [99], Hinch and Leal model [98], Hybrid model of Advani and Tucker [100], Orthotropic closure models [101], and the fully symmetric quadratic model [102, 103]. All these models can be applied to fibers, spheroids, and other axisymmetric particles. The time evolution of the

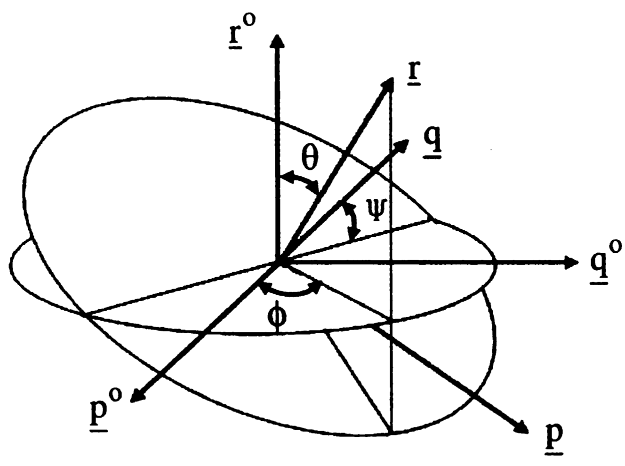

Figure 6.1. Description of the Euler angles used in this chapter.

second-order orientation tensor $<\mathbf{pp}>$ is solved to obtain the average orientation of the particles.

6.3 Predictions of orientation of non-axisymmetric particles

For rotating particles of arbitrary shape suspended in the fluid domain, a vector associated with the particle can be mapped from the reference configuration to the current configuration by using a rotation matrix **R**, which is defined by

$$\mathbf{R} = \mathbf{p}(t)\mathbf{p}^0 + \mathbf{q}(t)\mathbf{q}^0 + \mathbf{r}(t)\mathbf{r}^0 \tag{6.11}$$

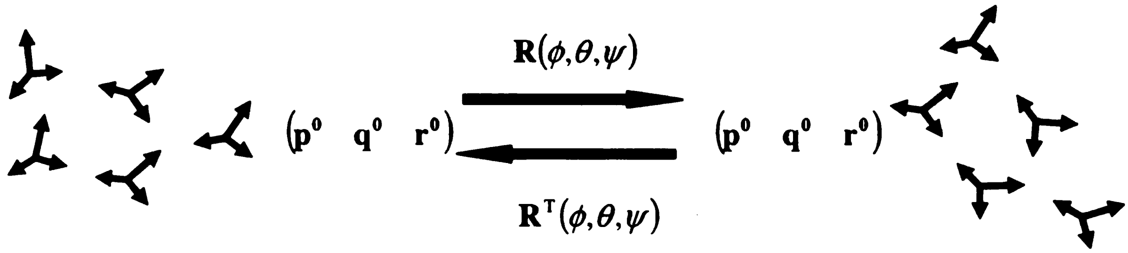

Figure 6.2. Mapping procedure of a vector associated with the particle between the reference configuration and the current configuration.

where **p**, **q**, and **r** are three orthogonal axes of the particle in the current configuration and $\mathbf{p}^0$, $\mathbf{q}^0$, and $\mathbf{r}^0$ are the corresponding axes in the reference configuration shown in Figure 6.1. Since

$$\mathbf{R} \cdot \mathbf{R}^{\mathrm{T}} = \mathbf{I} \tag{6.12}$$

a vector can also be mapped from the current configuration to the reference configuration. The mapping procedure is shown in the Figure 6.2. This rotation matrix **R** depends on the three Euler angles by the following relation

$$\mathbf{R} = \begin{pmatrix} -\sin\psi & +\cos\psi & 0 \\ -\cos\psi & -\sin\psi & 0 \\ 0 & 0 & +1 \end{pmatrix} \begin{pmatrix} +\cos\theta & 0 & -\sin\theta \\ 0 & +1 & 0 \\ +\sin\theta & 0 & +\cos\theta \end{pmatrix} \begin{pmatrix} +\sin\phi & -\cos\phi & 0 \\ +\cos\phi & +\sin\phi & 0 \\ 0 & 0 & +1 \end{pmatrix} \tag{6.13}$$

The ranges of the three Euler angles are

$$0 \le \psi \le 2\pi \tag{6.14}$$

$$0 \le \phi \le 2\pi \tag{6.15}$$

$$0 \le \theta \le \pi \tag{6.16}$$

Instead of using Euler angles, the orientation of the particle is represented by a rotation matrix **R**, which can be written in the component form as $R_{i\alpha}$ as well. A convention is employed to use the Greek suffixes to evaluate a tensor in the reference configuration and Latin suffixes in the current configuration.

For the rigid particles suspension, an orientation probability distribution function $\mathcal{N}(\mathbf{R}, t)$ is introduced so that $\mathcal{N} d\tau$ gives at time t the fraction of particles whose orientation states lie within a small region of orientation space $d\tau (\equiv \sin\theta d\theta d\phi d\psi)$. $\mathcal{N}(\mathbf{R}, t)$ satisfies the normalization condition:

$$\int_{\text{orientation}} \mathcal{N}(\mathbf{R}, t) d\tau = 1 \tag{6.17}$$

According to the conservation law in orientation space, the orientation states of particles is governed by the continuity equation

$$\frac{\mathcal{N}}{t} + \nabla \cdot \mathcal{F} = 0 \tag{6.18}$$

where $\mathcal{F}$ is the probability flux vector in orientation space and ∇ is the gradient vector in that space. It is shown in Rallison's paper [106], if f is any scalar function of orientation, then

$$(\nabla f) = \varepsilon_{kij} R_{i\alpha} \frac{\partial f}{\partial R_{j\alpha}} \tag{6.19}$$

The probability flux

$$\mathcal{F} = \mathcal{N} \boldsymbol{\omega} \tag{6.20}$$

in which $\boldsymbol{\omega}$ is the angular velocity of particles.

In studying force-free particles suspended in a flow field with no external couples exerted on them, there are two separate contributions on the angular velocity of the particle. One is the hydrodynamic contribution from the surrounding fluid straining motion and one is from the Brownian couples [106]. Ignoring the influence of the Brownian motion of the particles, the angular velocity of the particle is

$$\boldsymbol{\omega} = \boldsymbol{\omega}^{\mathrm{H}} = \boldsymbol{\Omega} + \frac{1}{2}\mathbf{B} : \mathbf{S} \tag{6.21}$$

where $\boldsymbol{\Omega} = -\frac{1}{2}\boldsymbol{\varepsilon} : \mathbf{W}$ is the angular velocity of the flow field at the infinity, $\mathbf{S}$ is the strain rate, $\mathbf{W}$ is the vorticity tensor of the fluid, and $\mathbf{B}$ is a third-order material tensor introduced by Bretherton [8]. The geometry of such particles (e.g. ellipsoids) and their interactions with the surrounding fluid are described by the third order tensor $\mathbf{B}$ instead of the single parameter often used for axisymmetric particles (spheroids). By using (6.19) it can obtained that

$$\nabla \cdot \boldsymbol{B} = -2\mathbf{F} \tag{6.22}$$

in which

$$F_{ij} = \frac{1}{2}\left(\varepsilon_{ijk}B_{kjl} + \varepsilon_{kjl}B_{kil}\right) \tag{6.23}$$

Substituting the angular velocity (6.21) into the continuity equation (6.18), the probability conservation equation can be obtained as [106]

$$\frac{\partial \mathcal{N}}{\partial t} + W_{ij}R_{j\alpha}\frac{\partial \mathcal{N}}{\partial R_{i\alpha}} + \frac{1}{2}B_{jpq}E_{pq}\varepsilon_{kij}R_{i\alpha}\frac{\partial \mathcal{N}}{\partial R_{j\alpha}} - \mathcal{N}E_{ij}F_{ij} = 0 \tag{6.24}$$

6.4 Algebraic restrictions on averaged orientation tensors

At an any given point in a particle-filled system, the state of orientation can be described with a forth and an eighth-order averaged orientation tensors, respectively defined by:

$$< R_{i\alpha}R_{j\beta} >= \int_{\text{orientation}} R_{i\alpha}R_{j\beta}\mathcal{N}(\mathbf{R}, t)d\tau \tag{6.25}$$

$$< R_{i\alpha}R_{j\beta}R_{k\gamma}R_{l\delta} >= \int_{\text{orientation}} R_{i\alpha}R_{j\beta}R_{k\gamma}R_{l\delta}\mathcal{N}(\mathbf{R}, t)d\tau \tag{6.26}$$

It is noticed that the average orientation tensor state does not change if switching each pair of indices in $\left\langle R_{i\alpha}R_{j\beta}\right\rangle$ and $\left\langle R_{i\alpha}R_{j\beta}R_{k\gamma}R_{l\delta}\right\rangle$

$$\left\langle R_{i\alpha}R_{j\beta}\right\rangle = \left\langle R_{j\beta}R_{i\alpha}\right\rangle \tag{6.27}$$

and

$$\begin{aligned}\left\langle R_{i\alpha}R_{j\beta}R_{k\gamma}R_{l\delta}\right\rangle &= \left\langle R_{j\beta}R_{i\alpha}R_{k\gamma}R_{l\delta}\right\rangle = \left\langle R_{k\gamma}R_{j\beta}R_{i\alpha}R_{l\delta}\right\rangle = \left\langle R_{l\delta}R_{j\beta}R_{k\gamma}R_{i\alpha}\right\rangle \\ &= \left\langle R_{i\alpha}R_{k\gamma}R_{j\beta}R_{l\delta}\right\rangle = \left\langle R_{i\alpha}R_{l\delta}R_{k\gamma}R_{j\beta}\right\rangle = \left\langle R_{i\alpha}R_{j\beta}R_{l\delta}R_{k\gamma}\right\rangle\end{aligned} \tag{6.28}$$

Furthermore, since $\mathbf{R}^{\mathrm{T}} \cdot \mathbf{R} = \mathbf{R} \cdot \mathbf{R}^{\mathrm{T}} = \mathbf{I}$, the following relations can be obtained

$$\langle R_{31}R_{31}\rangle = 1 - (\langle R_{11}R_{11}\rangle + \langle R_{21}R_{21}\rangle) \tag{6.29}$$

$$\langle R_{32}R_{32}\rangle = 1 - (\langle R_{12}R_{12}\rangle + \langle R_{22}R_{22}\rangle) \tag{6.30}$$

$$\langle R_{33}R_{33}\rangle = 1 - (\langle R_{13}R_{13}\rangle + \langle R_{23}R_{23}\rangle) \tag{6.31}$$

$$\langle R_{31}R_{32}\rangle = -(\langle R_{11}R_{12}\rangle + \langle R_{21}R_{22}\rangle) \tag{6.32}$$

$$\langle R_{31}R_{33}\rangle = -(\langle R_{11}R_{13}\rangle + \langle R_{21}R_{23}\rangle) \tag{6.33}$$

$$\langle R_{32}R_{31}\rangle = -(\langle R_{11}R_{13}\rangle + \langle R_{22}R_{23}\rangle) \tag{6.34}$$

Using the symmetry and projection conditions, 39 independent entries of **a** can be listed by $\langle R_{11}R_{11}\rangle$, $\langle R_{11}R_{12}\rangle$, $\langle R_{11}R_{13}\rangle$, $\langle R_{11}R_{21}\rangle$, $\langle R_{11}R_{22}\rangle$, $\langle R_{11}R_{23}\rangle$, $\langle R_{11}R_{31}\rangle$, $\langle R_{11}R_{32}\rangle$, $\langle R_{11}R_{33}\rangle$, $\langle R_{12}R_{12}\rangle$, $\langle R_{12}R_{13}\rangle$, $\langle R_{12}R_{21}\rangle$, $\langle R_{12}R_{22}\rangle$, $\langle R_{12}R_{23}\rangle$, $\langle R_{12}R_{31}\rangle$, $\langle R_{12}R_{32}\rangle$, $\langle R_{12}R_{33}\rangle$, $\langle R_{13}R_{13}\rangle$, $\langle R_{13}R_{21}\rangle$, $\langle R_{13}R_{22}\rangle$, $\langle R_{13}R_{23}\rangle$, $\langle R_{13}R_{31}\rangle$, $\langle R_{13}R_{32}\rangle$, $\langle R_{13}R_{33}\rangle$, $\langle R_{21}R_{21}\rangle$, $\langle R_{21}R_{22}\rangle$, $\langle R_{21}R_{23}\rangle$, $\langle R_{21}R_{31}\rangle$, $\langle R_{21}R_{32}\rangle$, $\langle R_{21}R_{33}\rangle$, $\langle R_{22}R_{22}\rangle$, $\langle R_{22}R_{23}\rangle$, $\langle R_{22}R_{31}\rangle$, $\langle R_{22}R_{32}\rangle$, $\langle R_{22}R_{33}\rangle$, $\langle R_{23}R_{23}\rangle$, $\langle R_{23}R_{31}\rangle$, $\langle R_{23}R_{32}\rangle$, and $\langle R_{23}R_{33}\rangle$. Since

$$\mathrm{tr}\left\langle \mathbf{R}^{\mathrm{T}} \cdot \mathbf{R}\right\rangle = \mathrm{tr}\left\langle \mathbf{R} \cdot \mathbf{R}^{\mathrm{T}}\right\rangle = \mathrm{tr}(\mathbf{I}) = 3 \tag{6.35}$$

the eighth order orientation tensor should also satisfy the following projection properties

$$\left\langle R_{i\alpha}R_{i\alpha}R_{k\gamma}R_{l\delta}\right\rangle = \left\langle R_{i\alpha}R_{j\beta}R_{i\alpha}R_{l\delta}\right\rangle = \left\langle R_{i\alpha}R_{j\beta}R_{k\gamma}R_{i\alpha}\right\rangle$$

$$= \left\langle R_{i\alpha}R_{j\beta}R_{j\beta}R_{l\delta}\right\rangle = \left\langle R_{i\alpha}R_{j\beta}R_{k\gamma}R_{j\beta}\right\rangle = \left\langle R_{i\alpha}R_{j\beta}R_{k\gamma}R_{k\gamma}\right\rangle = 3 < \mathbf{RR} > \tag{6.36}$$

Similarly to the analysis of suspensions of axisymmetric particles, it is convenient from a computational view to use an alternative approach based on the moments of the probability distribution function. The derivation of equation (6.24) can be rewritten in terms of average orientation tensors. An evolution equation for the second moment of the probability distribution may be obtained by multiplying (6.24) by $\langle \mathbf{RR} \rangle$ and integrating over all orientations. The time derivative of the fourth order orientation tensor can be expressed as [106]

$$\frac{\partial \left\langle R_{s\gamma}R_{t\delta}\right\rangle}{\partial t} - W_{sm}\left\langle R_{m\gamma}R_{t\delta}\right\rangle + \left\langle R_{s\gamma}R_{m\delta}\right\rangle W_{mt}$$

$$= -\frac{1}{2}\varepsilon_{\alpha\mu\gamma}B^{0}_{\alpha\beta\theta}\left\langle R_{s\mu}R_{t\delta}R_{p\beta}R_{q\theta}\right\rangle S_{pq} - \frac{1}{2}\varepsilon_{\alpha\mu\delta}B^{0}_{\alpha\beta\theta}\left\langle R_{s\gamma}R_{t\mu}R_{p\beta}R_{q\theta}\right\rangle S_{pq} \tag{6.37}$$

(6.37) gives the evolution of $\langle \mathbf{RR} \rangle$ in terms of $\langle \mathbf{RRRR} \rangle$. To solve the second moment equation describing the evolution of the particle orientation (6.37) it is necessary to know the eighth-order orientation tensor $\langle \mathbf{RR} \rangle$. Closure problems are introduced in (6.37) due to the unknown eighth-order orientation tensor $\langle \mathbf{RRRR} \rangle$. A fully symmetric quadratic model for the eighth-order tensor $\langle \mathbf{RRRR} \rangle$ is constructed in the following section.

6.5 Symmetry operator

According to the above discussion the only information available about the structure of the eighth-order tensor are its symmetry and projection properties. This indicates that higher order tensors can be reconstructed form combinations of lower order tensors and the unit tensor. It is customary to make the following hypothesis

$$\langle \mathbf{RRRR} \rangle = \mathbb{F}(\langle \mathbf{RR} \rangle) \tag{6.38}$$

The operator $\mathbb{F}$ should satisfy the six fold symmetry and six fold projection properties. To ensure the symmetry of the eighth-order tensor, a symmetry operator S is introduced with six terms in the form of

$$\mathrm{S}(\mathbf{X},\mathbf{Y}) = \mathbf{XY} + \mathbf{XY}^{\mathrm{T23}} + \mathbf{XY}^{\mathrm{T24}} + \mathbf{XY} + \mathbf{YX}^{\mathrm{T23}} + \mathbf{YX}^{\mathrm{T24}} \tag{6.39}$$

where $\mathbf{XY}^{\mathrm{Txy}}$ indicates a switch of the x^{th} pair and y^{th} pair of indices of the dyadic $\mathbf{X}, \mathbf{Y}$ and $\mathbf{X}$ and $\mathbf{Y}$ are symmetric forth-order tensor ($\mathbf{X} = \mathbf{X}^{\mathrm{T12}}$ and $\mathbf{Y} = \mathbf{Y}^{\mathrm{T12}}$). Satisfaction of the six symmetry properties implies that the permutation of any pair of indices of a dyadic must give the same result. Thus, $\mathrm{S}(\mathbf{X},\mathbf{Y})$ is a six-fold symmetry operator. Permuting all six combinations of indices can prove the symmetry property of $\mathrm{S}(\mathbf{X},\mathbf{Y})$ by

$$\begin{aligned}
\mathrm{S}(\mathbf{X},\mathbf{Y}) &= \mathbf{X}_{i\alpha j\beta}\mathbf{Y}_{k\gamma l\delta} + \mathbf{X}_{i\alpha k\gamma}\mathbf{Y}_{j\beta l\delta} + \mathbf{X}_{i\alpha l\delta}\mathbf{Y}_{k\gamma j\beta} + \mathbf{Y}_{i\alpha j\beta}\mathbf{X}_{k\gamma l\delta} + \mathbf{Y}_{i\alpha k\gamma}\mathbf{X}_{j\beta l\delta} + \mathbf{Y}_{i\alpha l\delta}\mathbf{X}_{k\gamma j\beta} \\
&\overset{i\alpha \leftrightarrow j\beta}{=} \mathbf{X}_{j\beta i\alpha}\mathbf{Y}_{k\gamma l\delta} + \mathbf{X}_{j\beta k\gamma}\mathbf{Y}_{i\alpha l\delta} + \mathbf{X}_{j\beta l\delta}\mathbf{Y}_{k\gamma i\alpha} + \mathbf{Y}_{j\beta i\alpha}\mathbf{X}_{k\gamma l\delta} + \mathbf{Y}_{j\beta k\gamma}\mathbf{X}_{i\alpha l\delta} + \mathbf{Y}_{j\beta l\delta}\mathbf{X}_{k\gamma i\alpha} \\
&\overset{i\alpha \leftrightarrow k\gamma}{=} \mathbf{X}_{k\gamma j\beta}\mathbf{Y}_{i\alpha l\delta} + \mathbf{X}_{k\gamma i\alpha}\mathbf{Y}_{j\beta l\delta} + \mathbf{X}_{k\gamma l\delta}\mathbf{Y}_{i\alpha j\beta} + \mathbf{Y}_{k\gamma j\beta}\mathbf{X}_{i\alpha l\delta} + \mathbf{Y}_{k\gamma i\alpha}\mathbf{X}_{j\beta l\delta} + \mathbf{Y}_{k\gamma l\delta}\mathbf{X}_{i\alpha j\beta} \\
&\overset{i\alpha \leftrightarrow l\delta}{=} \mathbf{X}_{l\delta j\beta}\mathbf{Y}_{k\gamma i\alpha} + \mathbf{X}_{l\delta k\gamma}\mathbf{Y}_{j\beta i\alpha} + \mathbf{X}_{l\delta i\alpha}\mathbf{Y}_{k\gamma j\beta} + \mathbf{Y}_{l\delta j\beta}\mathbf{X}_{k\gamma i\alpha} + \mathbf{Y}_{l\delta k\gamma}\mathbf{X}_{j\beta i\alpha} + \mathbf{Y}_{l\delta i\alpha}\mathbf{X}_{k\gamma j\beta} \\
&\overset{j\beta \leftrightarrow k\gamma}{=} \mathbf{X}_{i\alpha k\gamma}\mathbf{Y}_{j\beta l\delta} + \mathbf{X}_{i\alpha j\beta}\mathbf{Y}_{k\gamma l\delta} + \mathbf{X}_{i\alpha l\delta}\mathbf{Y}_{j\beta k\gamma} + \mathbf{Y}_{i\alpha k\gamma}\mathbf{X}_{j\beta l\delta} + \mathbf{Y}_{i\alpha j\beta}\mathbf{X}_{k\gamma l\delta} + \mathbf{Y}_{i\alpha l\delta}\mathbf{X}_{j\beta k\gamma} \\
&\overset{j\beta \leftrightarrow l\delta}{=} \mathbf{X}_{i\alpha l\delta}\mathbf{Y}_{k\gamma j\beta} + \mathbf{X}_{i\alpha k\gamma}\mathbf{Y}_{l\delta j\beta} + \mathbf{X}_{i\alpha j\beta}\mathbf{Y}_{k\gamma l\delta} + \mathbf{Y}_{i\alpha l\delta}\mathbf{X}_{k\gamma j\beta} + \mathbf{Y}_{i\alpha k\gamma}\mathbf{X}_{l\delta j\beta} + \mathbf{Y}_{i\alpha j\beta}\mathbf{X}_{k\gamma l\delta} \\
&\overset{k\gamma \leftrightarrow l\delta}{=} \mathbf{X}_{i\alpha j\beta}\mathbf{Y}_{k\gamma l\delta} + \mathbf{X}_{i\alpha l\delta}\mathbf{Y}_{j\beta k\gamma} + \mathbf{X}_{i\alpha k\gamma}\mathbf{Y}_{l\delta j\beta} + \mathbf{X}_{i\alpha j\beta}\mathbf{Y}_{k\gamma l\delta} + \mathbf{X}_{i\alpha l\delta}\mathbf{Y}_{j\beta k\gamma} + \mathbf{X}_{i\alpha k\gamma}\mathbf{Y}_{l\delta j\beta}
\end{aligned} \tag{6.40}$$

where $\overset{i\alpha \leftrightarrow j\beta}{=}$ means to switch the indices of $i\alpha$ with $j\beta$.

6.6 Construction of the eighth-order orientation tensor

A fully symmetric quadratic closure model is constructed based on the hypothesis of equation (6.38). Four operators are needed to represent a closed form of (6.38):

$$\begin{aligned} \mathrm{P}_1 &= \mathrm{S}(\boldsymbol{\delta}, \boldsymbol{\delta}) \\ &= 2\left(\delta_{i\alpha j\beta}\delta_{k\gamma l\delta} + \delta_{i\alpha k\gamma}\right) \end{aligned} \tag{6.41}$$

$$\begin{aligned} \mathrm{P}_2 &= \mathrm{S}(\boldsymbol{\delta}, \langle \mathbf{RR} \rangle) \\ &= \left[\left\langle R_{i\alpha} R_{j\beta}\right\rangle \delta_{k\gamma l\delta} + \left\langle R_{i\alpha} R_{k\gamma}\right\rangle \delta_{j\beta l\delta} + \langle R_{i\alpha} R_{l\delta}\rangle \delta_{k\gamma j\beta} + \right. \\ &\quad \left. \delta_{i\alpha j\beta}\left\langle R_{k\gamma} R_{l\delta}\right\rangle + \delta_{i\alpha k\gamma}\left\langle R_{j\beta} R_{l\delta}\right\rangle + \delta_{i\alpha l\delta}\left\langle R_{k\gamma} R_{j\beta}\right\rangle\right] \end{aligned} \tag{6.42}$$

$$\begin{aligned} \mathrm{P}_3 &= \mathrm{S}(\langle \mathbf{RR} \rangle, \langle \mathbf{RR} \rangle) \\ &= 2\left(\delta_{i\alpha j\beta}\left\langle \mathbf{R}_{k\gamma}\mathbf{R}_{l\delta}\right\rangle + \delta_{i\alpha k\gamma}\left\langle \mathbf{R}_{j\beta}\mathbf{R}_{l\delta}\right\rangle + \delta_{i\alpha l\delta}\left\langle \mathbf{R}_{k\gamma}\mathbf{R}_{j\beta}\right\rangle\right) \end{aligned} \tag{6.43}$$

$$\begin{aligned} P_4 &= \mathrm{S}\left(\boldsymbol{\delta}, \left(\langle \mathbf{RR} \rangle : \langle \mathbf{RR} \rangle^{\mathrm{T}12}\right)\right) \\ &= \delta_{i\alpha j\beta}\left\langle R_{k\gamma} R_{m\phi}\right\rangle \left\langle R_{m\phi} R_{l\delta}\right\rangle + \delta_{i\alpha k\gamma}\left\langle R_{j\beta} R_{m\phi}\right\rangle \left\langle R_{m\phi} R_{l\delta}\right\rangle \\ &\quad + \delta_{i\alpha l\delta}\left\langle R_{k\gamma} R_{m\phi}\right\rangle \left\langle R_{m\phi} R_{j\beta}\right\rangle + \left\langle R_{i\alpha} R_{m\phi}\right\rangle \left\langle R_{m\phi} R_{j\beta}\right\rangle \delta_{k\gamma l\delta} \\ &\quad + \left\langle R_{i\alpha} R_{m\phi}\right\rangle \left\langle R_{m\phi} R_{k\gamma}\right\rangle \delta_{j\beta l\delta} + \left\langle R_{i\alpha} R_{m\phi}\right\rangle \left\langle R_{m\phi} R_{l\delta}\right\rangle \delta_{k\gamma j\beta} \end{aligned} \tag{6.44}$$

where P_1 is a constant term, P_2 is a linear term of $\langle \mathbf{RR} \rangle$, and both P_3, and P_4 are quadratic terms of $\langle \mathbf{RR} \rangle$. $\boldsymbol{\delta}$ is a 4th order symmetry tensor with unit entries that transposes an arbitrary tensor under double dot product, i.e. $\boldsymbol{\delta} : \langle \mathbf{RRRR} \rangle = \langle \mathbf{RRRR} \rangle^{\mathrm{T}12}$, and

$\langle \mathbf{RRRR} \rangle : \boldsymbol{\delta} = \langle \mathbf{RRRR} \rangle^{T34}$. The components of $\boldsymbol{\delta}$ is shown as the followings:

$$\boldsymbol{\delta} = \begin{pmatrix} \begin{pmatrix} 1 & 0 & 0 \\ 0 & 0 & 0 \\ 0 & 0 & 0 \end{pmatrix} & \begin{pmatrix} 0 & 1 & 0 \\ 0 & 0 & 0 \\ 0 & 0 & 0 \end{pmatrix} & \begin{pmatrix} 0 & 0 & 1 \\ 0 & 0 & 0 \\ 0 & 0 & 0 \end{pmatrix} \\ \begin{pmatrix} 0 & 0 & 0 \\ 1 & 0 & 0 \\ 0 & 0 & 0 \end{pmatrix} & \begin{pmatrix} 0 & 0 & 0 \\ 0 & 1 & 0 \\ 0 & 0 & 0 \end{pmatrix} & \begin{pmatrix} 0 & 0 & 0 \\ 0 & 0 & 1 \\ 0 & 0 & 0 \end{pmatrix} \\ \begin{pmatrix} 0 & 0 & 0 \\ 0 & 0 & 0 \\ 1 & 0 & 0 \end{pmatrix} & \begin{pmatrix} 0 & 0 & 0 \\ 0 & 0 & 0 \\ 0 & 1 & 0 \end{pmatrix} & \begin{pmatrix} 0 & 0 & 0 \\ 0 & 0 & 0 \\ 0 & 0 & 1 \end{pmatrix} \end{pmatrix} \tag{6.45}$$

The FSQ model is constructed out of a linear combination of two different terms. The first term contains the constant term and the linear terms of $\langle \mathbf{RR} \rangle$, the second contains constant term, and the linear and quadratic terms of $\langle \mathbf{RR} \rangle$

$$\langle \mathbf{RRRR} \rangle_1 = \alpha_{11} \mathrm{P}_1 + \alpha_{12} \mathrm{P}_2 \tag{6.46}$$

$$\langle \mathbf{RRRR} \rangle_2 = \alpha_{21} \mathrm{P}_1 + \alpha_{23} \mathrm{P}_3 + \alpha_{24} \mathrm{P}_4 \tag{6.47}$$

and the closure model is given by

$$\langle \mathbf{RRRR} \rangle = \mathbb{F}(\langle \mathbf{RRRR} \rangle) = (1 - C_2) \langle \mathbf{RRRR} \rangle_1 + C_2 \langle \mathbf{RRRR} \rangle_2 \tag{6.48}$$

$\langle \mathbf{RRRR} \rangle_1$ and $\langle \mathbf{RRRR} \rangle_2$ constructed by (6.46) and (6.47) are symmetric and the coefficients are selected so that contraction property (6.36) should be satisfied. After contraction of the linear closure and the quadratic closure that satisfy projection and symmetry properties the following coefficients can be obtained

$$\alpha_{11} = -\frac{9}{286} \tag{6.49}$$

$$\alpha_{12} = \frac{3}{13} \tag{6.50}$$

$$\alpha_{21} = -\frac{3(2J_2 - J_1{}^2)}{143J_1} \tag{6.51}$$

$$\alpha_{23} = -\frac{3}{2J_1} \tag{6.52}$$

$$\alpha_{24} = \frac{6}{13J_1} \tag{6.53}$$

in which J_1, and J_2 are the first two invariants of the fourth-order tensor $\langle \mathbf{RR} \rangle$ [110] with the following expressions

$$J_1 = -\mathrm{tr}\left(\langle \mathbf{RR} \rangle\right) \tag{6.54}$$

and

$$J_2 = -\frac{1}{2}\left(\langle R_{i\alpha}R_{i\alpha}\rangle \left\langle R_{j\beta}R_{j\beta}\right\rangle - \left\langle R_{i\alpha}R_{m\phi}\right\rangle \left\langle R_{m\phi}R_{i\alpha}\right\rangle\right) \tag{6.55}$$

Substituting these coefficients into (6.46) and (6.47), the two terms of the closure model can be rewritten as

$$\langle \mathbf{RRRR} \rangle_1 = -\frac{9}{286}\mathrm{S}\left(\boldsymbol{\delta}, \boldsymbol{\delta}\right) + \frac{3}{13}\mathrm{S}\left(\boldsymbol{\delta}, \mathbf{a}\right) \tag{6.56}$$

$$\langle \mathbf{RRRR} \rangle_2 = -\frac{3(2J_2 - J_1^2)}{143J_1}\mathrm{S}\left(\boldsymbol{\delta}, \boldsymbol{\delta}\right) - \frac{3}{2J_1}\mathrm{S}\left(\mathbf{a}, \mathbf{a}\right) + \frac{6}{13J_1}\mathrm{S}\left(\boldsymbol{\delta}, \langle \mathbf{RR} \rangle\right) \tag{6.57}$$

Substituting (6.56) and (6.57) into (6.48), the closure model for the fourth moment orientation tensor can be obtained as

$$\begin{aligned} < \mathbf{RRRR} > = \quad & (1 - C_2)\left[-\frac{9}{286}\mathrm{S}\left(\boldsymbol{\delta}, \boldsymbol{\delta}\right) + \frac{3}{13}\mathrm{S}\left(\boldsymbol{\delta}, \mathbf{a}\right)\right] \\ & + C_2\left[-\frac{3(2J_2 - J_1^2)}{143J_1}\mathrm{S}\left(\boldsymbol{\delta}, \boldsymbol{\delta}\right) - \frac{3}{2J_1}\mathrm{S}\left(\mathbf{a}, \mathbf{a}\right) + \frac{6}{13J_1}\mathrm{S}\left(\boldsymbol{\delta}, \langle \mathbf{RR} \rangle\right)\right] \end{aligned} \tag{6.58}$$

which preserve both the six-fold symmetry and six-fold projection properties.

For suspensions of spheroids, to satisfy the following sufficient condition for realizability of the orientation dyadic (i.e., microstructure), i.e.,

$$\mathbf{z} \cdot < \mathbf{pp} > \cdot\, \mathbf{z} \geq 0 \tag{6.59}$$

C_2 has been shown to be

$$C_2 = \frac{8 + 45\mathrm{III}_{\mathbf{b}}}{18(1 + 9\mathrm{III}_{\mathbf{b}})} \tag{6.60}$$

in which $\mathbf{b} = <\mathbf{pp}> - \frac{1}{3}\boldsymbol{\delta}$ is the anisotropic orientation tensor for spheroids and $\mathrm{III}_{\mathbf{b}} = \mathrm{tr}(\mathbf{b}\cdot\mathbf{b}\cdot\mathbf{b})$ the third invariant of $\mathbf{b}$ [111,112]. For suspensions of non-axisymmetric particles, C_2 is still in development. The tensor calculation associated with this chapter can be found in Appendix A.

6.7 Conclusions

As suggested by Rallison [106], it may be practical to predict the microstructure of a suspension of rigid , non-axisymmetric particles by using the rotation operator as a state variable rather than the Euler angles. This research has identified a closure for the 4th-order moment of the orientation distribution function in terms of the 2nd-order moment that satisfies all six-fold symmetry and projection properties of the exact 4th-order moment. This result may provide a means to improve the accuracy of estimating the rotary diffusion coefficient from return-to-isotropy experiments.

CHAPTER 7

PREDICTION OF FLOW-INDUCED ORIENTATION AND SPATIAL MIGRATION OF PARTICLES

7.1 Introduction

Particle migrations in suspension flows are of importance to a variety of scientific and engineering applications, e.g. the transport of sediments, chromotography, composite materials processing, sequestration processes in porous media, and secondary oil recovery techniques. For suspensions with micron size particles, for which inertia effects and Brownian diffusion can be neglected, the interaction between the particles adds a random component to their motion that is additional to the deterministic translation along streaming in the slow viscous environment. This random component results in migration of particles, which was first identified by Leighton [113]. Some valuable information on the many-particle interactions have been simulated by Stokesian Dynamics and boundary element methods [72, 114–118]. The experiments of Segré and Silberberg [119, 120] have large influence on fluid mechanics studies of migration and lift of particles. They studied the migration of dilute suspensions of neutrally buoyant spheres in a pipe flow at Reynolds numbers between 2 and 700. The particles migrate from the wall and centerline and accumulate at about 0.6 of a pipe radius from the centerline. Karnis et al., verified the same phenomenon and observed that particles migrate faster for larger flow rate and closer to the axis for the larger rigid sphere. Aubert et al. [121, 122] found that there were some forms of migration in all flows, curved or uncurved; however, in parallel flows he found that there could be no migration perpendicular to the direction of flow; that is, the polymer just lags or precedes the flow along a single streamline. He found further that cross-streamline migration occurs in curvilinear (e.g., circular Couette) flow when he approximated the curved flow as a quadratic. Flow-induced polymer migration is treated in a rather intuitive though mathematically formal way by Sekhon et al. to study the effects due to the hydrodynamic interaction as well as flow geometry [123].

Two different approaches have been used to develop models capable of describing various multiphase flow regimes. The first case is known as the Dilute phase approach, also called the Lagrangian approach, in which the fluid phase is treated as a continuum and the particle trajectories are calculated for the equation of particle motions. Lagrangian method is used in modelling the dynamics of a single particle or a dilute suspension [10, 14, 124, 125]. The second approach is known as the Dense phase approach, sometimes also called the Eulerian (or two-fluid) approach. In this approach, each phase (or component) directly influences the motion and the behavior of the other phase and the particle phase also is treated as a continuum. This method is used widely in fluidization [126], gas-solid flows [127], pneumatic conveying [128], and suspensions [129].

Two continuum theories are developed in the dense phase approach: Mixture theory and Averaging theory [130]. Both theories are based on the assumption that each phase may be mathematically described as a continuum. The ideas of Mixture theory can be traced back to the branch of mechanics [131–134]. The fundamental assumption in Mixture theory is that at any instant time, all phases are present at every material point. In contrast, the Averaging method directly modifies the classical transport equations to account for the discontinuities for 'jump' conditions at moving boundaries between the phases [135, 136]. The modified balance equations must then be averaged in either space, time or statistical to arrive at an acceptable local form [23, 137, 138]. Some difference of the equations of two-fluid by Mixture theory and by Ensemble Average theory can be found in [134].

Three essential parts are composed of the formulation in the Eulerian approach: the derivation of field equations, constitutive equations, and interfacial conditions. The field equations state the conservation principles for, e.g. the mass, momentum, and energy. Constitutive equations close the equation system by taking into account the structure of the flow field and material properties by experiment correlations. It's noted that both of the Mixture approach and the Averaging approach are not closed and methods of closure, or the constitutive equations for the interaction terms, are required to put the equations of motion into a form suitable for application. Because of its close relation to measuring techniques, the Averaging method is most widely used in the multiphase flows.

7.2 Hydrodynamics of ensembles of particles

7.2.1 Theory of ensemble averaging

As mentioned in the previous section, there are several kinds of averaging methods, i.e., time average, volume average, and ensemble average can be applied in the average approach to solve for the multiphase flow. Comparing with the other averaging methods, ensemble averaging method has some advantages and is widely used in the current analysis of multiphase flow [23, 134, 135, 139, 140]. First, the data acquired by time and/or volume averaging can be easily used as the "sample" of the ensemble. Second, ensemble averaging does not require that a control volume contain a large number of particles in any given realization. Third, ensemble averaging is easily implemented. Forth, the ensemble average allows for that all realizations are only approximations of the ideal. Detail information on the ensemble average is given by Drew and Passman [135]. The definition of ensemble average is

$$\bar{f}(\mathbf{x}, t) = \int_{\epsilon} f(\mathbf{x}, t; \mu) dm(\mu) \tag{7.1}$$

where $dm(\cdot)$ is the density for the measure (probability) on the set of all precesses ϵ. Some results can be applied to the ensemble average in order to average the equations of motion:

(1) Reynolds rules

$$\overline{c_1 f_1 + c_2 f_2} = c_1 \overline{f_1} + c_2 \overline{f_2} \tag{7.2}$$

(2) Treating generalized function

$$\int_{\Omega} \phi(\mathbf{x}, t) \frac{\partial f(\mathbf{x}, t)}{\partial t} dv dt = - \int_{\Omega} \frac{\partial \phi(\mathbf{x}, t)}{\partial t} f(\mathbf{x}, t) dv dt \tag{7.3}$$

and

$$\int_\Omega \phi(\mathbf{x},t)\nabla f(\mathbf{x},t)dvdt = -\int_\Omega \nabla\phi(\mathbf{x},t)f(\mathbf{x},t)dvdt \tag{7.4}$$

in which ϕ is a test function belongs to Φ, Ω a compact set in space and time to support $\phi \in \Phi$.

(3) Interface Delta function and Topological Equation

$$\frac{\partial X_k}{\partial n} = \mathbf{n}_k \cdot \nabla X_k \tag{7.5}$$

This is the interface Delta function where X_k is the characteristic function as

$$X_k(\mathbf{x},t) = \begin{cases} 1 & \text{if phase } k \text{ occupies } \mathbf{x} \\ 0 & \text{otherwise} \end{cases} \tag{7.6}$$

The Topological equation is

$$\frac{\partial X_k}{\partial t} + \mathbf{v}_i \cdot \nabla X_k = 0 \tag{7.7}$$

(4) Gauss and Leibniz rules

$$\begin{aligned} \overline{X_k \nabla f} &= \overline{\nabla X_k f} - \overline{f \nabla X_k} \\ &= \nabla \overline{(X_k f)} - \overline{f_{ki} \nabla X_k} \end{aligned} \tag{7.8}$$

This is called the Gauss rule in which f_{ki} is the value of the function f evaluated on the component k side of the interface.

Similarly, the Leibnitz rule is

$$\begin{aligned} \overline{X_k \frac{\partial f}{\partial t}} &= \overline{\frac{\partial X_k f}{\partial t}} - \overline{f \frac{\partial X_k}{\partial t}} \\ &= \frac{\partial \overline{X_k f}}{\partial t} - \overline{f_{ki} \frac{\partial X_k}{\partial t}} \end{aligned} \tag{7.9}$$

7.2.2 Averaged balanced equations

A two-fluid model is used in the balanced of mass, and momentum equations can be obtained by taking the product of the balanced equations with the phase indicator, X_k, manipulating using the product rule for differentiation, and then performing the averaging process. Mass balanced equation can be written as

$$\frac{\overline{X_k \rho}}{\partial t} + \nabla \cdot \overline{X_k \rho \mathbf{v}} = \overline{\rho \left(\frac{\partial X_k}{\partial t} + \mathbf{v} \cdot \nabla X_k \right)} \tag{7.10}$$

By using the topological equation 7.7, the right-hand side can be reduced to

$$\Gamma_k = \overline{[\rho(\mathbf{v} - \mathbf{v_i})] \cdot \nabla X_k} \tag{7.11}$$

This is the interfacial source of mass due to the phase change. If $(\mathbf{v} - \mathbf{v_i}) \cdot \mathbf{n} = 0$, then $\boldsymbol{\Gamma}_k = 0$. The averaged density and averaged velocity of phase k can be defined by

$$\alpha_k \bar{\rho}_k = \overline{X_k \rho} \tag{7.12}$$

$$\alpha_k \bar{\rho}_k \bar{\mathbf{v}}_k = \overline{X_k \rho \mathbf{v}} \tag{7.13}$$

Substituting (7.11 - 7.13) into (7.10), the averaged balanced of mass for the phase k can be obtained by

$$\frac{\partial \alpha_k \bar{\rho}_k}{\partial t} + \nabla \cdot \alpha_k \bar{\rho}_k \bar{\mathbf{v}}_k = \boldsymbol{\Gamma}_k \tag{7.14}$$

Multiplying the equation of balance of momentum by X_k and taking average to it, the averaged momentum equation for phase k can be obtained

$$\frac{\partial \overline{X_k \rho \mathbf{v}}}{\partial t} + \nabla \cdot \overline{X_k \rho \mathbf{v}\mathbf{v}} = \nabla \cdot \overline{X_k \mathbf{T}} + \overline{X_k \rho \mathbf{g}} + \overline{\rho \mathbf{v}[(\mathbf{v} - \mathbf{v}_i) \cdot \nabla X_k] - \mathbf{T} \cdot \nabla X_k} \tag{7.15}$$

in which $\mathbf{T}$ is the stress tensor, and $\mathbf{g}$ is the body force, e.g., gravity and magnesium. Defining the averaged stress by

$$\alpha_k \overline{\mathbf{T}}_k = \overline{X_k \mathbf{T}}, \tag{7.16}$$

the Reynolds stress by

$$\alpha_k \mathbf{T}_k^{Re} = -\overline{X_k \rho \mathbf{v}_k^{\prime} \mathbf{v}_k^{\prime}}, \tag{7.17}$$

the interfacial velocity by

$$\mathbf{v}_{ki}^{m} = \overline{\rho \mathbf{v}(\mathbf{v} - \mathbf{v}_i) \cdot \nabla X_k} \tag{7.18}$$

and the interfacial force by

$$\mathbf{M}_k = -\overline{\mathbf{T} \cdot \nabla X_k} \tag{7.19}$$

finally the equation of balance of momentum can be reduced to

$$\frac{\partial \alpha_k \bar{\rho}_k \bar{\mathbf{v}}_k}{\partial t} + \nabla \cdot \alpha_k \bar{\rho}_k \bar{\mathbf{v}}_k \bar{\mathbf{v}}_k = \nabla \cdot \alpha_k (\overline{\mathbf{T}}_k + \mathbf{T}_k^{Re}) + \alpha_k \bar{\rho}_k \mathbf{g} + \mathbf{M}_k + \mathbf{v}_{ki}^{m} \Gamma_k \tag{7.20}$$

7.3 Equations of motion and orientation for a dilute suspension

To distinguish each constituent of two-phase flows, subscripts "f" and "s" are used to represent the continuous phase (fluid) and the solid phase (particle) respectively. If the concentration of the solid phase is α, the concentration of the fluid phase will be

$$\alpha_f = 1 - \alpha_s = 1 - \alpha \tag{7.21}$$

The "−" over the variables means ensemble averaged quantities. For convenience, the overline may be taken off to yield simpler expressions. Assuming $\Gamma_{d/f} = 0$, the conversation equations for mass of the constituents are

$$\frac{\partial \alpha}{\partial t} + \nabla \cdot \alpha \mathbf{v}_s = 0 \tag{7.22}$$

$$\frac{\partial (1 - \alpha)}{\partial t} + \nabla \cdot (1 - \alpha) \mathbf{v}_f = 0 \tag{7.23}$$

The corresponding equations of momentum for the dilute suspension are of the form

$$\alpha\rho_s\left(\frac{\partial \mathbf{v}_s}{\partial t} + \mathbf{v}_s \cdot \nabla \mathbf{v}_s\right) = \nabla \cdot \alpha \mathbf{T}_s + \alpha\rho_s \mathbf{g} + \mathbf{M}_s \tag{7.24}$$

$$(1-\alpha)\rho_f\left(\frac{\partial \mathbf{v}_f}{\partial t} + \mathbf{v}_f \cdot \nabla \mathbf{v}_f\right) = \nabla \cdot (1-\alpha)\mathbf{T}_f + \alpha\rho_f \mathbf{g} - \mathbf{M}_s \tag{7.25}$$

In the above, α is the concentration of the solid phase. ρ_s, and ρ_f are the partial densities of the solid and fluid phase respectively; the mass weighted averaged of solid and fluid velocity are $\mathbf{v}_s$ and $\mathbf{v}_f$ respectively; the phase interaction force per unit volume is denoted by $\mathbf{M}_s$ and the mass-weighted stress for the solid and fluid phase are $\mathbf{T}_s$ and $\mathbf{T}_s$ respectively.

For dilute suspensions, the interaction between the particles is negligible. According to (6.10) the orientation of the particles can be written as

$$\frac{\mathrm{D}\mathbf{a}}{\mathrm{D}t} = -\mathbf{W} \cdot \mathbf{a} - \mathbf{a} \cdot \mathbf{W}^{\mathrm{T}} + \lambda(\mathbf{S} \cdot \mathbf{a} + \mathbf{a} \cdot \mathbf{S} - 2\mathbf{S} : \mathbf{A}) \tag{7.26}$$

7.4 Stress model

It is noted that the averaged balanced equations are not closed. In order to make the above equations solvable, constitutive relations must be obtained for the phase interaction force and the phase stresses. There are many distinctly different modes. Hwang and Shen [141, 142] provided a derivation of the solid phase stress using a a control volume/control surface approach. Consider a mixture of an incompressible Newtonian fluid and rigid particles with a uniform size. The fluid and solid phase stress may be decomposed, respectively, as

$$\mathbf{T}_f = -p_f \mathbf{I} + \mathbf{T}'_f \tag{7.27}$$

and

$$\mathbf{T}_s = -p_s \mathbf{I} + \mathbf{T}'_s \tag{7.28}$$

where $-p_f$ and $-p_s$ are the phase pressures, $\mathbf{I}$ is the unit tensor, and $\mathbf{T}'_s$ and $\mathbf{T}'_f$ the deviatoric parts of the phase stresses. The deviatoric parts of the phases can be decomposed, respectively, as

$$\mathbf{T}'_f = \mathbf{T}_\nu + \mathbf{T}_t \tag{7.29}$$

and

$$\mathbf{T}'_s = \mathbf{T}_c + \mathbf{T}_k + \mathbf{T}_p \tag{7.30}$$

in which $\mathbf{T}_\nu$ is the fluid viscous stress, $\mathbf{T}_t$ the fluid turbulence stress (or Reynolds stress), $\mathbf{T}_c$ the collision/contact stress, $\mathbf{T}_k$ the kinetic stress (equivalent to the solid turbulence stress) and $\mathbf{T}_p$ the particle-presence stress resulting from the hydrodynamic forces acting on the particles.

Consider dilute suspensions of rigid particles in an incompressible Newtonian flows at a low Reynolds number. Due to the low Reynolds number, the fluid is laminar. Hence

$$\mathbf{T}_t = \mathbf{0} \tag{7.31}$$

For dilute suspensions, the concentration of the particle approaches zero so that there is no particle collisions, consequently

$$\mathbf{T}_c = \mathbf{0} \tag{7.32}$$

Furthermore, driven by a laminar fluid motion and a stationary body force, particles do not fluctuate. In the absence of particle collision induced random motion, this implies

$$\mathbf{T}_k = \mathbf{0} \tag{7.33}$$

For the Newtonian fluid considered here there shear stress is well defined as

$$\mathbf{T}_\nu = \frac{\mu}{2}[\nabla \mathbf{v}_f + (\nabla \mathbf{v}_f)^{\mathrm{T}}] \tag{7.34}$$

The physical interpretation for $\mathbf{T}_p$ was first given by Batchelor [21, 143] using a volume averaging concept. The resulting stress has the following form

$$T_{p\,ij} = \frac{1}{V_0}\left(\int_{A_0} \Sigma_{ik} n_k r_j dA - \int_{V_0} \partial_k \Sigma_{ik} r_j dV\right) \tag{7.35}$$

where V_0 and A_0 are the volume and the surface of a single particle, Σ_{ik} the hydrodynamically induced local stress at dA on the surface of a particle or at dV in side a particle, n_k is the kth component of a unit outward normal on the particle's surface and r_j is the jth component of the position vector of the infinitesimals dA or dV. The averaged particle stress for uniform suspensions of ellipsoids with neglecting the inertia force is written as

$$\mathbf{T}_p = k\mathbf{A} : \mathbf{S} \tag{7.36}$$

in which $\mathbf{A}$ is the forth order orientation tensor of the particles, k a factor depending on the fiber length and the fiber concentration. The expression for k is

$$k = \frac{\pi \mu_f v L^3}{6 \ln 2L/d} f(\varepsilon) \tag{7.37}$$

where vL^3 the volume fraction of the particles, $f(\varepsilon) = \dfrac{1}{1 - 1.5\varepsilon}$, and $\varepsilon = [\ln 2L/d]^{-1}$. The concentration ratio of the particle in suspension is

$$\alpha = \pi d^2 L v/4 = \pi v L^3/(4\alpha_p^2) \tag{7.38}$$

in which $\alpha_p = L/d$ is the aspect ratio of the particle. It can be seen that the factor k depends more on the concentration ratio of the particles [107].

An alternative formulation of the solid phase stress is given by Hwang and Shen [141] based on the concept of utilizing a control surface and considering stress as the force per unit area on such a surface. The resulting formulation of this stress is identical to Batchelor's [21]. Because the stress components $\mathbf{T}_k$ and $\mathbf{T}_c$ are strictly modelled from the momentum transfer rate across a control surface, it is different from volume-averaging of internal solid stress. In order to be consistent with the concept of deriving $\mathbf{T}_k$ and $\mathbf{T}_c$, a control volume/control surface approach is adopted to derive the particle-presence stress $\mathbf{T}_p$ by Hwang and Shen [141]. The form of particle-presence stress is

$$T_{pij} = \frac{n}{\alpha}\left(\int_{A_0} \Sigma_{ik} n_k r_j dA - \int_{V_0} \partial_k \Sigma_{ik} r_j dV\right) \tag{7.39}$$

$$= \frac{1}{V_0}\left(\int_{A_0} \Sigma_{ik} n_k r_j dA - \int_{V_0} \partial_k \Sigma_{ik} r_j dV\right) \tag{7.40}$$

which is identical to Batchelor's [21] result for a slow flow of a dilute uniform fluid-solid mixture. For this flow, the particle-presence pressure is the form

$$p_p = \frac{R^3}{3V_0}\int_0^{2\pi}\int_0^{2\pi} p \sin\phi d\phi d\theta \tag{7.41}$$

7.5 Interfacial force

In [142], the derivation of the phase interaction term $\mathbf{M}_s$ is provided based on the same concept of control volume/control surface approach used in deriving $\mathbf{T}_p$. The form of $\mathbf{M}_s$ is

$$\mathbf{M}_s = \frac{\alpha}{V_0}\mathbf{h} - \nabla \cdot (\alpha \mathbf{T}_p) \tag{7.42}$$

where $\mathbf{h}$ is the hydrodynamic force, acting on a single particle, V_0 the volume of a single particle. For a dilute mixture, $\mathbf{h}$ is approximated by hydrodynamic forces of a single particle in an infinite fluid flow. With the additional assumption of low Reynolds number of the particle and fluid, $\mathbf{h}$ is composed of several contribution as the follows:

$$\mathbf{h} = \mathbf{f}_s + \mathbf{f}_a + V_0 \nabla \cdot \mathbf{T}_f \tag{7.43}$$

in which $\mathbf{f}_s$ is the Stokes drag acting on a particle, $\mathbf{f}_a$ the additional forces including the added mass effect, the Basset force [75] and the Saffman [144] force due to the fluid inertia. Substituting (7.43) into (7.42), the phase interaction is given by

$$\mathbf{M}_s = \frac{\alpha}{V_0}(\mathbf{f}_s + \mathbf{f}_a) + \alpha \nabla \cdot \mathbf{T}_f - \nabla \cdot (\alpha \mathbf{T}_p) \tag{7.44}$$

The analytical hydrodynamic force on a single particle suspending in unbounded creeping flows with a constant velocity gradient is derived in Chapter 2. Induced by the linear shear flow the particle may rotate and translate inside the flow. The hydrodynamic force described in the rotating coordinate system is

$$\mathbf{f}'_s = \mathbf{K}'(\mathbf{v}'_f - \mathbf{v}'_s) \tag{7.45}$$

where $\mathbf{v}'_f$ and $\mathbf{v}'_s$ are the velocities of the surrounding fluid and particle respectively, $\mathbf{K}'$ is a resistance tensor. If a spheroid suspending in linear shear flow with no slip boundary at the interface, $\mathbf{K}'$ is given as

$$\mathbf{K}' = -\frac{6}{5}\pi r_0 \mu \begin{pmatrix} -5+2\varepsilon & 0 & 0 \\ 0 & -5+2\varepsilon & 0 \\ 0 & 0 & -5+\varepsilon \end{pmatrix} \tag{7.46}$$

where ε is the deformation coefficient defined in Chapter 2. The hydrodynamic force described in the fixed coordinate system has the form

$$\begin{aligned} \mathbf{f}_s &= \mathbf{K}(\mathbf{v}_f - \mathbf{v}_s) && (7.47) \\ &= \mathbf{R}^{\mathrm{T}} \cdot \mathbf{K}' \cdot \mathbf{R}(\mathbf{v}_f - \mathbf{v}_s) && (7.48) \end{aligned}$$

in which $\mathbf{R}^{\mathrm{T}}$ is the transformation matrix between the rotating coordinate system and the fixed coordinate system, defined in (2.78). It is known that the orientation of the particle is defined by

$$\mathbf{p} = \begin{pmatrix} \sin\theta\sin\phi \\ -\sin\theta\cos\phi \\ \cos\theta \end{pmatrix} \tag{7.49}$$

Hence, the dyadic of **pp** is

$$\begin{aligned} \mathbf{a} &= \mathbf{pp} \\ &= \begin{pmatrix} \sin^2\theta\sin^2\phi & -\cos\phi\sin^2\theta\sin\phi & \cos\theta\sin\theta\sin\phi \\ -\cos\phi\sin^2\theta\sin\phi & \cos^2\phi\sin^2\theta & -\cos\theta\cos\phi\sin\theta \\ \cos\theta\sin\theta\sin\phi & -\cos\theta\cos\phi\sin\theta & \cos^2\theta \end{pmatrix} \end{aligned} \tag{7.50}$$

Substituting (2.78) into (7.47) and comparing with (7.50), then

$$\mathbf{K} = -\frac{6}{5}\pi r_0 \mu \left[(-5 + 2\varepsilon)\mathbf{I} - \varepsilon\mathbf{a}\right] \tag{7.51}$$

If the influence of addition force acting on spheroids is not considered for a general transient flow, the phase interfacial force can be written as the follows:

$$\mathbf{M}_s = \frac{\alpha}{V_0}[\mathbf{K}(\mathbf{v}_f - \mathbf{v}_s)] + \alpha\nabla\cdot\mathbf{T}_f - \nabla\cdot(\mathbf{T}_p) \tag{7.52}$$

where $V_0 = \frac{4}{3}\pi r_0^3(1-\varepsilon)$ for a spheroid. From (7.52), it can been seen that the interaction force on the particles depends on the velocity difference between the solid phase and the fluid phase, the averaged orientation of the particles, the viscous stress term, and the particle stress term. As discussed in Chapter 2, the variable ε in (7.51) is the deformation of a particle from a sphere. The **K** matrix is accurate to $O(\varepsilon^2)$. Hence, the model for the interfacial force on the particles shown by (7.52) is valid for a small number of ε.

7.6 Summery

A numerical model is developed to describe solid-fluid two phase flows using a continuum approach. A so-called Eulerian-Eulerian technique is adopted to deal with the motion of the spherical particles and Newtonian fluid. Based on the moments of the distribution function, the evolution of the second moment of the orientation tensor is used to govern the orientation of particles statistically. The concept of control volume/control surface method is used to develop closure models for the stresses and interfacial force on the particles. The model for the interfacial force is valid for small deformation of the particles from spheres.

CHAPTER 8

SIMULATION OF THE FLOW INDUCED FIBER ORIENTATION AND MIGRATION USING A FINITE ELEMENT METHOD

8.1 Governing equations for 2-dimension problems

8.1.1 Basic assumptions

In this chapter, a simple 2-dimensional problem is investigated by using the finite element method to solve the governing equations. According to the governing equations of the dilute suspension system introduced in Chapter 7, some further assumptions are taken into account to build the equations of motion for the 2-dimensional problems.

Velocities of the fluid and the particles in the x direction are assumed to be zeros. Particles rotates in the y-z plane induced by the surrounding flow fields. Due to their weak contributions the components of the orientation state **a**, i.g. a_{xy} and a_{xz} and the components of the particle stress term T_{pxx}, T_{pxy}, and T_{pxz} are assumed to be zeros. Even though the normal stress component T_{pxx} is not exact zeros for the FSQ closure model, it is negligible compared with the effect of the magnitudes of the other components, i.g. T_{pyy}, T_{pyz}, and T_{pzz}. According to the normalization condition of the orientation of a particle, the component of a_{xx} can be determined by $a_{xx} = 1 - a_{yy} - a_{zz}$. Therefore for 2-dimensional problems, both the velocity field of fluids and particles have two independent entries v_{fy}, v_{fz} and v_{sy}, v_{sz}; due to the symmetric property $a_{yz} = a_{zy}$ and the normalization condition $a_{xx} = 1 - a_{yy} - a_{zz}$, the average orientation tensor **a** has three independent entries, i.g. a_{yy}, a_{zz}, and a_{yz}; only three independent entries T_{pyy}, T_{pzz}, and T_{pyz} are evaluated for the particle stress term $\mathbf{T}_p$. Including the concentration ratio of the particles and the pressure of the fluid, there are totally **12** unknowns for the 2-dimensional suspension system, namely $v_{sy}, v_{sz}, v_{fy}, v_{fz}, T_{pyy}, T_{pzz}, T_{pyz}, a_{yy}, a_{zz}, a_{yz}, \alpha$, and p_f.

The fourth order orientation tensor **A** in (7.26) and (7.36) requires a closure model for it. The fully symmetry model [102, 103, 145] developed at Michigan State University is applied in the following simulations. This closure model retains all the six symmetry and projection properties of the fourth order tensor. Different forms of this model have been discussed in the work of Mandal [145]. Herein, only linear and quadratic terms in the fully symmetric model are considered (the so-called FSQ model) in implementing the equations. The coefficient C_2 in the FSQ model depends on the third invariant $\mathrm{III_b}$ of the anisotropic part of the averaged orientation tensor [111,112]. It has been noticed that when $C_2 = 0.37$, the closure model can provide pretty good results for simple shear flows as well as other different flow field, i.e.g. uniaxial flow [145]. For simplicity a constant value of $C_2 = 0.37$ is selected in the FSQ model.

The computed microstructure can be interpreted with the help of eigenvalues and eigenvectors of **a**. The eigenvalues of **a** has the property of $1/3 \leq \lambda \leq 1.0$, in which λ_{max} is the maximum eigenvalue in the domain. Furthermore, if $\lambda \simeq 1$ (i.e. $\lambda_{min} \simeq 0.0$), fibers are aligned in the direction of corresponding eigen vector. On the other hand, if $\lambda_{max} \simeq 1/3$ (i.e. $\lambda_{min} \simeq 1/3$), fibers are orientated randomly in all directions. Setting $\mathbf{e}_{max}$ as the normalized eigen vector associated with the maximum eigenvalue, the microstructure has been interpreted by plotting $\left(\lambda_{max} - \frac{1}{3}\right)/\frac{2}{3}$. This will result in a vector of zero length for a random orientation state and unit length for a uniaxial alignment state.

8.1.2 Governing equations

The simplified governing equations for the migration and alignment of ellipsoidal particles are presented below.

(1) **Continuity equation of solids**

Vector form:

$$\frac{\partial \alpha}{\partial t} + \nabla \cdot (\alpha \mathbf{v}_s) = 0 \tag{8.1}$$

Component form:

$$\frac{\partial \alpha}{\partial t} + \alpha\left(\frac{\partial v_{sy}}{\partial y} + \frac{\partial v_{sz}}{\partial z}\right) + \left(v_{sy}\frac{\partial \alpha}{\partial y} + v_{sz}\frac{\partial \alpha}{\partial z}\right) = 0 \tag{8.2}$$

(2) **Continuity equation of fluids**

Vector form:

$$\frac{\partial(1-\alpha)}{\partial t}+\nabla\cdot[(1-\alpha)\mathbf{v}_f]=0 \tag{8.3}$$

Component form:

$$-\frac{\partial\alpha}{\partial t}+(1-\alpha)\left(\frac{\partial v_{fy}}{\partial y}+\frac{\partial v_{fz}}{\partial z}\right)-\left(v_{fy}\frac{\partial\alpha}{\partial y}+v_{fz}\frac{\partial\alpha}{\partial z}\right)=0 \tag{8.4}$$

(3) **Momentum equations of solids**

Vector form:

$$\rho_s\alpha\left(\frac{\partial\mathbf{v}_s}{\partial t}+\mathbf{v}_s\cdot\nabla\mathbf{v}_s\right)-\frac{\alpha}{V_0}\mathbf{K}(\mathbf{v}_f-\mathbf{v}_s)-\alpha\nabla\cdot\left[-p_f\mathbf{I}+2\mu_f\nabla\mathbf{S}\right]-\rho_s\alpha\mathbf{g}=0 \tag{8.5}$$

$$\begin{aligned}&\rho_s\alpha\left(\frac{\partial v_{si}}{\partial t}+v_{sj}\frac{\partial v_{si}}{\partial x_j}\right)+\left(\frac{9\alpha\mu_f}{10r_0^2(1-\varepsilon)}\right)\left[(-5+2\varepsilon)\delta_{ij}-\varepsilon a_{ij}\right]\left(v_{fj}-v_{sj}\right)\\&-\alpha\frac{\partial}{\partial x_j}\left[-p_f\delta_{ij}+\mu_f\left(\frac{\partial v_{fi}}{\partial x_j}+\frac{\partial v_{fj}}{\partial x_i}\right)\right]-\rho_s\alpha g_i=0\end{aligned} \tag{8.6}$$

y-Component form:

$$\begin{aligned}&\rho_s\alpha\left(\frac{\partial v_{sy}}{\partial t}\right)+\rho_s\alpha\left(v_{sy}\frac{\partial v_{sy}}{\partial y}+v_{sz}\frac{\partial v_{sy}}{\partial z}\right)\\&+\left(\frac{9\alpha\mu_f}{10r_0^2(1-\varepsilon)}\right)\left[(-5+2\varepsilon)-\varepsilon a_{yy}\right]\left(v_{fy}-v_{sy}\right)+\left(\frac{9\alpha\mu_f}{10r_0^2(1-\varepsilon)}\right)\left[-\varepsilon a_{yz}\right]\left(v_{fz}-v_{sz}\right)\\&-\alpha\frac{\partial}{\partial y}\left[-p_f+\mu_f\left(\frac{\partial v_{fy}}{\partial y}+\frac{\partial v_{fy}}{\partial y}\right)\right]-\alpha\frac{\partial}{\partial z}\left[\mu_f\left(\frac{\partial v_{fy}}{\partial z}+\frac{\partial v_{fz}}{\partial y}\right)\right]-\rho_s\alpha g_y=0\end{aligned} \tag{8.7}$$

z-Component form:

$$\begin{aligned}&\rho_s\alpha\left(\frac{\partial v_{sz}}{\partial t}\right)+\rho_s\alpha\left(v_{sy}\frac{\partial v_{sz}}{\partial y}+v_{sz}\frac{\partial v_{sz}}{\partial z}\right)\\&+\left(\frac{9\alpha\mu_f}{10r_0^2(1-\varepsilon)}\right)\left[-\varepsilon a_{yz}\right]\left(v_{fy}-v_{sy}\right)+\left(\frac{9\alpha\mu_f}{10r_0^2(1-\varepsilon)}\right)\left[(-5+2\varepsilon)-\varepsilon a_{zz}\right]\left(v_{fz}-v_{sz}\right)\\&-\alpha\frac{\partial}{\partial y}\left[\mu_f\left(\frac{\partial v_{fz}}{\partial y}+\frac{\partial v_{fy}}{\partial z}\right)\right]-\alpha\frac{\partial}{\partial z}\left[-p_f+\mu_f\left(\frac{\partial v_{fz}}{\partial z}+\frac{\partial v_{fz}}{\partial z}\right)\right]-\rho_s\alpha g_z=0\end{aligned} \tag{8.8}$$

(4) **Momentum equations of fluids**

Vector form:

$$\rho_f(1-\alpha)\left(\frac{\partial \mathbf{v}_f}{\partial t}+\mathbf{v}_f\cdot\nabla\mathbf{v}_f\right)-(1-2\alpha)\nabla\cdot\left[-p_f\mathbf{I}+2\mu\nabla\mathbf{S}\right] \tag{8.9}$$

$$+\left[-p_f\mathbf{I}+2\mu\nabla\mathbf{S}\right]\cdot\nabla\alpha+\frac{\alpha}{V_0}\mathbf{K}(\mathbf{v}_f-\mathbf{v}_s)-\nabla\cdot\left(\alpha\mathbf{T}_p\right)-\rho_f(1-\alpha)\mathbf{g}=0$$

$$\rho_f(1-\alpha)\left(\frac{\partial v_{fi}}{\partial t}+v_{fj}\frac{\partial v_{fi}}{\partial x_j}\right)-(1-2\alpha)\frac{\partial}{\partial x_j}\left[-p_f\delta_{ij}+\mu_f\left(\frac{\partial v_{fi}}{\partial x_j}+\frac{\partial v_{fj}}{\partial x_i}\right)\right] \tag{8.10}$$

$$+\left[-p_f\delta_{ij}+\mu_f\left(\frac{\partial v_{fi}}{\partial x_j}+\frac{\partial v_{fj}}{\partial x_i}\right)\right]\frac{\partial\alpha}{\partial x_j}-\left(\frac{9\alpha\mu_f}{10r_0^2(1-\varepsilon)}\right)\left[(-5+2\varepsilon)\delta_{ij}-\varepsilon a_{ij}\right]\left(v_{fj}-v_{sj}\right)$$

$$-\alpha\frac{\partial}{\partial x_j}T_{pij}-T_{pij}\frac{\partial\alpha}{\partial x_j}-\rho_f(1-\alpha)g_i=0$$

y-Component form:

$$\rho_f(1-\alpha)\left(\frac{\partial v_{fy}}{\partial t}\right)+\rho_f(1-\alpha)\left(v_{fy}\frac{\partial v_{fy}}{\partial y}+v_{fz}\frac{\partial v_{fy}}{\partial z}\right) \tag{8.11}$$

$$-(1-2\alpha)\frac{\partial}{\partial y}\left[-p_f+\mu_f\left(\frac{\partial v_{fy}}{\partial y}+\frac{\partial v_{fy}}{\partial y}\right)\right]-(1-2\alpha)\frac{\partial}{\partial z}\left[\mu_f\left(\frac{\partial v_{fy}}{\partial z}+\frac{\partial v_{fz}}{\partial y}\right)\right]$$

$$+\left[-p_f+\mu_f\left(\frac{\partial v_{fy}}{\partial y}+\frac{\partial v_{fy}}{\partial y}\right)\right]\frac{\partial\alpha}{\partial y}+\left[\mu_f\left(\frac{\partial v_{fy}}{\partial z}+\frac{\partial v_{fz}}{\partial y}\right)\right]\frac{\partial\alpha}{\partial z}$$

$$-\left(\frac{9\alpha\mu_f}{10r_0^2(1-\varepsilon)}\right)\left[(-5+2\varepsilon)-\varepsilon a_{yy}\right]\left(v_{fy}-v_{sy}\right)-\left(\frac{9\alpha\mu_f}{10r_0^2(1-\varepsilon)}\right)\left[-\varepsilon a_{yz}\right]\left(v_{fz}-v_{sz}\right)$$

$$-\alpha\frac{\partial}{\partial y}T_{pyy}-\alpha\frac{\partial}{\partial z}T_{pyz}-T_{pyy}\frac{\partial\alpha}{\partial y}-T_{pyz}\frac{\partial\alpha}{\partial z}-\rho_f(1-\alpha)g_y=0$$

z-Component form:

$$\rho_f(1-\alpha)\left(\frac{\partial v_{fz}}{\partial t}\right)+\rho_f(1-\alpha)\left(v_{fy}\frac{\partial v_{fz}}{\partial y}+v_{fz}\frac{\partial v_{fz}}{\partial z}\right) \tag{8.12}$$

$$-(1-2\alpha)\frac{\partial}{\partial y}\left[\mu_f\left(\frac{\partial v_{fz}}{\partial y}+\frac{\partial v_{fy}}{\partial z}\right)\right]-(1-2\alpha)\frac{\partial}{\partial z}\left[-p_f+\mu_f\left(\frac{\partial v_{fz}}{\partial z}+\frac{\partial v_{fz}}{\partial z}\right)\right]$$

$$+\left[+\mu_f\left(\frac{\partial v_{fz}}{\partial y}+\frac{\partial v_{fy}}{\partial z}\right)\right]\frac{\partial\alpha}{\partial y}+\left[-p_f+\mu_f\left(\frac{\partial v_{fz}}{\partial z}+\frac{\partial v_{fz}}{\partial z}\right)\right]\frac{\partial\alpha}{\partial z}$$

$$-\left(\frac{9\alpha\mu_f}{10r_0^2(1-\varepsilon)}\right)\left[-\varepsilon a_{yz}\right]\left(v_{fy}-v_{sy}\right)-\left(\frac{9\alpha\mu_f}{10r_0^2(1-\varepsilon)}\right)\left[(-5+2\varepsilon)-\varepsilon a_{zz}\right]\left(v_{fz}-v_{sz}\right)$$

$$-\alpha\frac{\partial}{\partial y}T_{pyz}-\alpha\frac{\partial}{\partial z}T_{pzz}-T_{pyz}\frac{\partial\alpha}{\partial y}-T_{pzz}\frac{\partial\alpha}{\partial z}-\rho_f(1-\alpha)g_z=0$$

(5) **Particle stress**

Tensor form:

$$\mathbf{T}_p = k\mathbf{A} : \mathbf{S} \tag{8.13}$$

yy-Component form:

$$\begin{aligned}
T_{pyy} \quad & -\frac{1}{5}\left[-1 + C_2 + 2C_2\left(1 - a_{yy} - a_{zz}\right)^2\right]\frac{\partial v_{fy}}{\partial y} \\
& -\frac{1}{7}\left[-1 + C_2 + 2C_2\left(1 - a_{yy} - a_{zz}\right)^2\right]\frac{\partial v_{fz}}{\partial z} \\
& -\frac{a_{yy}}{35}\left[10\left(30 - 65C_2 + 94C_2a_{yy}\right)\frac{\partial v_{fy}}{\partial y} + \left(5 - 40C_2 + 35C_2a_{yy}\right)\frac{\partial v_{fz}}{\partial z}\right] \\
& -\frac{a_{zz}}{35}\left[\left(5 - 5C_2 + 35C_2a_{yy} + 4C_2a_{zz}\right)\frac{\partial v_{fy}}{\partial y}\right. \\
& \qquad \left. +10\left(1 - C_2 + 7C_2a_{yy} - C_2a_{zz}\right)\frac{\partial v_{fz}}{\partial z}\right] \\
& -\frac{3a_{yz}}{35}\left[\left(5 - 5C_2 + 25C_2a_{yy} - 10C_2a_{zz}\right)\left(\frac{\partial v_{fy}}{\partial z} + \frac{\partial v_{fz}}{\partial y}\right)\right. \\
& \qquad \left. +C_2a_{yz}\left(-14\frac{\partial v_{fy}}{\partial y} + 20\frac{\partial v_{fz}}{\partial z}\right)\right] = 0
\end{aligned} \tag{8.14}$$

zz-Component form:

$$\begin{aligned}
T_{pzz} \quad & -\frac{1}{7}\left[-1 + C_2 + 2C_2\left(1 - a_{yy} - a_{zz}\right)^2\right]\frac{\partial v_{fy}}{\partial y} \\
& -\frac{1}{5}\left[-1 + C_2 + 2C_2\left(1 - a_{yy} - a_{zz}\right)^2\right]\frac{\partial v_{fz}}{\partial z} \\
& -\frac{a_{yy}}{35}\left[10\left(1 - C_2 - C_2a_{yy}\right)\frac{\partial v_{fy}}{\partial y} + \left(5 - 5C_2 + 4C_2a_{yy}\right)\frac{\partial v_{fz}}{\partial z}\right]
\end{aligned} \tag{8.15}$$

$$\begin{aligned}
& -\frac{a_{zz}}{35}\left[5\left(1 - 8C_2 + 14C_2a_{yy} + 7C_2a_{zz}\right)\frac{\partial v_{fy}}{\partial y}\right. \\
& \qquad \left. +\left(30 - 65C_2 + 35C_2a_{yy} + 94C_2a_{zz}\right)\frac{\partial v_{fz}}{\partial z}\right] \\
& -\frac{3a_{yz}}{35}\left[\left(5 - 5C_2 - 10C_2a_{yy} + 25C_2a_{zz}\right)\left(\frac{\partial v_{fy}}{\partial z} + \frac{\partial v_{fz}}{\partial y}\right)\right. \\
& \qquad \left. +C_2a_{yz}\left(20\frac{\partial v_{fy}}{\partial y} - 14\frac{\partial v_{fz}}{\partial z}\right)\right] \\
& = 0
\end{aligned} \tag{8.16}$$

yz-Component form:

$$
\begin{aligned}
T_{pyz} \quad & -\frac{1}{35}\left[-1+C_2+2C_2\left(1-a_{yy}-a_{zz}\right)^2\right]\frac{\partial v_{fy}}{\partial z} \\
& -\frac{1}{35}\left[-1+C_2+2C_2\left(1-a_{yy}-a_{zz}\right)^2\right]\frac{\partial v_{fz}}{\partial y} \\
& -\frac{1}{35}\left[\left(5-5C_2-8C_2a_{yy}\right)\left(\frac{\partial v_{fy}}{\partial z}+\frac{\partial v_{fz}}{\partial y}\right)\right]a_{yy} \\
& -\frac{1}{35}\left[\left(5-5C_2+35C_2a_{yy}-8C_2a_{zz}\right)\left(\frac{\partial v_{fy}}{\partial z}+\frac{\partial v_{fz}}{\partial y}\right)\right]a_{zz} \\
& -\left[\frac{1}{7}\left(2-9C_2+24C_2a_{yy}+3C_2a_{zz}\right)\left(\frac{\partial v_{fy}}{\partial z}\right)+\frac{54}{35}C_2a_{yz}\left(\frac{\partial v_{fy}}{\partial z}+\frac{\partial v_{fz}}{\partial y}\right)\right. \\
& \qquad \left.+\frac{1}{7}\left(2-9C_2+3C_2a_{yy}+24C_2a_{zz}\right)\left(\frac{\partial v_{fz}}{\partial z}\right)\right]a_{yz} \\
& = 0
\end{aligned}
\tag{8.17}
$$

(6) **Orientation equations**

Vector form:

$$
\frac{\partial \mathbf{a}}{\partial t}+\mathbf{v}_f\cdot\nabla\mathbf{a}+\mathbf{W}\cdot\mathbf{a}+\mathbf{a}\cdot\mathbf{W}-\lambda\left(\mathbf{S}\cdot\mathbf{a}+\mathbf{a}\cdot\mathbf{S}-2\mathbf{S}:\mathbf{a}\right)=0 \tag{8.18}
$$

yy-Component form:

$$
\begin{aligned}
& \frac{\partial a_{yy}}{\partial t}+\left(v_{fy}\frac{\partial a_{yy}}{\partial y}+v_{fz}\frac{\partial a_{yy}}{\partial z}\right) \\
& +\frac{2\lambda}{35}\left[-1+C_2+2C_2\left(1-a_{yy}-a_{zz}\right)^2\right]\left(7\frac{\partial v_{fy}}{\partial y}+5\frac{\partial v_{fz}}{\partial z}\right) \\
& +\frac{2\lambda}{35}\left[\left(-5-65C_2+94C_2a_{yy}\right)\frac{\partial v_{fy}}{\partial y}+\left(5-8C_2+7C_2a_{yy}\right)\frac{\partial v_{fz}}{\partial z}\right]a_{yy} \\
& +\frac{2\lambda}{35}\left[\begin{array}{l}\left(5-5C_2+35C_2a_{yy}+4C_2a_{zz}\right)\frac{\partial v_{fy}}{\partial y} \\ +\left(10-10C_2+70C_2a_{yy}-10C_2a_{zz}\right)\frac{\partial v_{fz}}{\partial z}\end{array}\right]a_{zz} \\
& -\frac{1}{35}\left\{\begin{array}{l}12\lambda C_2a_{yz}\left(7\frac{\partial v_{fy}}{\partial y}-10\frac{\partial v_{fz}}{\partial z}\right) \\ -5\left[7+\lambda\left(-1-6C_2+30C_2a_{yy}-12C_2a_{zz}\right)\right]\frac{\partial v_{fz}}{\partial y} \\ +5\left[7+\lambda\left(1+6C_2-30C_2a_{yy}+12C_2a_{zz}\right)\right]\frac{\partial v_{fy}}{\partial z}\end{array}\right\}a_{yz} \\
& = 0
\end{aligned}
\tag{8.19}
$$

zz-Component form:

$$
\begin{aligned}
&\frac{\partial a_{zz}}{\partial t}+\left(v_{fy}\frac{\partial a_{zz}}{\partial y}+v_{fz}\frac{\partial a_{zz}}{\partial z}\right) \\
&+\frac{2\lambda}{35}\left[-1+C_2+2C_2\left(1-a_{yy}-a_{zz}\right)^2\right]\left(5\frac{\partial v_{fy}}{\partial y}+7\frac{\partial v_{fz}}{\partial z}\right) \\
&-\frac{2\lambda}{35}\left[\left(-10+10C_2+10C_2a_{yy}\right)\frac{\partial v_{fy}}{\partial y}+\left(-5+5C_2-4C_2a_{yy}\right)\frac{\partial v_{fz}}{\partial z}\right]a_{yy} \\
&+\frac{2\lambda}{35}\left[\begin{array}{l}\left(5-8C_2+14C_2a_{yy}+7C_2a_{zz}\right)\frac{\partial v_{fy}}{\partial y} \\ +\left(-5-65C_2+35C_2a_{yy}+94C_2a_{zz}\right)\frac{\partial v_{fz}}{\partial z}\end{array}\right]a_{zz} \\
&-\frac{1}{35}\left\{\begin{array}{l}12\lambda C_2a_{yz}\left(-10\frac{\partial v_{fy}}{\partial y}+7\frac{\partial v_{fz}}{\partial z}\right) \\ +5\left[-7+\lambda\left(1+6C_2+12C_2a_{yy}-30C_2a_{zz}\right)\right]\frac{\partial v_{fy}}{\partial z} \\ +5\left[7+\lambda\left(1+6C_2+12C_2a_{yy}-30C_2a_{zz}\right)\right]\frac{\partial v_{fz}}{\partial y}\end{array}\right\}a_{yz} \\
&=0
\end{aligned}
\tag{8.20}
$$

yz-Component form:

$$
\begin{aligned}
&\frac{\partial a_{yz}}{\partial t}+\left(v_{fy}\frac{\partial a_{yz}}{\partial y}+v_{fz}\frac{\partial a_{yz}}{\partial z}\right) \\
&+\frac{2\lambda}{35}\left[-1+C_2+2C_2\left(1-a_{yy}-a_{zz}\right)^2\right]\left(\frac{\partial v_{fy}}{\partial z}+\frac{\partial v_{fz}}{\partial y}\right) \\
&-\frac{1}{70}\left\{\begin{array}{l}\left[-35+\lambda\left(15+20C_2+32C_2a_{yy}\right)\right]\frac{\partial v_{fy}}{\partial z} \\ +\left[35+\lambda\left(15+20C_2+32C_2a_{yy}\right)\right]\frac{\partial v_{fz}}{\partial y}\end{array}\right\}a_{yy} \\
&-\frac{1}{70}\left\{\begin{array}{l}\left[-35+\lambda\left(15+20C_2+-140C_2a_{yy}+32C_2a_{zz}\right)\right]\frac{\partial v_{fz}}{\partial y} \\ +\left[35+\lambda\left(15+20C_2-140C_2a_{yy}+32C_2a_{zz}\right)\right]\frac{\partial v_{fy}}{\partial z}\end{array}\right\}a_{zz} \\
&+\frac{3\lambda}{35}\left\{\begin{array}{l}36C_2a_{yz}\left(\frac{\partial v_{fy}}{\partial z}+7\frac{\partial v_{fz}}{\partial y}\right) \\ +\left(-5-30C_2+80C_2a_{yy}+10C_2a_{zz}\right)\frac{\partial v_{fy}}{\partial y} \\ +\left(-5-30C_2+10C_2a_{yy}+80C_2a_{zz}\right)\frac{\partial v_{fz}}{\partial z}\end{array}\right\}a_{yz} \\
&=0
\end{aligned}
\tag{8.21}
$$

8.1.3 Boundary conditions

The boundary conditions imposed on the geometry are

(1) Dirichlet boundary conditions:

$$\mathbf{v}_{f/s} = \mathbf{f}_u \quad \text{on} \quad \Gamma_u \tag{8.22}$$

(2) Neumann boundary conditions:

$$\mathbf{t} = \left(-p\mathbf{I} + \mu_f\left[\left(\nabla\mathbf{v}_f\right) + \left(\nabla\mathbf{v}_f\right)^T\right]\right)\cdot\mathbf{n} \quad \text{on} \quad \Gamma_u \tag{8.23}$$

where $\mathbf{n}$ is the unit normal to the boundary and Γ_u and Γ_t are Dirichlet boundary and Neumann boundary and shown in Figure 8.2 [146].

8.2 Mixed finite element model

8.2.1 Weak form

The finite element method is used to solve this problem numerically. The starting point to develop the finite element models of (8.3)-(8.21) is their weak statements. The weak forms of (8.3)-(8.21) over an element Ω^e can be obtained by a three-step procedure. These steps are briefly reviewed here. First we multiply the differential equations with different wight functions, and integrate over the element. To distribute differentiation equally among all variables such that the finite element approximation functions satisfy the continuity requirement it is necessary to take integration by parts in the second step. The third step consists in expressing the boundary integral terms as functions of known quantities. The weak form development is shown below.

(1) Weak form of the momentum equation of solids

$$\int_{\Omega} \mathbf{W}_{vs} \left\{ \rho_s \alpha \left(\frac{\partial v_{si}}{\partial t} + v_{sj} \frac{\partial v_{si}}{\partial x_j} \right) \right\} d\Omega \tag{8.24}$$
$$+ \int_{\Omega} \mathbf{W}_{vs} \left\{ \left(\frac{9\alpha\mu_f}{10 r_0^2 (1-\varepsilon)} \right) \left[(-5 + 2\varepsilon)\delta_{ij} - \varepsilon a_{ij} \right] \left(v_{fj} - v_{sj} \right) - \rho_s \alpha g_i \right\} d\Omega$$
$$+ \int_{\Omega} \left\{ \frac{\partial \mathbf{W}_{vs}\alpha}{\partial x_j} \left[-p_f \delta_{ij} + \mu_f \left(\frac{\partial v_{fi}}{\partial x_j} + \frac{\partial v_{fj}}{\partial x_i} \right) \right] \right\} d\Omega - \int_{\Gamma} W_v \alpha t_i d\Gamma = 0$$

(2) Weak form of the momentum equation of fluids

$$\int_{\Omega} \mathbf{W}_{vf} \left\{ \rho_f (1-\alpha) \left(\frac{\partial v_{fi}}{\partial t} + v_{fj} \frac{\partial v_{fi}}{\partial x_j} \right) \right\} d\Omega \tag{8.25}$$
$$+ \int_{\Omega} \left\{ \frac{\partial \mathbf{W}_{vf}(1-2\alpha)}{\partial x_j} \left[-p_f \delta_{ij} + \mu_f \left(\frac{\partial v_{fi}}{\partial x_j} + \frac{\partial v_{fj}}{\partial x_i} \right) \right] \right\} d\Omega - \int_{\Gamma} W_{vf}(1-2\alpha) t_i d\Gamma$$
$$+ \int_{\Omega} \mathbf{W}_{vf} \left\{ \left[-p_f \delta_{ij} + \mu_f \left(\frac{\partial v_{fi}}{\partial x_j} + \frac{\partial v_{fj}}{\partial x_i} \right) \right] \frac{\partial \alpha}{\partial x_j} \right\} d\Omega$$
$$- \int_{\Omega} \mathbf{W}_{vf} \left\{ \left(\frac{9\alpha\mu_f}{10 r_0^2 (1-\varepsilon)} \right) \left[(-5 + 2\varepsilon)\delta_{ij} - \varepsilon a_{ij} \right] \left(v_{fj} - v_{sj} \right) \right\} d\Omega$$
$$- \int_{\Omega} \mathbf{W}_{vf} \left\{ \alpha \frac{\partial}{\partial x_j} T_{pij} - T_{pij} \frac{\partial \alpha}{\partial x_j} - \rho_f (1-\alpha) g_i \right\} d\Omega = 0$$

(3) Weak form of the particle stress

$$\int_{\Omega} \mathbf{W}_{Tp} \left\{ \mathbf{T}_p - k\mathbf{A} : \mathbf{S} \right\} d\Omega = 0 \tag{8.26}$$

(4) Weak form of the average orientation state

$$\int_{\Omega} \mathbf{W}_{\mathrm{a}} \left\{ \frac{\mathrm{D}\mathbf{a}}{\mathrm{D}t} + \mathbf{W} \cdot \mathbf{a} + \mathbf{a} \cdot \mathbf{W}^{\mathrm{T}} - \lambda (\mathbf{S} \cdot \mathbf{a} + \mathbf{a} \cdot \mathbf{S} - 2\mathbf{S} : \mathbf{A}) \right\} d\Omega = 0 \tag{8.27}$$

(5) Weak form of the continuity equation of solids

$$\int_{\Omega} \mathbf{W}_{\alpha} \left(\frac{\partial \alpha}{\partial t} + \nabla \cdot \alpha \mathbf{v}_s \right) d\Omega = 0 \tag{8.28}$$

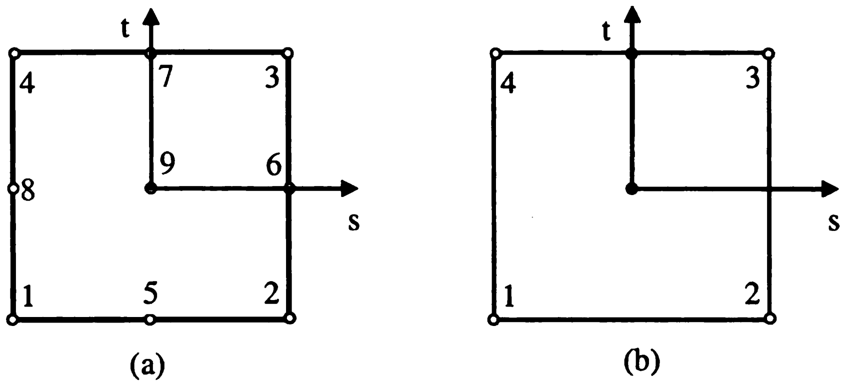

Figure 8.1. Quadrilateral elements used for the finite element model. (a) A nine-node bi-quadratic element is used for the shape function of velocities. (b) A four-node continuous-bilinear element is used for the shape function of the pressure of fluids.

(6) Weak form of the continuity equation of fluids

$$\int_{\Omega} -\mathbf{W}_{pf} \left[\frac{\partial(1-\alpha)}{\partial t} + \nabla \cdot (1-\alpha)\mathbf{v}_f \right] d\Omega = 0 \tag{8.29}$$

where $\mathbf{W}$ are the weight functions and the superscripts v_s, v_f, Tp, a, α, and pf denotes the weighting functions for the velocity of solids, velocity of fluids, particle stress, orientation tensor, concentration ratio, and pressure of fluids respectively.

8.2.2 Finite element model

Since Galerkin method is applied in finite element models, the same interpolation functions as the weight functions (isoparametric) are used to approximate the dependent variables v_{si}, v_{fi}, T_{pij}, a_{ij}, α, and p_f. Suppose the dependent variables are approximated by expansions of the form

$$v_{si} \approx \sum_{j=1}^{N_1} W_{vs}^j v_{si}^j = \mathbf{W}_{vs}^{\mathrm{T}} \mathbf{v}_{si} \tag{8.30}$$

$$v_{fi} \approx \sum_{j=1}^{N_2} W_{vf}^{j} v_{fi}^{j} = \mathbf{W}_{vf}^{\mathrm{T}} \mathbf{v}_{fi} \tag{8.31}$$

$$T_{p\,ij} \approx \sum_{j=1}^{N_3} W_{Tp}^{j} T_{pij}^{j} = \mathbf{W}_{T}^{\mathrm{T}} \mathbf{T}_{pij} \tag{8.32}$$

$$a_{ij} \approx \sum_{j=1}^{N_4} W_{a}^{j} \mathbf{a}^{j} = \mathbf{W}_{a}^{\mathrm{T}} \mathbf{a}_{ij} \tag{8.33}$$

$$\alpha \approx \sum_{j=1}^{N_5} W_{\alpha}^{j} \alpha_{j} = \mathbf{W}_{\alpha}^{\mathrm{T}} \alpha_{i} \tag{8.34}$$

$$p_f \approx \sum_{j=1}^{N_6} W_{p}^{j} p_{fj} = \mathbf{W}_{p}^{\mathrm{T}} \mathbf{p}_{fi} \tag{8.35}$$

Lagrangian type of polynomials are used for the interpolation functions. In order to prevent an overconstrained system of discrete equations, the interpolation functions for pressure should be at least one order lower than that used to velocities field to satisfy the LBB (Ladyzehskaya, Babuske, Brezzi) conditions [147]. For two-dimensional flows nine-node rectangular element shown in Figure 8.1(a). The velocity component, and other variables, i.g. particle stress tensor, and the orientation state tensor are approximated by bi-quadratic Lagrangian functions. These functions are expressed in terms of the normalized coordinates s, t for the element, which vary from -1 to 1, given as the following

$$N = \frac{1}{4} \begin{Bmatrix} (s^2 - s)(t^2 - t) \\ (s^2 + s)(t^2 - t) \\ (s^2 + s)(t^2 + t) \\ (s^2 - s)(t^2 + t) \\ 2(1 - s^2)(t^2 - t) \\ 2(s^2 + s)(1 - t^2) \\ 2(1 - s^2)(t^2 + t) \\ 2(s^2 - s)(1 - t^2) \\ 2(1 - s^2)(1 - t^2) \end{Bmatrix} \tag{8.36}$$

A 4-node continuous-bilinear element shown in Figure 8.1(b) is used to approximate the pressure of fluids. The bilinear interpolation functions are defined as

$$M = \frac{1}{4}\left\{\begin{array}{c} (1-s)(1-t) \\ (1+s)(1-t) \\ (1+s)(1+t) \\ (s^2-s)(t^2+t) \\ (1-s)(1+t) \end{array}\right\} \tag{8.37}$$

Substituting (8.30-8.35) to (8.24-8.29), we can get the matrix form of the weak from of the governing equations

$$\mathbf{M}\frac{\partial}{\partial t}\begin{pmatrix} v_{sy} \\ v_{sz} \\ v_{fy} \\ v_{fz} \\ T_{pyy} \\ T_{pzz} \\ T_{pyz} \\ a_{yy} \\ a_{zz} \\ a_{yz} \\ \alpha \\ p_f \end{pmatrix} + \mathbf{K}\begin{pmatrix} v_{sy} \\ v_{sz} \\ v_{fy} \\ v_{fz} \\ T_{pyy} \\ T_{pzz} \\ T_{pyz} \\ a_{yy} \\ a_{zz} \\ a_{yz} \\ \alpha \\ p_f \end{pmatrix} = \mathbf{F} \tag{8.38}$$

in which **M** is the mass matrix, **K** the stiffness matrix, and **F** the force vector. Their explicit forms are shown in Appendix A. Eq. (8.38) can be rewritten into a more symbolic format as

$$\mathbf{M}\dot{\mathbf{U}} + \mathbf{K}\mathbf{U} = \mathbf{F} \tag{8.39}$$

where

$$\mathbf{U} = \begin{pmatrix} v_{sy} & v_{sz} & v_{fy} & v_{fz} & T_{pyy} & T_{pzz} & T_{pyz} & a_{yy} & a_{zz} & a_{yz} & \alpha & p_f \end{pmatrix}^{\mathrm{T}} \tag{8.40}$$

In (8.40) there are 12 unknowns and 12 equations. Suitable boundary conditions and initial conditions are needed to solve this equation. The general form of (8.40) is nonlinear and time-dependent. Therefore, the first order backward difference scheme is applied with a relaxation factor of 0.5 and a Picard iterative method is adopted to obtain the solution. A finite element code is developed to predict the flow induced orientation and migration of suspensions in complex geometry by using Matlab7.0.

8.3 Simulation of a plane Poiseuille flow

Consider the slow flow with particle suspension between two long parallel plates at rest shown in Figure 8.2(a). This flow is driven by a pressure gradient in the axial direction. This kind of flow is often called a plane Poiseuille flow. When the length of the plate is very large compared to both the width and the distance between the plates, it is a case of a plane flow. 2H and 2L denote, respectively, the distance between and the length of the plates [see Figure 8.2]. At the inlet both of the velocity profiles for the fluids and particle V_0 have been specified as a parabolic function of z. Particles are ejected randomly at the inlet with the constant concentration ratio of 0.01 (a semidilute concentration if $L/d = 50$). The parameters associated with glycerin for the material of fluids and sand for the material of particles have been used in this problem, i.e. density of fluids $\rho_f = 1260kg/m^3$, density of solids $\rho_s = 2500kg/m^3$, dynamic viscosity of the fluid $\mu_f = 1.5Ns/m^2$. Due to the axial-symmetry in this problem, it suffices to model only half of the domain. BL, BR, BB, and BU shown in Figure 8.2(b) represent the left, right, bottom, and the upper boundary of the half domain respectively. The boundary conditions for the half domain are set as the

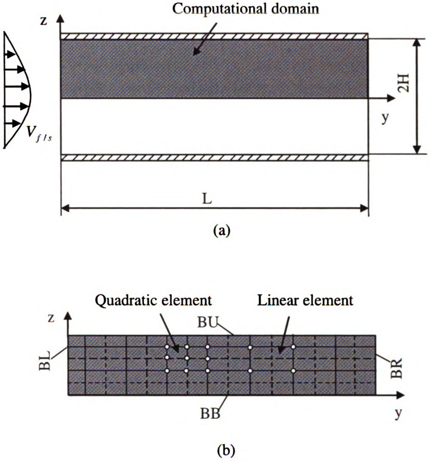

Figure 8.2. Domain and mesh for a plane Poiseuille flow with particle suspensions. (a) Geometry, computational domain, and (b) the finite element mesh used for the analysis of the slow flow with particle suspensions between parallel plates.

following:

At BL:

$$v_{fy} = v_{sy} = -\frac{z^2}{2} + \frac{H^2}{2} \tag{8.41}$$

$$v_{fz} = v_{sz} = -\frac{z^2}{2} + \frac{H^2}{2} \tag{8.42}$$

$$t_y = p_f \tag{8.43}$$

$$t_z = -\mu_f \frac{\partial v_{fy}}{\partial z} \tag{8.44}$$

$$\mathbf{a} = \begin{pmatrix} 1/3 & 0 & 0 \\ 0 & 1/3 & 0 \\ 0 & 0 & 1/3 \end{pmatrix} \quad \text{(random orientation)} \tag{8.45}$$

$$\alpha = 0.01 \tag{8.46}$$

At BR:

$$v_{sz} = v_{fz} = 0 \tag{8.47}$$

$$\frac{\partial v_{fy}}{\partial y} = \frac{\partial v_{sy}}{\partial y} = 0 \tag{8.48}$$

At BU:

$$v_{fy} = v_{sy} = 0 \tag{8.49}$$

$$v_{fz} = v_{sz} = 0 \tag{8.50}$$

$$t_y = 0 \tag{8.51}$$

$$t_z = -p_f \tag{8.52}$$

At BB:

$$v_{fz} = v_{sz} = 0 \tag{8.53}$$

$$\frac{\partial v_{fy}}{\partial z} = \frac{\partial v_{sy}}{\partial z} = 0 \tag{8.54}$$

$$t_y = 0 \tag{8.55}$$

$$t_z = p_f \tag{8.56}$$

In the mixed finite element model, it is necessary to specify the pressure at least at one node. In the present case, the node at $(y, z) = (L, 0)$ is specified to have zero pressure. All the fibers in the computational domain have been set initially random . At the initial time, the velocity of the fluids and solids are set to be the same parabolic function of z as the boundary condition at the inlet (BL).

In this problem the average Reynolds number is specified as 36 at the inlet and deformation coefficient $\varepsilon = 0.2$. The computational domain is meshed by $12 \times 6 = 96$ nine-node quadratic elements for the velocity variable, and $12 \times 6 = 96$ four-node bilinear elements for the pressure. Fiber orientation states at different time are shown in Figure 8.3. Dot points at the inlet and near the center line indicate that the fibers are randomly oriented at these regions. Away from the center line fibers become oriented faster and rotate inside the fluids (i.e. λ_{max} is higher near the wall than the center region). The particle stresses due to the presence of fibers depend on the orientation tensor $\mathbf{a}$ of the particles and the strain rate of the fluids. The contour of main eigenvalue of the particle stress and its corresponding eigenvector are shown in Figure 8.4. It can been seen that the main eigenvalue of the particle stress $\mathbf{T}_p$ is higher near the wall than the center region. Uniform suspension at the initial time is assumed for this problem. At different times, the concentration ratio α of the particles still keeps uniform shown in Figure 8.5. No migration is found for this case. The pressure fields are shown in the Figure 8.6 at different times. The pressure field is not same at any downstream cross section. The pressure is higher near the inlet than that

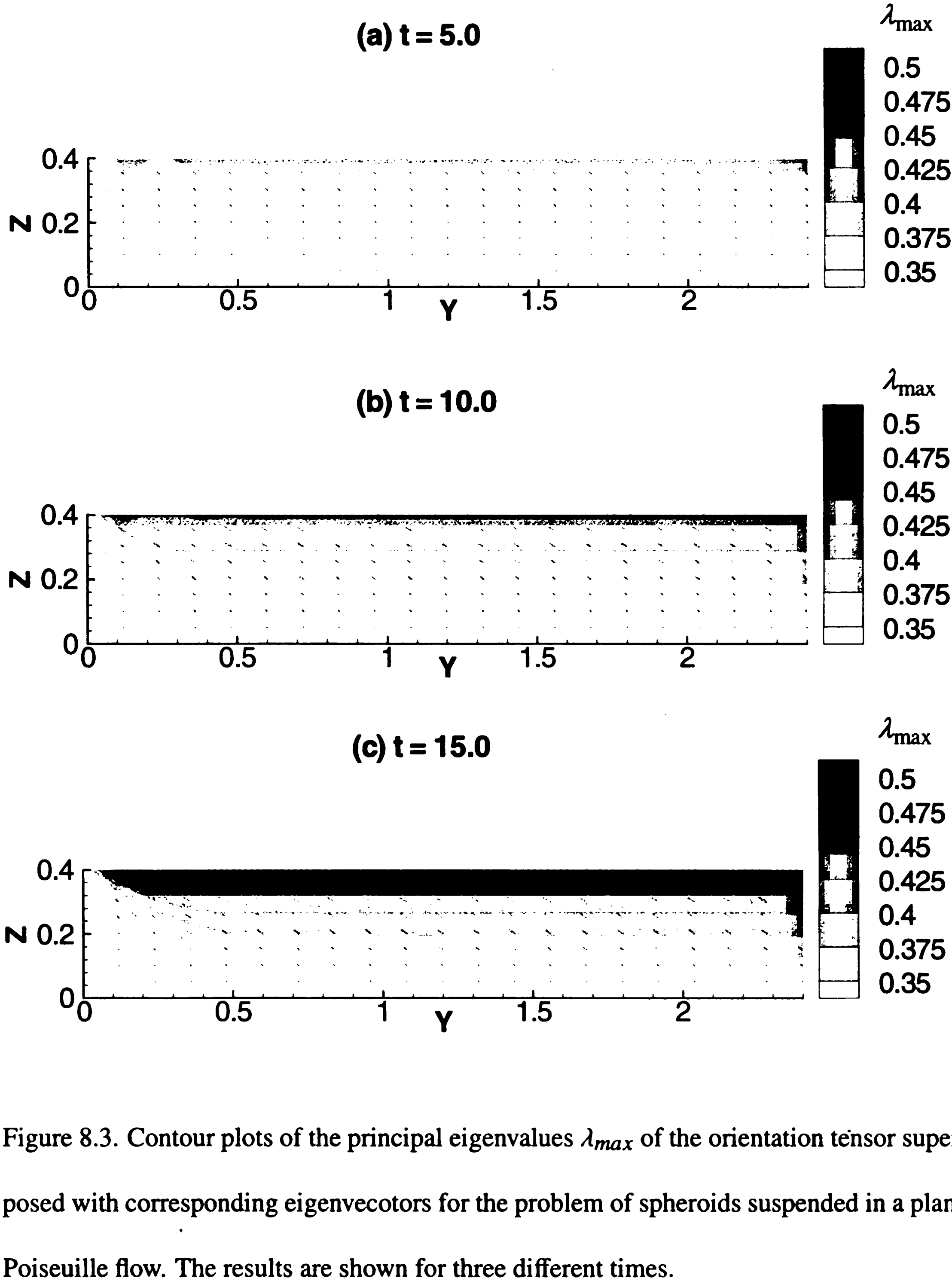

Figure 8.3. Contour plots of the principal eigenvalues λ_{max} of the orientation tensor superposed with corresponding eigenvecotors for the problem of spheroids suspended in a plane Poiseuille flow. The results are shown for three different times.

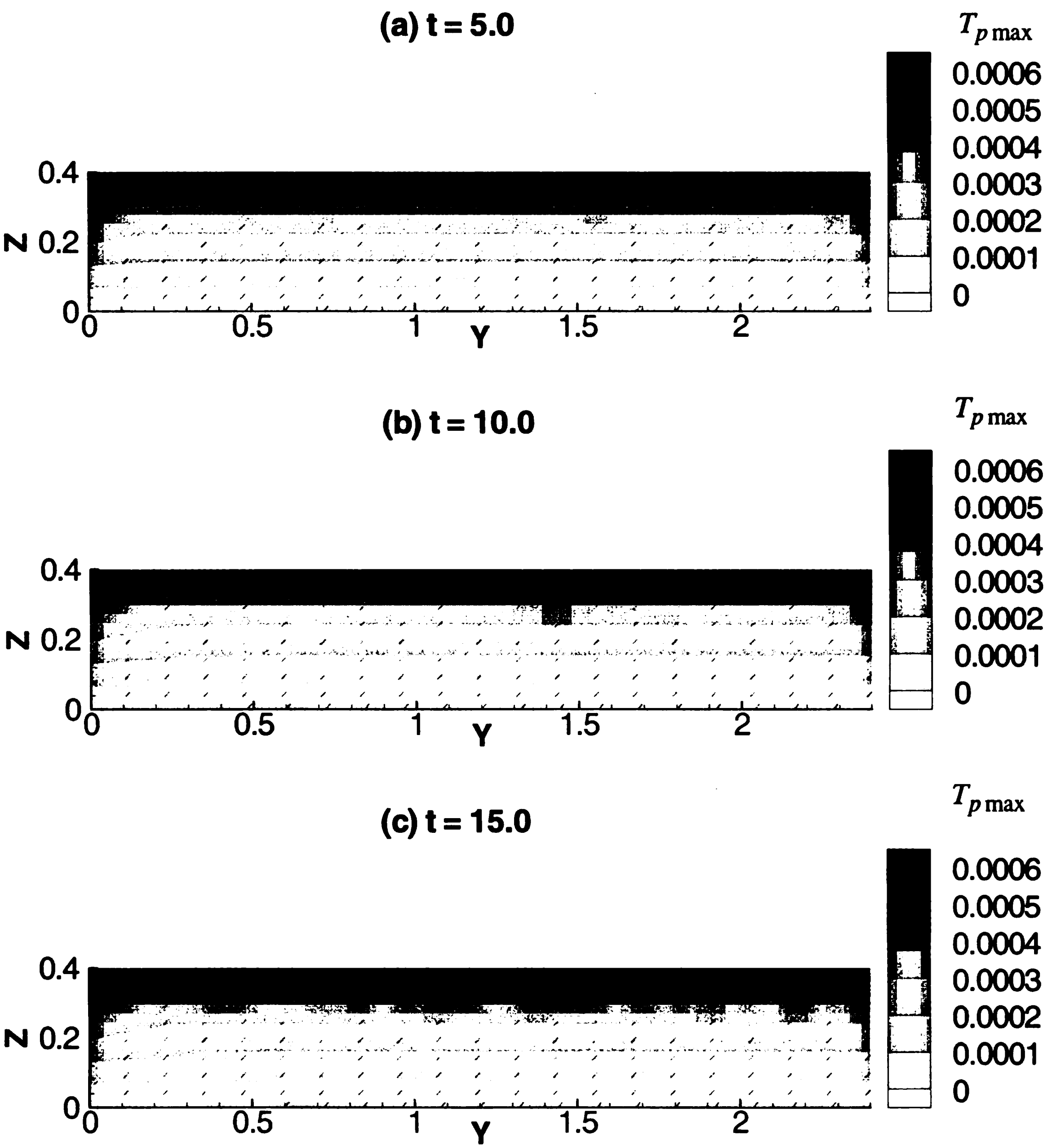

Figure 8.4. Contour plots of the principal eigenvalues T_{pmax} of the particle stress superposed with corresponding main eigenvecotors for the problem of spheroids suspended in a plane Poiseuille flow.

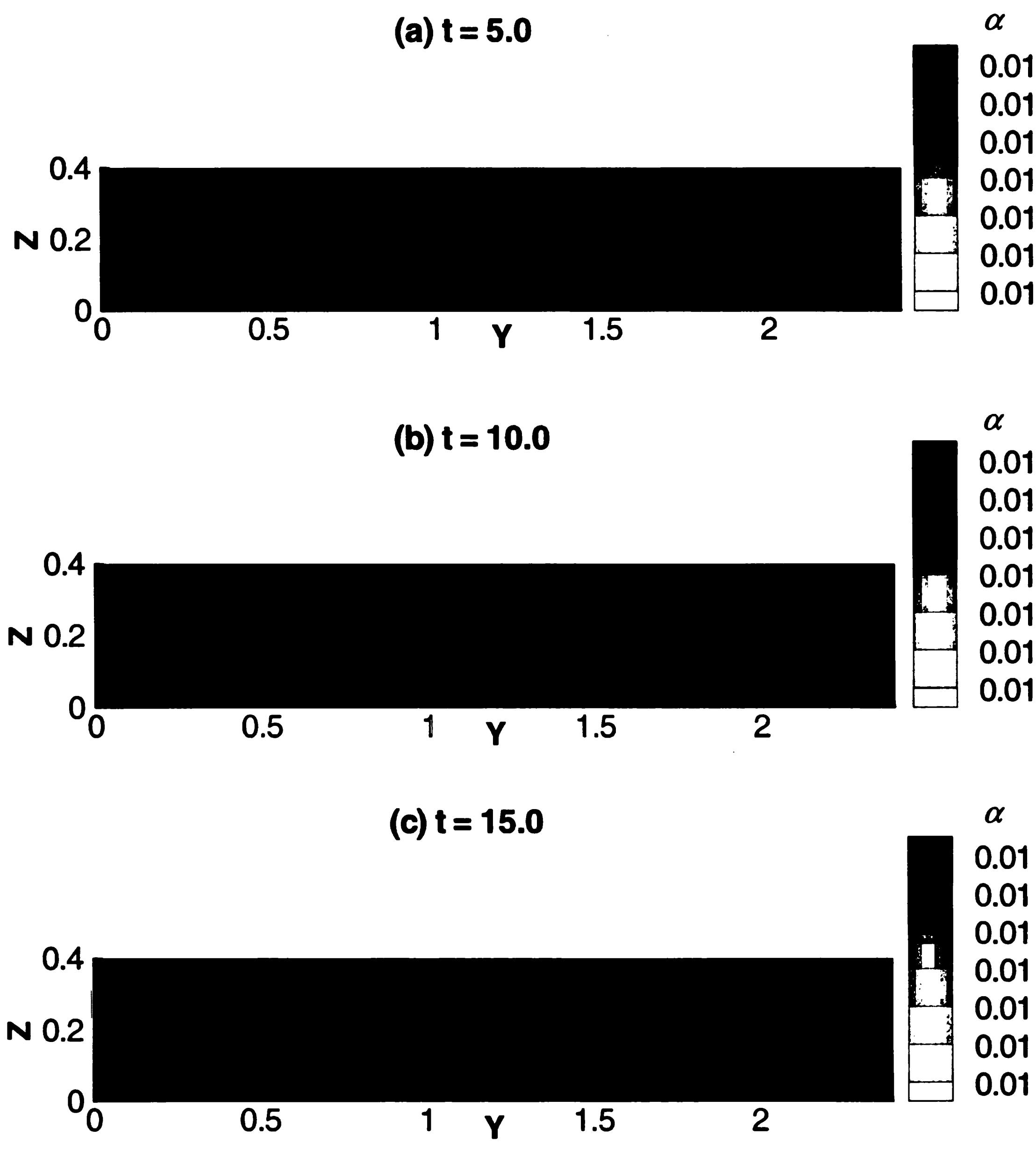

Figure 8.5. Contour plots of concentration of the particles α for the problem of spheroids suspended in a plane Poiseuille flow

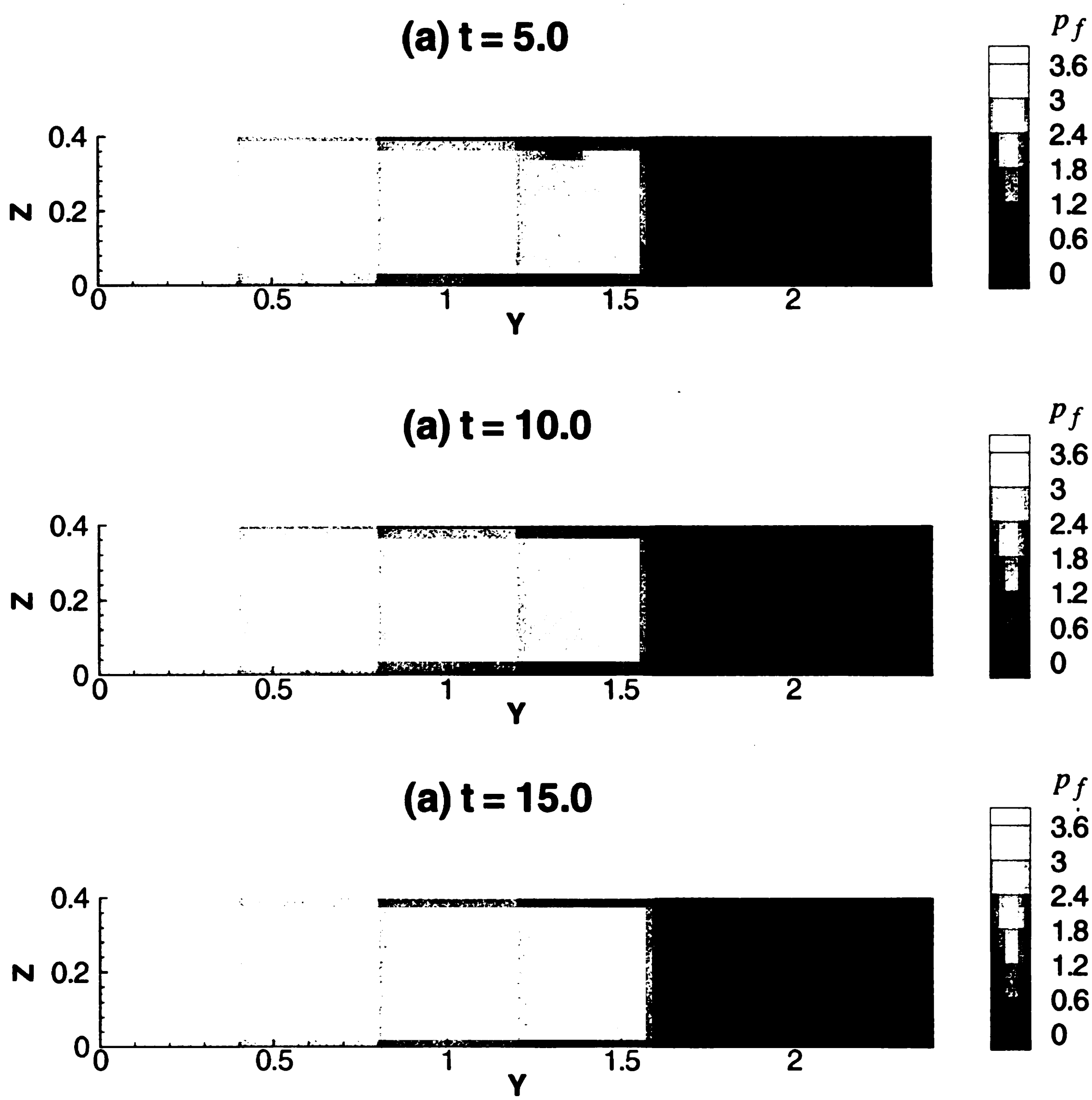

Figure 8.6. Contour plots of the fluid pressure p_f for the problem of spheroids suspended in a plane Poiseuille flow

near the outlet. The specified parabolic velocity profile at the inlet is changed a little in the downstream due to the particle stress, the fluid has some behaviors of non-Newtonian flow to some extents.

CHAPTER 9

SUMMARY AND CONCLUSIONS

In the first part of this dissertation, various factors affecting the hydrodynamics of a single particle suspended in a viscous fluid are studied. These factors include the presence of slip on the particle surface, the influence of flow fields, non-Newtonian viscosity, and the presence of inertia forces. The drag force and rotary motion of a single particle are analytically computed to study the effects of all these phenomena. In the second part, a closure model for the orientation tensor of nearly arbitrary shape particles is developed and a framework is proposed to estimate the alignment and spatial migration of spheroidal particles. The findings associated with these studies are presented below.

The dynamics of a rigid particle shaped as a slightly deformed sphere surface in creeping flows is studied with consideration of slip on the particle surface. Analytical expressions are obtained for the hydrodynamic force and torque exerted by the fluid on a deformed sphere using an asymptotic method wherein the normalized amplitude of the deviation from sphericity is assumed to be a small parameter. The Stokes' resistance calculated by this method is validated by comparing with existing solutions of the limiting cases of no slip and perfect slip. The analytical results for the axial and equatorial drag and torque on a slightly deformed spheroid reproduce previously reported results for three limiting cases: the perfect slip case, the no-slip case, and the case with an aspect ratio of unity (sphere). This new theory has thus the potential to account for the presence of slip in multiphase flows. In addition, the equations describing the motion of a deformed sphere with a slip surface induced by a simple shear flow are also derived and solved. The motion of the deformed sphere is shown to differ significantly from the no-slip case for low values of a dimensionless parameter that incorporates the coefficient of sliding friction. The period of the motion of a deformed sphere is longer, and for cases where the coefficient of sliding friction is low, the spheroid rotates to a fixed angle and reaches a steady orientation state.

Analytical expressions for the drag force on a slightly deformed sphere suspended in quadratic and cubic flows are derived by assuming that there is no slip on the interface between the particle and the surrounding fluid. For a slightly deformed sphere, no rotary motion is induced by the quadratic flow while periodic motion is induced by a cubic flow with no slip. Comparison with the motion of a deformed sphere in a linear shear flow reveals that the period of the motion of particle in a cubic flow is much longer if the same coefficients as for the cubic flow are used.

Consideration of inertial forces on the uniform motion of a particle can be achieved for a viscous flow by using Burgess' general solution for Oseen flows. No-slip and slip boundary conditions are considered on the interface between the particle and the fluid respectively. Two kinds of geometry of the particle,. a sphere and a slightly deformed sphere, are studied. Four cases are calculated respectively according to different boundary conditions on the interface and the shape of the particle. They are: (1) the motion of a sphere with nonslip,

(2) the motion of a sphere with slip, (3) the motion of a deformed sphere with no slip, and (4) the motion of a deformed sphere with slip. Both of the solutions for case (2), case (3) and case (4) can be reduced to the solution of case (1) by letting the slip coefficient β and the deformation coefficient ε equal to zero. The error between the solution of case (4) when the slip coefficient goes to ∞ and the solution of case (3) is negligible when the velocity and the diameter of the particle are small. The boundary condition at infinity is well satisfied and the boundary condition at the interface is approximately satisfied if the length dimension of the particle or the velocity of the particle is small.

It is well recognized that numerous fluids cannot be described by a Newtonian constitutive model and the influence of a non-Newtonian viscosity is studied by allowing the viscosity to vary with the shear rate. A Power-Law model is used to predict the viscosity of the fluid. The no-slip boundary condition is also applied on the interface. It is found that the non-Newtonian flow has much influence to the motion of a deformed sphere.

The consideration of particles of arbitrary shape as led to the development of a new closure model to complete the description of the motion of ensembles of rigid particles of complex shapes. Each particle is non-axisymmetric and its orientation is described with a second order tensor $< \mathbf{R} >$. An evolution equation for the second moment of the distribution function, which forms a fourth order tensor $< \mathbf{RR} >$, is used in order to obtain the average orientation of the particles in homogeneous flows. As suggested by Rallison (1978), the rotation operator is used to predict the microstructure of a suspension of rigid , non-axisymmetric particles as a state variable rather than the Euler angles. This dissertation has identified a closure for the 4th moment of the orientation distribution function in terms of the 2nd moment that satisfies all six-fold symmetry and projection properties of the exact the 4th moment.

In the last part of this work, models describing solid-liquid two-phase flows are developed using a continuum approach. A so-called Eulerian-Eulerian technique is adopted to deal with the motion and migration of the particles and the fluid. Based on the moments of the distribution function, the evolution of the second moment of the orientation tensor is used to govern the orientation of particles statistically. The concept of control volume/control surface method is used to develop closure models for the stresses and interfacial force. The Fully Symmetric Quadratic model, developed at Michigan State University, is applied to close the problem associated with computing the orientation tensor. A finite element code is developed to simulate the alignment and migration of dilute suspensions of spheroids in a flowing liquid. Simulations results for flow between two parallel plates show that at the inlet and near the center line the fibers are randomly oriented while away from the center line fibers become oriented faster and rotate inside the fluids and no migration is found for the plane Poiseuille flow.

APPENDICES

A. Tensor notation used in this dissertation

Dot product

Dot product of two vectors $(\mathbf{a}, \mathbf{b})$ is as the follows

$$\mathbf{a} \cdot \mathbf{b} = \sum_{i=1}^{3} a_i b_i = a_1 b_1 + a_2 b_2 + a_3 b_3 \tag{A-1}$$

Dot product of two second-order tensor $(\mathbf{A}, \mathbf{B})$ is as follows

$$\mathbf{A} \cdot \mathbf{B} = \sum_{i=1}^{3} \sum_{l=1}^{3} \mathbf{e}_i \mathbf{e}_l \left(\sum_{j=1}^{3} A_{ij} B_{jl} \right) \tag{A-2}$$

$$= \begin{pmatrix} A_{11}B_{11} + A_{12}B_{21} + A_{13}B_{31} & A_{11}B_{12} + A_{12}B_{22} + A_{13}B_{32} & A_{11}B_{13} + A_{12}B_{23} + A_{13}B_{33} \\ A_{21}B_{11} + A_{22}B_{21} + A_{23}B_{31} & A_{21}B_{12} + A_{22}B_{22} + A_{23}B_{32} & A_{21}B_{13} + A_{22}B_{23} + A_{23}B_{33} \\ A_{31}B_{11} + A_{32}B_{21} + A_{33}B_{31} & A_{31}B_{12} + A_{32}B_{22} + A_{33}B_{32} & A_{31}B_{13} + A_{32}B_{23} + A_{33}B_{33} \end{pmatrix}$$

Double dot product

Double dot product of two second-order tensor $(\mathbf{A}, \mathbf{B})$ is as follows

$$\begin{aligned} \mathbf{A} : \mathbf{B} = & \sum_{i=1}^{3} \sum_{j=1}^{3} A_{ij} B_{ji} \\ = & A_{11}B_{11} + A_{12}B_{21} + A_{13}B_{31} \\ & + A_{21}B_{21} + A_{22}B_{22} + A_{23}B_{32} \\ & + A_{31}B_{13} + A_{32}B_{23} + A_{33}B_{33} \end{aligned} \tag{A-3}$$

Double dot product of two fourth-order tensor $(\mathbf{A}, \mathbf{B})$ is as follows

$$\mathbf{A} : \mathbf{B} = \sum_{i=1}^{3} \sum_{\alpha=1}^{3} \sum_{l=1}^{3} \sum_{\delta=1}^{3} \mathbf{e}_i \mathbf{e}_\alpha \mathbf{e}_l \mathbf{e}_\delta \left(\sum_{j=1}^{3} \sum_{\beta=1}^{3} A_{i\alpha j\beta} B_{\beta jl\delta} \right) \tag{A-4}$$

Dyadic product

Dyadic product of two vectors $(\mathbf{x}, \mathbf{y})$ is as follows

$$\mathbf{a} \otimes \mathbf{b} = \sum_{i=1}^{3}\sum_{j=1}^{3} x_i y_j \mathbf{e}_i \mathbf{e}_j \tag{A-5}$$

$$= \begin{pmatrix} a_1b_1 & a_1b_2 & a_1b_3 \\ a_2b_1 & a_2b_2 & a_2b_3 \\ a_3b_1 & a_3b_2 & a_3b_3 \end{pmatrix}$$

Dyadic product of two second-order tensors $(\mathbf{A}, \mathbf{B})$ is as follows

$$\mathbf{A} \otimes \mathbf{B} = \sum_{i}^{3}\sum_{\alpha}^{3}\sum_{j}^{3}\sum_{\beta}^{3} A_{i\alpha}\, B_{j\beta}\, \mathbf{e}_i\, \mathbf{e}_\alpha\, \mathbf{e}_j\, \mathbf{e}_\beta = \tag{A-6}$$

$$\begin{pmatrix}
A_{11}B_{11} & A_{11}B_{12} & A_{11}B_{13} & A_{12}B_{11} & A_{12}B_{12} & A_{12}B_{13} & A_{13}B_{11} & A_{13}B_{12} & A_{13}B_{13} \\
A_{11}B_{21} & A_{11}B_{22} & A_{11}B_{23} & A_{12}B_{21} & A_{12}B_{22} & A_{12}B_{23} & A_{13}B_{21} & A_{13}B_{22} & A_{13}B_{23} \\
A_{11}B_{31} & A_{11}B_{32} & A_{11}B_{33} & A_{12}B_{31} & A_{12}B_{32} & A_{12}B_{33} & A_{13}B_{31} & A_{13}B_{32} & A_{13}B_{33} \\
A_{21}B_{11} & A_{21}B_{12} & A_{21}B_{13} & A_{22}B_{11} & A_{22}B_{12} & A_{22}B_{13} & A_{23}B_{11} & A_{23}B_{12} & A_{23}B_{13} \\
A_{21}B_{21} & A_{21}B_{22} & A_{21}B_{23} & A_{22}B_{21} & A_{22}B_{22} & A_{22}B_{23} & A_{23}B_{21} & A_{23}B_{22} & A_{23}B_{23} \\
A_{21}B_{31} & A_{21}B_{32} & A_{21}B_{33} & A_{22}B_{31} & A_{22}B_{32} & A_{22}B_{33} & A_{23}B_{31} & A_{23}B_{32} & A_{23}B_{33} \\
A_{31}B_{11} & A_{31}B_{12} & A_{31}B_{13} & A_{32}B_{11} & A_{32}B_{12} & A_{32}B_{13} & A_{33}B_{11} & A_{33}B_{12} & A_{33}B_{13} \\
A_{31}B_{21} & A_{31}B_{22} & A_{31}B_{23} & A_{32}B_{21} & A_{32}B_{22} & A_{32}B_{23} & A_{33}B_{21} & A_{33}B_{22} & A_{33}B_{23} \\
A_{31}B_{31} & A_{31}B_{32} & A_{31}B_{33} & A_{32}B_{31} & A_{32}B_{32} & A_{32}B_{33} & A_{33}B_{31} & A_{33}B_{32} & A_{33}B_{33}
\end{pmatrix}$$

Dyadic product of two fourth-order tensors $(\mathbf{A}, \mathbf{B})$ is as follows

$$\mathbf{A} \otimes \mathbf{B} = \sum_{i}^{3}\sum_{\alpha}^{3}\sum_{j}^{3}\sum_{\beta}^{3}\sum_{k}^{3}\sum_{\gamma}^{3}\sum_{l}^{3}\sum_{\delta}^{3} A_{i\alpha j\beta}\, B_{k\gamma l\delta}\, \mathbf{e}_i\, \mathbf{e}_\alpha\, \mathbf{e}_j\, \mathbf{e}_\beta\, \mathbf{e}_k\, \mathbf{e}_\gamma\, \mathbf{e}_l\, \mathbf{e}_\delta \tag{A-7}$$

B. Matrix form of the weak form of the governing equations

Mass matrix $\mathbf{M}$

$$\mathbf{M} = \begin{bmatrix} M^{1,1} & 0 & 0 & 0 & 0 & 0 & 0 & 0 & 0 & 0 & 0 & 0 \\ 0 & M^{2,2} & 0 & 0 & 0 & 0 & 0 & 0 & 0 & 0 & 0 & 0 \\ 0 & 0 & M^{3,3} & 0 & 0 & 0 & 0 & 0 & 0 & 0 & 0 & 0 \\ 0 & 0 & 0 & M^{4,4} & 0 & 0 & 0 & 0 & 0 & 0 & 0 & 0 \\ 0 & 0 & 0 & 0 & 0 & 0 & 0 & 0 & 0 & 0 & 0 & 0 \\ 0 & 0 & 0 & 0 & 0 & 0 & 0 & 0 & 0 & 0 & 0 & 0 \\ 0 & 0 & 0 & 0 & 0 & 0 & 0 & 0 & 0 & 0 & 0 & 0 \\ 0 & 0 & 0 & 0 & 0 & 0 & 0 & M^{8,8} & 0 & 0 & 0 & 0 \\ 0 & 0 & 0 & 0 & 0 & 0 & 0 & 0 & M^{9,9} & 0 & 0 & 0 \\ 0 & 0 & 0 & 0 & 0 & 0 & 0 & 0 & 0 & M^{10,10} & 0 & 0 \\ 0 & 0 & 0 & 0 & 0 & 0 & 0 & 0 & 0 & 0 & M^{11,11} & 0 \\ 0 & 0 & 0 & 0 & 0 & 0 & 0 & 0 & 0 & 0 & M^{12,11} & 0 \end{bmatrix} \tag{B-1}$$

Entries of the mass matrix

$$M^{1,1} = \int_\Omega W_{vs}\rho_s(W_\alpha^{\mathrm{T}}\alpha)W_{vs}^{\mathrm{T}}d\Omega \tag{B-2}$$

$$M^{2,2} = \int_\Omega W_{vs}\rho_s(W_\alpha^{\mathrm{T}}\alpha)W_{vs}^{\mathrm{T}}d\Omega \tag{B-3}$$

$$M^{3,3} = \int_\Omega W_{vf}\rho_f(1 - W_\alpha^{\mathrm{T}}\alpha)W_{vf}^{\mathrm{T}}d\Omega \tag{B-4}$$

$$M^{4,4} = \int_\Omega W_{vf}\rho_f(1 - W_\alpha^{\mathrm{T}}\alpha)W_{vf}^{\mathrm{T}}d\Omega \tag{B-5}$$

$$M^{8,8} = \int_\Omega W_a W_a^{\mathrm{T}}d\Omega \tag{B-6}$$

$$M^{9,9} = \int_\Omega W_a W_a^{\mathrm{T}}d\Omega \tag{B-7}$$

$$M^{10,10} = \int_\Omega W_a W_a^{\mathrm{T}}d\Omega \tag{B-8}$$

$$M^{11,11} = \int_\Omega W_\alpha W_\alpha^{\mathrm{T}}d\Omega \tag{B-9}$$

$$M^{12,11} = \int_{\Omega} W_{\alpha} W_{\alpha}^{\mathrm{T}} d\Omega \tag{B-10}$$

Stiffness matrix **K**

$$\mathbf{K} = \begin{pmatrix} K^{1,1} & K^{1,2} & K^{1,3} & K^{1,4} & 0 & 0 & 0 & 0 & 0 & 0 & 0 & K^{1,12} \\ K^{2,1} & K^{2,2} & K^{2,3} & K^{2,4} & 0 & 0 & 0 & 0 & 0 & 0 & 0 & K^{2,12} \\ K^{3,1} & K^{3,2} & K^{3,3} & K^{3,4} & K^{3,5} & 0 & K^{3,7} & 0 & 0 & 0 & K^{3,11} & K^{3,12} \\ K^{4,1} & K^{4,2} & K^{4,3} & K^{4,4} & 0 & K^{4,6} & K^{4,7} & 0 & 0 & 0 & K^{4,11} & K^{4,12} \\ 0 & 0 & K^{5,3} & K^{5,4} & K^{5,5} & 0 & 0 & K^{5,8} & K^{5,9} & K^{5,10} & 0 & 0 \\ 0 & 0 & K^{6,3} & K^{6,4} & 0 & K^{6,6} & 0 & K^{6,8} & K^{6,9} & K^{6,10} & 0 & 0 \\ 0 & 0 & K^{7,3} & K^{7,4} & 0 & 0 & 0 & K^{7,8} & K^{7,9} & K^{7,10} & 0 & 0 \\ 0 & 0 & K^{8,3} & K^{8,4} & 0 & 0 & 0 & K^{8,8} & K^{8,9} & K^{8,10} & 0 & 0 \\ 0 & 0 & K^{9,3} & K^{9,4} & 0 & 0 & 0 & K^{9,8} & K^{9,9} & K^{9,10} & 0 & 0 \\ 0 & 0 & K^{10,3} & K^{10,4} & 0 & 0 & 0 & K^{10,8} & K^{10,9} & K^{10,10} & 0 & 0 \\ K^{11,1} & K^{11,2} & 0 & 0 & 0 & 0 & 0 & 0 & 0 & 0 & K^{11,11} & 0 \\ 0 & 0 & K^{12,3} & K^{12,4} & 0 & 0 & 0 & 0 & 0 & 0 & K^{12,11} & 0 \end{pmatrix} \tag{B-11}$$

Entries of the stiffness matrix

$$\begin{aligned} K^{1,1} = & \int_{\Omega} W_{vs}\rho_s\alpha\left(\left(W_{vs}^{\mathrm{T}}v_{sy}\right)\frac{\partial W_{vs}^{\mathrm{T}}}{\partial y} + \left(W_{vs}^{\mathrm{T}}v_{sz}\right)\frac{\partial W_{vs}^{\mathrm{T}}}{\partial z}\right)d\Omega \\ & + \int_{\Omega} W_{vs}^{\mathrm{T}}\frac{9(W_{\alpha}^{\mathrm{T}}\alpha)\mu}{10r_0^2(1-\varepsilon)}\left[(-5+2\varepsilon) - \varepsilon(W_a^{\mathrm{T}}a_{yy})\right](-W_{vs}^{\mathrm{T}})d\Omega \end{aligned} \tag{B-12}$$

$$K^{1,2} = \int_{\Omega} W_{vs}^{\mathrm{T}}\frac{9(W^{\alpha^{\mathrm{T}}}\alpha)\mu}{10r_0^2(1-\varepsilon)}\left[\varepsilon(W_a^{\mathrm{T}}a_{yz})\right](-W_{vs}^{\mathrm{T}})d\Omega \tag{B-13}$$

$$\begin{aligned} K^{1,3} = & \int_{\Omega} W_{vs}\frac{9(W_{\alpha}^{\mathrm{T}}\alpha)\mu}{10r_0^2(1-\varepsilon)}\left[(-5+2\varepsilon) - \varepsilon(W_a^{\mathrm{T}}a_{yy})\right](-W_{vf}^{\mathrm{T}})d\Omega \\ & + \int_{\Omega}\left[\frac{\partial W_{vs}}{\partial y}(W_{\alpha}^{\mathrm{T}}\alpha) + W_{vs}\left(\frac{\partial W_{\alpha}^{\mathrm{T}}}{\partial y}\alpha\right)\right]2\mu\frac{\partial W_{vs}^{\mathrm{T}}}{\partial y}d\Omega \\ & + \int_{\Omega}\left[\frac{\partial W_{vs}}{\partial z}(W_{\alpha}^{\mathrm{T}}\alpha) + W_{vs}\left(\frac{\partial W_{vf}^{\mathrm{T}}}{\partial z}\right)\right]\mu\frac{\partial W_{vf}^{\mathrm{T}}}{\partial z}d\Omega \end{aligned} \tag{B-14}$$

$$K^{1,4} = +\int_{\Omega}\left[\frac{\partial W_{vs}}{\partial z}(W_{\alpha}^{\mathrm{T}}\alpha) + W_{vs}\left(\frac{\partial W_{vf}^{\mathrm{T}}}{\partial z}\right)\right]\mu\frac{\partial W_{vf}^{\mathrm{T}}}{\partial y} \tag{B-15}$$

$$+\int_{\Omega} W_{vs}\frac{9(W_{\alpha}^{\mathrm{T}}\alpha)\mu}{10r_0^2(1-\varepsilon)}\left[\varepsilon(W_a^{\mathrm{T}}a_{yz})W_{vf}^{\mathrm{T}}\right]d\Omega$$

$$K^{2,1} = -\int_{\Omega} W_{vs}\frac{9(W_{\alpha}^{\mathrm{T}}\alpha)\mu}{10r_0^2(1-\varepsilon)}\left[\varepsilon(W_a^{\mathrm{T}}a_{yz})\right]\left(-W_{vs}^{\mathrm{T}}\right)d\Omega\, v_{sy} \tag{B-16}$$

$$K^{2,2} = +\int_{\Omega} W_{vs}\rho_s\left(W_{\alpha}^{\mathrm{T}}\alpha\right)\left(\left(W_{vs}^{\mathrm{T}}v_{sy}\right)\frac{\partial W_{vs}^{\mathrm{T}}}{\partial y} + \left(W_{vs}^{\mathrm{T}}v_{sz}\right)\frac{\partial W_{vs}^{\mathrm{T}}}{\partial z}\right)d\Omega\, v_{sz} \tag{B-17}$$

$$+\int_{\Omega} W_{vs}\frac{9(W_{\alpha}^{\mathrm{T}}\alpha)\mu}{10r_0^2(1-\varepsilon)}\left[(-5+2\varepsilon) - \varepsilon(W_a^{\mathrm{T}}a_{zz})\right]\left(-W_{vs}^{\mathrm{T}}\right)d\Omega$$

$$K^{2,3} = +\int_{\Omega}\left[\frac{\partial W_{vs}}{\partial y}\left(W_{\alpha}^{\mathrm{T}}\alpha\right) + W_{vs}\left(\frac{\partial W_{\alpha}^{\mathrm{T}}}{\partial y}\alpha\right)\right]\left[+\mu\left(\frac{\partial W_{vf}^{\mathrm{T}}}{\partial z}\right)\right]d\Omega \tag{B-18}$$

$$+\int_{\Omega} W_{vs}\frac{9(W_{\alpha}^{\mathrm{T}}\alpha)\mu}{10r_0^2(1-\varepsilon)}\left[\varepsilon\left(W_{\alpha}^{\mathrm{T}}\alpha_{yz}\right)\right]\left(-W_{vf}^{\mathrm{T}}\right)d\Omega$$

$$-\int_{\Gamma_L} W_{vs}(W_{\alpha}^{\mathrm{T}}\alpha)\left(-\mu\frac{\partial W_{vf}^{\mathrm{T}}}{\partial z}\right)d\Gamma$$

$$K^{2,4} = +\int_{\Omega} W_{vs}^{\mathrm{T}}\frac{9(W_{\alpha}^{\mathrm{T}}\alpha)\mu}{10r_0^2(1-\varepsilon)}\left[(-5+2\varepsilon) - \varepsilon\left(W_{\alpha}^{\mathrm{T}}\alpha_{zz}\right)\right]\left(W_{vf}^{\mathrm{T}}\right)d\Omega \tag{B-19}$$

$$\int_{\Omega}\left[\frac{\partial W_{vs}}{\partial y}\left(W_{\alpha}^{\mathrm{T}}\alpha\right) + W_{vs}\left(\frac{\partial W_{\alpha}^{\mathrm{T}}}{\partial y}\alpha\right)\right]\left[+\mu\left(\frac{\partial W_{vf}^{\mathrm{T}}}{\partial y}\right)\right]d\Omega$$

$$\int_{\Omega}\left[\frac{\partial W_{vs}}{\partial z}\left(W_{\alpha}^{\mathrm{T}}\alpha\right) + W_{vs}\left(\frac{\partial W_{\alpha}^{\mathrm{T}}}{\partial z}\alpha\right)\right]\left[+2\mu\left(\frac{\partial W_{vf}^{\mathrm{T}}}{\partial z}\right)\right]d\Omega$$

$$K^{2,12} = \int_{\Omega}\left[\frac{\partial W_{vs}}{\partial z}\left(W_{\alpha}^{\mathrm{T}}\alpha\right) + W_{vs}\left(\frac{\partial W_{\alpha}^{\mathrm{T}}}{\partial z}\alpha\right)\right](-W_{pf}^{\mathrm{T}})d\Omega \tag{B-20}$$

$$-\int_{\Gamma_U} W_{vs}(-W_{pf}^{\mathrm{T}})d\Gamma - \int_{\Gamma_B} W_{vs}(W_{pf}^{\mathrm{T}})d\Gamma$$

$$K^{3,1} = +\int_{\Omega} W_{vf}\left(-\frac{9(W_{\alpha}^{\mathrm{T}}\alpha)\mu}{10r_0^2(1-\varepsilon)}\right)\left[(-5+2\varepsilon) - \varepsilon\left(W_{\alpha}^{\mathrm{T}}\alpha_{yy}\right)\right](-W_{vs}^{\mathrm{T}})d\Omega \tag{B-21}$$

$$K^{3,2} = + \int_{\Omega} W_{vf} \left(-\frac{9(W_{\alpha}^{\mathrm{T}}\alpha)\mu}{10r_0^2(1-\varepsilon)} \right) \left[-\varepsilon \left(W_{\alpha}^{\mathrm{T}}\alpha_{yy} \right) \right] (-W_{vs}^{\mathrm{T}}) d\Omega \qquad \text{(B-22)}$$

$$\begin{aligned} K^{3,3} \;=\; & \int_{\Omega} W_{vf}\rho_f \left(1 - W_{\alpha}^{\mathrm{T}}\alpha\right) \left[\left(W_{vf}^{\mathrm{T}} v_{fy} \right) \frac{\partial W_{vf}^{\mathrm{T}}}{\partial y} + \left(W_{vf}^{\mathrm{T}} v_{fz} \right) \frac{\partial W_{vf}^{\mathrm{T}}}{\partial z} \right] d\Omega \qquad \text{(B-23)} \\ & \int_{\Omega} \left[\frac{\partial W_{vf}}{\partial y} \left(1 - 2W_{\alpha}^{\mathrm{T}}\alpha\right) - 2W_{vf} \left(\frac{\partial W_{\alpha}^{\mathrm{T}}}{\partial y} \alpha \right) \right] 2\mu_f \frac{\partial W_{vf}^{\mathrm{T}}}{\partial y} d\Omega \\ & \int_{\Omega} \left[\frac{\partial W_{vf}}{\partial z} \left(1 - 2W_{\alpha}^{\mathrm{T}}\alpha\right) - 2W_{vf} \left(\frac{\partial W_{\alpha}^{\mathrm{T}}}{\partial z} \alpha \right) \right] \mu_f \frac{\partial W_{vf}^{\mathrm{T}}}{\partial z} d\Omega \\ & \int_{\Omega} W_{vf} \left(-\frac{9(W_{\alpha}^{\mathrm{T}}\alpha)\mu}{10r_0^2(1-\varepsilon)} \right) \left[(-5 + 2\varepsilon) - \varepsilon \left(W_{\alpha}^{\mathrm{T}}\alpha_{yy} \right) \right] (-W_{vf}^{\mathrm{T}}) d\Omega \qquad \text{(B-24)} \end{aligned}$$

$$\begin{aligned} K^{3,4} \;=\; & \int_{\Omega} \left[\frac{\partial W_{vf}}{\partial z} \left(1 - 2W_{\alpha}^{\mathrm{T}}\alpha\right) - 2W_{vf} \left(\frac{\partial W_{\alpha}^{\mathrm{T}}}{\partial z} \alpha \right) \right] \mu_f \frac{\partial W_{vf}^{\mathrm{T}}}{\partial y} d\Omega \\ & \int_{\Omega} W_{vf} \left(-\frac{9(W_{\alpha}^{\mathrm{T}}\alpha)\mu}{10r_0^2(1-\varepsilon)} \right) \left[-\varepsilon \left(W_{\alpha}^{\mathrm{T}}\alpha_{yz} \right) \right] (-W_{vf}^{\mathrm{T}}) d\Omega \end{aligned}$$

$$K^{3,5} = + \int_{\Omega} W_{vf} \left(-W_{\alpha}^{\mathrm{T}}\alpha \frac{\partial W_{Tp}^{\mathrm{T}}}{\partial y} \right) d\Omega \qquad \text{(B-25)}$$

$$K^{3,7} = + \int_{\Omega} W_{vf} \left(-W_{\alpha}^{\mathrm{T}}\alpha \frac{\partial W_{Tp}^{\mathrm{T}}}{\partial z} \right) d\Omega \qquad \text{(B-26)}$$

$$\begin{aligned} K^{3,11} \;=\; & \int_{\Omega} W_{vf} \left[-\left(W_{Tp}^{\mathrm{T}} T_{pyy} \right) \frac{\partial W_{\alpha}^{\mathrm{T}}}{\partial y} - \left(W_{Tp}^{\mathrm{T}} T_{pyz} \right) \frac{\partial W_{\alpha}^{\mathrm{T}}}{\partial y} \right] d\Omega \qquad \text{(B-27)} \\ & - \int_{\Omega} W_{vf} \left(W_{pf}^{\mathrm{T}} p_f \right) \frac{\partial W_{\alpha}^{\mathrm{T}}}{\partial y} d\Omega + \int_{\Omega} W_{vf} 2\mu_f \left(\frac{\partial W_{vf}^{\mathrm{T}}}{\partial y} v_{fy} \right) \frac{\partial W_{\alpha}^{\mathrm{T}}}{\partial y} d\Omega \\ & + \int_{\Omega} W_{vf}\mu_f \left[\left(\frac{\partial W_{vf}^{\mathrm{T}}}{\partial z} v_{fy} \right) + \left(\frac{\partial W_{vf}^{\mathrm{T}}}{\partial y} v_{fz} \right) \right] \frac{\partial W_{\alpha}^{\mathrm{T}}}{\partial z} d\Omega \end{aligned}$$

$$\begin{aligned} K^{3,12} \;=\; & \int_{\Omega} \left[\frac{\partial W_{vf}^{\mathrm{T}}}{\partial y} \left(1 - 2W_{\alpha}^{\mathrm{T}}\alpha\right) - 2W_{vf} \left(\frac{\partial W_{\alpha}^{\mathrm{T}}}{\partial y} \alpha \right) \right] \left(-W_{pf}^{\mathrm{T}} \right) d\Omega \qquad \text{(B-28)} \\ & - \int_{\Gamma_L} W_{vf} \left(1 - 2W_{\alpha}^{\mathrm{T}}\alpha\right) W_{pf}^{\mathrm{T}} d\Gamma \end{aligned}$$

$$K^{4,1} = + \int_{\Omega} W_{vf}\left(-\frac{9\left(W_{\alpha}^{\mathrm{T}}\alpha\right)\mu}{10r_0^2(1-\varepsilon)}\right)\left[-\varepsilon\left(W_{\alpha}^{\mathrm{T}}\alpha_{yz}\right)\right](-W_{vs}^{\mathrm{T}})d\Omega \tag{B-29}$$

$$K^{4,2} = + \int_{\Omega} W_{vf}\left(-\frac{9\left(W_{\alpha}^{\mathrm{T}}\alpha\right)\mu}{10r_0^2(1-\varepsilon)}\right)\left[(-5+2\varepsilon)-\varepsilon\left(W_{\alpha}^{\mathrm{T}}\alpha_{zz}\right)\right](-W_{vs}^{\mathrm{T}})d\Omega \tag{B-30}$$

$$\begin{aligned} K^{4,3} \;=\; & \int_{\Omega}\left[\frac{\partial W_{vf}^{\mathrm{T}}}{\partial y}\left(1-2W_{\alpha}^{\mathrm{T}}\alpha\right)-2W_{vf}\left(\frac{\partial W_{\alpha}^{\mathrm{T}}}{\partial y}\alpha\right)\right]\mu_f\left(\frac{\partial W_{vf}^{\mathrm{T}}}{\partial z}\right)d\Omega \\ & + \int_{\Omega} W_{vf}\left(-\frac{9\left(W_{\alpha}^{\mathrm{T}}\alpha\right)\mu}{10r_0^2(1-\varepsilon)}\right)\left[-\varepsilon\left(W_{\alpha}^{\mathrm{T}}\alpha_{yz}\right)\right](-W_{vf}^{\mathrm{T}}) \\ & - \int_{\Gamma_L} W_{vf}\left(1-2W_{\alpha}^{\mathrm{T}}\alpha\right)\mu_f\left(-\frac{\partial W_{vf}^{\mathrm{T}}}{\partial z}\right)d\Gamma \end{aligned} \tag{B-31}$$

$$\begin{aligned} K^{4,4} \;=\; & \int_{\Omega} W_{vf}\rho_f\left(1-W_{\alpha}^{\mathrm{T}}\alpha\right)\left[\left(W_{vf}^{\mathrm{T}}v_{fy}\right)\frac{\partial W_{vf}^{\mathrm{T}}}{\partial y}+\left(W_{vf}^{\mathrm{T}}v_{fz}\right)\frac{\partial W_{vf}^{\mathrm{T}}}{\partial z}\right]d\Omega \\ & \int_{\Omega}\left[\frac{\partial W_{vf}}{\partial y}\left(1-2W_{\alpha}^{\mathrm{T}}\alpha\right)-2W_{vf}\left(\frac{\partial W_{\alpha}^{\mathrm{T}}}{\partial y}\alpha\right)\right]\mu_f\frac{\partial W_{vf}^{\mathrm{T}}}{\partial y}d\Omega \\ & \int_{\Omega}\left[\frac{\partial W_{vf}}{\partial z}\left(1-2W_{\alpha}^{\mathrm{T}}\alpha\right)-2W_{vf}\left(\frac{\partial W_{\alpha}^{\mathrm{T}}}{\partial z}\alpha\right)\right]2\mu_f\frac{\partial W_{vf}^{\mathrm{T}}}{\partial z}d\Omega \\ & \int_{\Omega} W_{vf}\left(-\frac{9(W_{\alpha}^{\mathrm{T}}\alpha)\mu}{10r_0^2(1-\varepsilon)}\right)\left[(-5+2\varepsilon)-\varepsilon\left(W_{\alpha}^{\mathrm{T}}\alpha_{zz}\right)\right]W_{vf}^{\mathrm{T}}d\Omega \end{aligned} \tag{B-32}$$

$$K^{4,6} = + \int_{\Omega} W_{v_f}\left[\left(-W_{\alpha}^{\mathrm{T}}\alpha\right)\frac{\partial W_{Tp}^{\mathrm{T}}}{\partial z}\right]d\Omega \tag{B-33}$$

$$K^{4,7} = + \int_{\Omega} W_{vf}\left[\left(-W_{\alpha}^{\mathrm{T}}\alpha\right)\frac{\partial W_{Tp}^{\mathrm{T}}}{\partial y}\right]d\Omega \tag{B-34}$$

$$\begin{aligned} K^{4,11} \;=\; & \int_{\Omega} W_{vf}\left[-\left(W_{Tp}^{\mathrm{T}}T_{pyz}\right)\frac{\partial W_{\alpha}^{\mathrm{T}}}{\partial y}-\left(W_{Tp}^{\mathrm{T}}T_{pzz}\right)\frac{\partial W_{\alpha}^{\mathrm{T}}}{\partial z}\right]d\Omega \\ & - \int_{\Omega} W_{vf}\left(W_{pf}^{\mathrm{T}}p_f\right)\frac{\partial W_{\alpha}^{\mathrm{T}}}{\partial z}d\Omega + \int_{\Omega} W_{vf}2\mu_f\left(\frac{\partial W_{vf}^{\mathrm{T}}}{\partial z}v_{fz}\right)\frac{\partial W_{\alpha}^{\mathrm{T}}}{\partial z}d\Omega \\ & + \int_{\Omega} W_{vf}\mu_f\left[\left(\frac{\partial W_{vf}^{\mathrm{T}}}{\partial y}v_{fz}\right)+\left(\frac{\partial W_{vf}^{\mathrm{T}}}{\partial z}v_{fy}\right)\right]\frac{\partial W_{\alpha}^{\mathrm{T}}}{\partial y}d\Omega \end{aligned} \tag{B-35}$$

$$K^{4,12} = \int_\Omega \left[\frac{\partial W_{vf}^{\mathrm{T}}}{\partial z} \left(1 - 2W_\alpha^{\mathrm{T}}\alpha\right) - 2W_{vf}\left(\frac{\partial W_\alpha^{\mathrm{T}}}{\partial z}\alpha\right)\right]\left(-W_{pf}^{\mathrm{T}}\right) d\Omega \tag{B-36}$$
$$+ \int_{\Gamma_U} W_{vf}\left(1 - 2W_\alpha^{\mathrm{T}}\alpha\right) W_{pf}^{\mathrm{T}} d\Gamma - \int_{\Gamma_B} W_{vf}\left(1 - 2W_\alpha^{\mathrm{T}}\alpha\right) W_{pf}^{\mathrm{T}} d\Gamma$$

$$K^{5,3} = -k\int_\Omega \frac{W_{vs}}{5}\left[-1 + C_2 + 2\left(1 - W_a^{\mathrm{T}}a_{yy} - W_a^{\mathrm{T}}a_{yy}a_{zz}\right)^2 C_2\right]\frac{\partial W_{vf}^{\mathrm{T}}}{\partial y} d\Omega \tag{B-37}$$

$$K^{5,4} = -k\int_\Omega \frac{W_{vs}}{7}\left[-1 + C_2 + 2\left(1 - W_a^{\mathrm{T}}a_{yy} - W_a^{\mathrm{T}}a_{yy}a_{zz}\right)^2 C_2\right]\frac{\partial W_{vf}^{\mathrm{T}}}{\partial z} d\Omega \tag{B-38}$$

$$K^{5,5} = \int_\Omega W_{vs}W_{Tp}^{\mathrm{T}} d\Omega \tag{B-39}$$

$$K^{5,8} = -k\int_\Omega \frac{W_{vs}}{35}\left\{\begin{array}{l}\left(30 - 65C_2 + 94C_2W_a^{\mathrm{T}}a_{yy}\right)\dfrac{\partial W_{vf}^{\mathrm{T}}}{\partial y}v_{fy} \\ +\left(5 - 40C_2 + 35C_2W_a^{\mathrm{T}}a_{yy}\right)\dfrac{\partial W_{vf}^{\mathrm{T}}}{\partial z}v_{fz}\end{array}\right\} W_a^{\mathrm{T}} d\Omega \tag{B-40}$$

$$K^{5,9} = -k\int_\Omega \frac{W_{vs}}{35}\left\{\begin{array}{l}\left(5 - 5C_2 + 35C_2W_a^{\mathrm{T}}a_{yy} + 4C_2W_a^{\mathrm{T}}a_{zz}\right)\dfrac{\partial W_{vf}^{\mathrm{T}}}{\partial y}v_{fy} \\ +10\left(1 - C_2 + 7C_2W_a^{\mathrm{T}}a_{yy} - C_2W_a^{\mathrm{T}}a_{zz}\right)\dfrac{\partial W_{vf}^{\mathrm{T}}}{\partial z}v_{fz}\end{array}\right\} W_a^{\mathrm{T}} d\Omega \tag{B-41}$$

$$K^{5,10} = -k\int_\Omega \frac{3W_{vs}}{35}\left\{\begin{array}{l}\left(5 - 5C_2 + 25C_2W_a^{\mathrm{T}}a_{yy} - 10C_2W_a^{\mathrm{T}}a_{zz}\right) \\ \left(\dfrac{\partial W_{vf}^{\mathrm{T}}}{\partial z}v_{fy} + \dfrac{\partial W_{vf}^{\mathrm{T}}}{\partial y}v_{fz}\right) \\ +C_2W_a^{\mathrm{T}}a_{yz}\left(-14\dfrac{\partial W_{vf}^{\mathrm{T}}}{\partial y}v_{fy} + 20\dfrac{\partial W_{vf}^{\mathrm{T}}}{\partial z}v_{fz}\right)\end{array}\right\} W_a^{\mathrm{T}} d\Omega \tag{B-42}$$

$$K^{6,3} = -k\int_\Omega \frac{W_{vs}}{7}\left[-1 + C_2 + 2\left(1 - W_a^{\mathrm{T}}a_{yy} - W_a^{\mathrm{T}}a_{yy}a_{zz}\right)^2 C_2\right]\frac{\partial W_{vf}^{\mathrm{T}}}{\partial y} d\Omega \tag{B-43}$$

$$K^{6,4} = -k\int_\Omega \frac{W_{vs}}{5}\left[-1 + C_2 + 2\left(1 - W_a^{\mathrm{T}}a_{yy} - W_a^{\mathrm{T}}a_{yy}a_{zz}\right)^2 C_2\right]\frac{\partial W_{vf}^{\mathrm{T}}}{\partial z} d\Omega \tag{B-44}$$

$$K^{6,6} = \int_\Omega W_{vs}W_{Tp}^{\mathrm{T}} d\Omega \tag{B-45}$$

$$K^{6,8} = -k\int_\Omega \frac{W_{vs}}{35}\left\{\begin{array}{l}10\left(1 - C_2 - C_2W_a^{\mathrm{T}}a_{yy}\right)\dfrac{\partial W_{vf}^{\mathrm{T}}}{\partial y}v_{fy} \\ +\left(5 - 5C_2 + 4C_2W_{aT}a_{yy}\right)\dfrac{\partial W_{vf}^{\mathrm{T}}}{\partial z}v_{fz}\end{array}\right\} W_a^{\mathrm{T}} d\Omega \tag{B-46}$$

$$K^{4,12} = \int_\Omega \left[\frac{\partial W_{vf}^{\mathrm{T}}}{\partial z} \left(1 - 2W_\alpha^{\mathrm{T}} \alpha\right) - 2W_{vf} \left(\frac{\partial W_\alpha^{\mathrm{T}}}{\partial z} \alpha \right) \right] \left(-W_{pf}^{\mathrm{T}}\right) d\Omega \tag{B-36}$$

$$+ \int_{\Gamma_U} W_{vf} \left(1 - 2W_\alpha^{\mathrm{T}} \alpha\right) W_{pf}^{\mathrm{T}} d\Gamma - \int_{\Gamma_B} W_{vf} \left(1 - 2W_\alpha^{\mathrm{T}} \alpha\right) W_{pf}^{\mathrm{T}} d\Gamma$$

$$K^{5,3} = -k \int_\Omega \frac{W_{vs}}{5} \left[-1 + C_2 + 2\left(1 - W_a^{\mathrm{T}} a_{yy} - W_a^{\mathrm{T}} a_{yy} a_{zz}\right)^2 C_2 \right] \frac{\partial W_{vf}^{\mathrm{T}}}{\partial y} d\Omega \tag{B-37}$$

$$K^{5,4} = -k \int_\Omega \frac{W_{vs}}{7} \left[-1 + C_2 + 2\left(1 - W_a^{\mathrm{T}} a_{yy} - W_a^{\mathrm{T}} a_{yy} a_{zz}\right)^2 C_2 \right] \frac{\partial W_{vf}^{\mathrm{T}}}{\partial z} d\Omega \tag{B-38}$$

$$K^{5,5} = \int_\Omega W_{vs} W_{Tp}^{\mathrm{T}} d\Omega \tag{B-39}$$

$$K^{5,8} = -k \int_\Omega \frac{W_{vs}}{35} \left\{ \begin{array}{c} \left(30 - 65C_2 + 94C_2 W_a^{\mathrm{T}} a_{yy}\right) \dfrac{\partial W_{vf}^{\mathrm{T}}}{\partial y} v_{fy} \\ + \left(5 - 40C_2 + 35C_2 W_a^{\mathrm{T}} a_{yy}\right) \dfrac{\partial W_{vf}^{\mathrm{T}}}{\partial z} v_{fz} \end{array} \right\} W_a^{\mathrm{T}} d\Omega \tag{B-40}$$

$$K^{5,9} = -k \int_\Omega \frac{W_{vs}}{35} \left\{ \begin{array}{c} \left(5 - 5C_2 + 35C_2 W_a^{\mathrm{T}} a_{yy} + 4C_2 W_a^{\mathrm{T}} a_{zz}\right) \dfrac{\partial W_{vf}^{\mathrm{T}}}{\partial y} v_{fy} \\ +10\left(1 - C_2 + 7C_2 W_a^{\mathrm{T}} a_{yy} - C_2 W_a^{\mathrm{T}} a_{zz}\right) \dfrac{\partial W_{vf}^{\mathrm{T}}}{\partial z} v_{fz} \end{array} \right\} W_a^{\mathrm{T}} d\Omega \tag{B-41}$$

$$K^{5,10} = -k \int_\Omega \frac{3W_{vs}}{35} \left\{ \begin{array}{l} \left(5 - 5C_2 + 25C_2 W_a^{\mathrm{T}} a_{yy} - 10C_2 W_a^{\mathrm{T}} a_{zz}\right) \\ \left(\dfrac{\partial W_{vf}^{\mathrm{T}}}{\partial z} v_{fy} + \dfrac{\partial W_{vf}^{\mathrm{T}}}{\partial y} v_{fz} \right) \\ +C_2 W_a^{\mathrm{T}} a_{yz} \left(-14 \dfrac{\partial W_{vf}^{\mathrm{T}}}{\partial y} v_{fy} + 20 \dfrac{\partial W_{vf}^{\mathrm{T}}}{\partial z} v_{fz} \right) \end{array} \right\} W_a^{\mathrm{T}} d\Omega \tag{B-42}$$

$$K^{6,3} = -k \int_\Omega \frac{W_{vs}}{7} \left[-1 + C_2 + 2\left(1 - W_a^{\mathrm{T}} a_{yy} - W_a^{\mathrm{T}} a_{yy} a_{zz}\right)^2 C_2 \right] \frac{\partial W_{vf}^{\mathrm{T}}}{\partial y} d\Omega \tag{B-43}$$

$$K^{6,4} = -k \int_\Omega \frac{W_{vs}}{5} \left[-1 + C_2 + 2\left(1 - W_a^{\mathrm{T}} a_{yy} - W_a^{\mathrm{T}} a_{yy} a_{zz}\right)^2 C_2 \right] \frac{\partial W_{vf}^{\mathrm{T}}}{\partial z} d\Omega \tag{B-44}$$

$$K^{6,6} = \int_\Omega W_{vs} W_{Tp}^{\mathrm{T}} d\Omega \tag{B-45}$$

$$K^{6,8} = -k \int_\Omega \frac{W_{vs}}{35} \left\{ \begin{array}{c} 10\left(1 - C_2 - C_2 W_a^{\mathrm{T}} a_{yy}\right) \dfrac{\partial W_{vf}^{\mathrm{T}}}{\partial y} v_{fy} \\ + \left(5 - 5C_2 + 4C_2 W_{aT} a_{yy}\right) \dfrac{\partial W_{vf}^{\mathrm{T}}}{\partial z} v_{fz} \end{array} \right\} W_a^{\mathrm{T}} d\Omega \tag{B-46}$$

$$K^{6,9} = -k\int_{\Omega} W_{vs}\left\{\begin{array}{l}\frac{1}{7}\left(1-8C_2+14C_2W_a^{\mathrm{T}}a_{yy}+7C_2W_a^{\mathrm{T}}a_{zz}\right)\frac{\partial W_{vf}^{\mathrm{T}}}{\partial y}v_{fy}\\ +\frac{1}{35}\left(30-65C_2+35C_2W_a^{\mathrm{T}}a_{yy}+94C_2W_a^{\mathrm{T}}a_{zz}\right)\frac{\partial W_{vf}^{\mathrm{T}}}{\partial z}v_{fz}\end{array}\right\}W_a^{\mathrm{T}}d\Omega \tag{B-47}$$

$$K^{6,10} = -k\int_{\Omega}\frac{3W_{vs}}{35}\left\{\begin{array}{l}\left(5-5C_2-10C_2W_a^{\mathrm{T}}a_{yy}+25C_2W_a^{\mathrm{T}}a_{zz}\right)\\ \left(\frac{\partial W_{vf}^{\mathrm{T}}}{\partial z}v_{fy}+\frac{\partial W_{vf}^{\mathrm{T}}}{\partial y}v_{fz}\right)\\ +C_2W_a^{\mathrm{T}}a_{yz}\left(20\frac{\partial W_{vf}^{\mathrm{T}}}{\partial y}v_{fy}-14\frac{\partial W_{vf}^{\mathrm{T}}}{\partial z}v_{fz}\right)\end{array}\right\}W_a^{\mathrm{T}}d\Omega \tag{B-48}$$

$$K^{7,3} = -k\int_{\Omega}\frac{W_{vs}}{35}\left[-1+C_2+2\left(1-W_a^{\mathrm{T}}a_{yy}-W_a^{\mathrm{T}}a_{yy}a_{zz}\right)^2C_2\right]\frac{\partial W_{vf}^{\mathrm{T}}}{\partial z}d\Omega \tag{B-49}$$

$$K^{7,4} = -k\int_{\Omega}\frac{W_{vs}}{35}\left[-1+C_2+2\left(1-W_a^{\mathrm{T}}a_{yy}-W_a^{\mathrm{T}}a_{yy}a_{zz}\right)^2C_2\right]\frac{\partial W_{vf}^{\mathrm{T}}}{\partial y}d\Omega \tag{B-50}$$

$$K^{7,7} = \int_{\Omega} W_{vs}W_{Tp}^{\mathrm{T}}d\Omega \tag{B-51}$$

$$K^{7,8} = -k\int_{\Omega}\frac{W_{vs}}{35}\left(5-5C_2-8C_2W_a^{\mathrm{T}}a_{yy}\right)\left(\frac{\partial W_{vf}^{\mathrm{T}}}{\partial z}v_{fy}+\frac{\partial W_{vf}^{\mathrm{T}}}{\partial y}v_{fz}\right)W_a^{\mathrm{T}}d\Omega \tag{B-52}$$

$$K^{7,9} = -k\int_{\Omega}\frac{W_{vs}}{35}\left(5-5C_2-35C_2W_a^{\mathrm{T}}a_{yy}-8C_2W_a^{\mathrm{T}}a_{zz}\right)\left(\frac{\partial W_{vf}^{\mathrm{T}}}{\partial z}v_{fy}+\frac{\partial W_{vf}^{\mathrm{T}}}{\partial y}v_{fz}\right)W_a^{\mathrm{T}}d\Omega \tag{B-53}$$

$$K^{7,10} = -k\int_{\Omega} W_{vs}\left\{\begin{array}{l}\frac{1}{7}\left(2-9C_2+24C_2W_a^{\mathrm{T}}a_{yy}+3C_2W_a^{\mathrm{T}}a_{zz}\right)\frac{\partial W_{vf}^{\mathrm{T}}}{\partial y}v_{fy}\\ +\frac{1}{7}\left(2-9C_2+24C_2W_a^{\mathrm{T}}a_{zz}+3C_2W_a^{\mathrm{T}}a_{yy}\right)\frac{\partial W_{vf}^{\mathrm{T}}}{\partial z}v_{fz}\\ +\frac{54}{35}C_2\left(W_a^{\mathrm{T}}a_{yz}\right)\left(\frac{\partial W_{vf}^{\mathrm{T}}}{\partial z}v_{fy}+\frac{\partial W_{vf}^{\mathrm{T}}}{\partial y}v_{fz}\right)\end{array}\right\}W_a^{\mathrm{T}}d\Omega \tag{B-54}$$

$$K^{8,3} = \int_{\Omega} W_a\left\{\frac{2\lambda}{5}\left[-1+C_2+2C_2\left(1-W_a^{\mathrm{T}}a_{yy}-W_a^{\mathrm{T}}a_{zz}\right)^2\right]\frac{\partial W_{vf}^{\mathrm{T}}}{\partial y}\right\}d\Omega \tag{B-55}$$

$$K^{8,3} = \int_{\Omega} W_a\left\{\frac{2\lambda}{7}\left[-1+C_2+2C_2\left(1-W_a^{\mathrm{T}}a_{yy}-W_a^{\mathrm{T}}a_{zz}\right)^2\right]\frac{\partial W_{vf}^{\mathrm{T}}}{\partial z}\right\}d\Omega \tag{B-56}$$

$$K^{8,8} = \int_\Omega W_a\left[\left(W_{vf}^{\mathrm{T}} v_{sy}\right)\frac{\partial W_a^{\mathrm{T}}}{\partial y} + \left(W_{vf}^{\mathrm{T}} v_{sz}\right)\frac{\partial W_a^{\mathrm{T}}}{\partial z}\right] d\Omega$$

$$+ \int_\Omega W_a \frac{2\lambda}{35}\left\{\begin{array}{l}\left(-5 - 65C_2 + 94C_2 W_a^{\mathrm{T}} a_{yy}\right)\dfrac{\partial W_{vf}^{\mathrm{T}}}{\partial y} v_{fy} \\ +\left(5 - 8C_2 + 7C_2 W_a^{\mathrm{T}} a_{yy}\right)\dfrac{\partial W_{vf}^{\mathrm{T}}}{\partial z} v_{fz}\end{array}\right\} W_a^{\mathrm{T}} d\Omega \quad \text{(B-57)}$$

$$K^{8,9} = + \int_\Omega W_a \frac{2\lambda}{35}\left\{\begin{array}{l}\left(-5 - 5C_2 + 35C_2 W_a^{\mathrm{T}} a_{yy} + 4C_2 W_a^{\mathrm{T}} a_{zz}\right)\dfrac{\partial W_{vf}^{\mathrm{T}}}{\partial y} v_{fy} \\ +\left(10 - 10C_2 + 70C_2 W_a^{\mathrm{T}} a_{yy} - 10C_2 W_a^{\mathrm{T}} a_{zz}\right)\dfrac{\partial W_{vf}^{\mathrm{T}}}{\partial z} v_{fz}\end{array}\right\} W_a^{\mathrm{T}} d\Omega \quad \text{(B-58)}$$

$$K^{8,10} = - \int_\Omega W_a \frac{1}{35}\left\{\begin{array}{l}12\lambda C_2\left(W_a^{\mathrm{T}} a_{yz}\right)\left(7\dfrac{\partial W_{vf}^{\mathrm{T}}}{\partial y} v_{fy} - 10\dfrac{\partial W_{vf}^{\mathrm{T}}}{\partial z} v_{fz}\right) \\ -5\left[7 + \lambda\left(-1 - 6C_2 + 30C_2 W_a^{\mathrm{T}} a_{yy} - 12C_2 W_a^{\mathrm{T}} a_{zz}\right)\right]\dfrac{\partial W_{vf}^{\mathrm{T}}}{\partial y} v_{fz} \\ +5\left[7 + \lambda\left(1 + 6C_2 - 30C_2 W_a^{\mathrm{T}} a_{yy} + 12C_2 W_a^{\mathrm{T}} a_{zz}\right)\right]\dfrac{\partial W_{vf}^{\mathrm{T}}}{\partial z} v_{fy}\end{array}\right\} W_a^{\mathrm{T}} d\Omega \quad \text{(B-59)}$$

$$K^{9,3} = \int_\Omega W_a\left\{\frac{2\lambda}{7}\left[-1 + C_2 + 2C_2\left(1 - W_a^{\mathrm{T}} a_{yy} - W_a^{\mathrm{T}} a_{zz}\right)^2\right]\frac{\partial W_{vf}^{\mathrm{T}}}{\partial y}\right\} d\Omega \quad \text{(B-60)}$$

$$K^{9,4} = \int_\Omega W_a\left\{\frac{2\lambda}{7}\left[-1 + C_2 + 2C_2\left(1 - W_a^{\mathrm{T}} a_{yy} - W_a^{\mathrm{T}} a_{zz}\right)^2\right]\frac{\partial W_{vf}^{\mathrm{T}}}{\partial z}\right\} d\Omega \quad \text{(B-61)}$$

$$K^{9,8} = + \int_\Omega W_a \frac{2\lambda}{35}\left\{\begin{array}{l}\left(-10 + 10C_2 + 10C_2 W_a^{\mathrm{T}} a_{yy}\right)\dfrac{\partial W_{vf}^{\mathrm{T}}}{\partial y} v_{fy} \\ +\left(-5 + 5C_2 - 4C_2 W_a^{\mathrm{T}} a_{yy}\right)\dfrac{\partial W_{vf}^{\mathrm{T}}}{\partial z} v_{fz}\end{array}\right\} W_a^{\mathrm{T}} d\Omega \quad \text{(B-62)}$$

$$K^{9,9} = \int_\Omega W_a\left[\left(W_{vf}^{\mathrm{T}} v_{sy}\right)\frac{\partial W_a^{\mathrm{T}}}{\partial y} + \left(W_{vf}^{\mathrm{T}} v_{sz}\right)\frac{\partial W_a^{\mathrm{T}}}{\partial z}\right] d\Omega \quad \text{(B-63)}$$

$$+ \int_\Omega W_a \frac{2\lambda}{35}\left\{\begin{array}{l}\left(5 - 8C_2 + 14C_2 W_a^{\mathrm{T}} a_{yy} + 7C_2 W_a^{\mathrm{T}} a_{zz}\right)\dfrac{\partial W_{vf}^{\mathrm{T}}}{\partial y} v_{fy} \\ +\left(-5 - 65C_2 + 35C_2 W_a^{\mathrm{T}} a_{yy} + 94C_2 W_{a^T} a_{zz}\right)\dfrac{\partial W_{vf}^{\mathrm{T}}}{\partial z} v_{fz}\end{array}\right\} W_a^{\mathrm{T}} d\Omega$$

$$K^{9,10} = -\int_\Omega W_a \frac{1}{35}\left\{\begin{array}{l} 12\lambda C_2\left(W_a^{\mathrm{T}} a_{yz}\right)\left(-10\frac{\partial W_{vf}^{\mathrm{T}}}{\partial y}v_{fy} + 7\frac{\partial W_{vf}^{\mathrm{T}}}{\partial z}v_{fz}\right) \\ +5\left[-7+\lambda\left(1+6C_2+12C_2 W_a^{\mathrm{T}} a_{yy} - 30C_2 W_a^{\mathrm{T}} a_{zz}\right)\right]\frac{\partial W_{vf}^{\mathrm{T}}}{\partial z}v_{fy} \\ +5\left[7+\lambda\left(1+6C_2+12C_2 W_a^{\mathrm{T}} a_{yy} - 30C_2 W_{aT} a_{zz}\right)\right]\frac{\partial W_{vf}^{\mathrm{T}}}{\partial y}v_{fz} \end{array}\right\} W_a^{\mathrm{T}} d\Omega \tag{B-64}$$

$$K^{10,3} = \int_\Omega W_a \left\{\frac{2\lambda}{35}\left[-1+C_2+2C_2\left(1-W_a^{\mathrm{T}} a_{yy} - W_a^{\mathrm{T}} a_{zz}\right)^2\right]\frac{\partial W_{vf}^{\mathrm{T}}}{\partial z}\right\} d\Omega \tag{B-65}$$

$$K^{10,4} = \int_\Omega W_a \left\{\frac{2\lambda}{35}\left[-1+C_2+2C_2\left(1-W_a^{\mathrm{T}} a_{yy} - W_a^{\mathrm{T}} a_{zz}\right)^2\right]\frac{\partial W_{vf}^{\mathrm{T}}}{\partial y}\right\} d\Omega \tag{B-66}$$

$$K^{10,8} = -\int_\Omega W_a \frac{1}{70}\left\{\begin{array}{l} \left[-35+\lambda\left(15+20C_2+32C_2 W_a^{\mathrm{T}} a_{yy}\right)\right]\frac{\partial W_{vf}^{\mathrm{T}}}{\partial z}v_{fy} \\ +\left[35+\lambda\left(15+20C_2+32C_2 W_{aT} a_{yy}\right)\right]\frac{\partial W_{vf}^{\mathrm{T}}}{\partial y}v_{fz} \end{array}\right\} W_a^{\mathrm{T}} d\Omega \tag{B-67}$$

$$K^{10,9} = -\int_\Omega W_a \frac{1}{70}\left\{\begin{array}{l} \left[-35+\lambda\left(15+20C_2+32C_2 W_a^{\mathrm{T}} a_{yy}\right)\right]\frac{\partial W_{vf}^{\mathrm{T}}}{\partial y}v_{fz} \\ +\left[35+\lambda\left(15+20C_2+32C_2 W_a^{\mathrm{T}} a_{yy}\right)\right]\frac{\partial W_{vf}^{\mathrm{T}}}{\partial z}v_{fy} \end{array}\right\} W_a^{\mathrm{T}} d\Omega \tag{B-68}$$

$$\begin{aligned} K^{10,10} &= \int_\Omega W_a\left[\left(W_{vf}^{\mathrm{T}} v_{sy}\right)\frac{\partial W_a^{\mathrm{T}}}{\partial y} + \left(W_{vf}^{\mathrm{T}} v_{sz}\right)\frac{\partial W_a^{\mathrm{T}}}{\partial z}\right] d\Omega \\ &+ \int_\Omega W_a \frac{32\lambda}{35}\left\{\begin{array}{l} \left(-5-30C_2+80C_2 W_a^{\mathrm{T}} a_{yy}+10C_2 W_a^{\mathrm{T}} a_{zz}\right)\frac{\partial W_{vf}^{\mathrm{T}}}{\partial y}v_{fy} \\ +36C_2 W_a^{\mathrm{T}} a_{yz}\left(\frac{\partial W_{vf}^{\mathrm{T}}}{\partial z}v_{fy} + \frac{\partial W_{vf}^{\mathrm{T}}}{\partial y}v_{fz}\right) \\ +\left(-5-30C_2+10C_2 W_a^{\mathrm{T}} a_{yy}+80C_2 W_a^{\mathrm{T}} a_{zz}\right)\frac{\partial W_{vf}^{\mathrm{T}}}{\partial z}v_{fz} \end{array}\right\} W_a^{\mathrm{T}} d\Omega \end{aligned} \tag{B-69}$$

$$K^{11,1} = -\int_\Omega W_\alpha\left(W_a^{\mathrm{T}}\alpha\right)\frac{\partial W_{vs}^{\mathrm{T}}}{\partial y} d\Omega \tag{B-70}$$

$$K^{11,2} = -\int_\Omega W_\alpha\left(W_a^{\mathrm{T}}\alpha\right)\frac{\partial W_{vs}^{\mathrm{T}}}{\partial z} d\Omega \tag{B-71}$$

$$K^{11,11} = \int_\Omega W_\alpha\left[\left(W_{vs}^{\mathrm{T}} v_{sy}\right)\frac{\partial W_\alpha^{\mathrm{T}}}{\partial y} + \left(W_{vs}^{\mathrm{T}} v_{sz}\right)\frac{\partial W_\alpha^{\mathrm{T}}}{\partial z}\right] d\Omega \tag{B-72}$$

$$K^{12,3} = -\int_{\Omega} W_{pf}\left(1 - W_a^{\mathrm{T}}\alpha\right)\frac{\partial W_{vs}^{\mathrm{T}}}{\partial z}d\Omega \tag{B-73}$$

$$K^{12,4} = -\int_{\Omega} W_{pf}\left(1 - W_a^{\mathrm{T}}\alpha\right)\frac{\partial W_{vs}^{\mathrm{T}}}{\partial y}d\Omega \tag{B-74}$$

$$K^{12,11} = \int_{\Omega} W_{pf}\left[\left(W_{vf}^{\mathrm{T}}v_{fy}\right)\frac{\partial W_{\alpha}^{\mathrm{T}}}{\partial y} + \left(W_{vf}^{\mathrm{T}}v_{fz}\right)\frac{\partial W_{\alpha}^{\mathrm{T}}}{\partial z}\right]d\Omega \tag{B-75}$$

Force vector

$$\mathbf{F} = \begin{pmatrix} f^1 & f^2 & f^3 & f^4 & 0 & 0 & 0 & 0 & 0 & 0 & 0 & 0 \end{pmatrix}^{\mathrm{T}} \tag{B-76}$$

Entries of the force vector

$$f^1 = +\int_{\Omega} W_{vs}\rho_s\left(W_{\alpha}^{\mathrm{T}}\alpha\right)g_y d\Omega \tag{B-77}$$

$$f^2 = +\int_{\Omega} W_{vs}\rho_s\left(W_{\alpha}^{\mathrm{T}}\alpha\right)g_z d\Omega \tag{B-78}$$

$$f^3 = +\int_{\Omega} W_{vf}\rho_f\left(1 - W_{\alpha}^{\mathrm{T}}\alpha\right)g_y d\Omega \tag{B-79}$$

$$f^4 = +\int_{\Omega} W_{vf}\rho_f\left(1 - W_{\alpha}^{\mathrm{T}}\alpha\right)g_z d\Omega \tag{B-80}$$

BIBLIOGRAPHY

[1] G.B. Jeffery. The motion of ellipsoidal particles immersed in a viscous fluid. *Proc. Royal Soc. Math. London*, 102:161–179, 1922.

[2] H. Brenner. The stokes resistance of an slightly deformed sphere. *Chem. Engng. Sci.*, 19:519–539, 1964.

[3] R. W. Burgess. The uniform motion of a sphere through a viscous liquid. *American Journal of Mathematics*, 38:81–96, 1916.

[4] J. Happel and H. Brenner. *Low Reynold number hydrodynamics with special applications to particulate media*. Prentice-Hall,N. J., 1965.

[5] S. Kim and S. J. Karrila. *Microhydrodynamics: principles and selected applications*. Bulterworlt-Heineman, 1991.

[6] H. Lamb. *Hydrodynamics*. Dover, New York, 1945.

[7] B. J. Trevelyan and S. G. Mason. Force-free particles. *Journal of Colloid Science*, 6:354–370, 1951.

[8] F. P. Bretherton. The motion of rigid particles in a shear flow at low reynolds number. *Journal of Fluid Mechanics*, 14:284–304, 1962.

[9] D. Broday, M.Fichman, M.Shapiro, and C.Gutfinger. Motion of spheroidal particles in vertal shear flows. *Phys. Fluids*, 1:86–100, 1999.

[10] D. J. Jeffery. The calculations for teh low reynolds number resistance functions for two unequal spheres. *Phys. Fluids*, 4:16–29, 1992.

[11] H. Keh and S. Chen. Low-reynolds-number hydrodynamic interactions in a suspension of spherical particles with slip surfaces. *Chemical Engineering Science*, 52:1789–1805, 1997.

[12] E. D. Wetzel and C. L. TuckerIII. Droplet deformation in dispersions with unequal viscosities and zero interfacial tension. *Journal of Fluid Mechanics*, 426:199–228, 2001.

[13] H. Niazmand and M. Renksizbulut. Surface effects on transient three-dimensional flows around rotating spheres at moderte reynolds number. *Computers and Fluids*, 32:1405–1433, 2003.

[14] H. Brenner. The stokes resistance of an arbitrary particle. *Chemical engineering science*, 27:1–25, 1963.

[15] H. Brenner and M. E. O'Neill. On the stokes resistance of multiparticle systems in a linear shear field. *Chemical engineering science*, 27:1421–1439, 1972.

[16] G. K. Batchelor. Brownian diffusion of particles with hydrodynamic interaction. *Journal of fluid mechanics*, 74:1–29, 1976.

[17] G. K. Batchelor. Sedimentation in a dilute polydisperse system of interacting spheres. part 1. general theory. *Journal of fluid mechanics*, 119:379–408, 1982.

[18] D. J. Jeffery and Y. Onishi. Calculation of the resistance and mobility functions for two unequal rigid spheres in low-reynolds-number flow. *Journal of fluid mechanics*, 139:261–290, 1984.

[19] E. J. Hinch and L. G. Leal. The effect of brownian motion on the rheological properties of a suspension of non-spherical particles. *Journal of Fluid Mechanics*, 52:683–712, 1972.

[20] M. Doi and S. F. Edwards. *The theory of polymer dynamics*. Clarendon Press, Oxford, 1987.

[21] G. K. Batchelor. The stress system in a suspension of force-free particles. *Journal of Fluid Mechanics*, 41:545–570, 1970.

[22] E. J. Hinch and L. G. Leal. Constitutive equations in suspension mechanics, part 1. general formulation. *Journal of Fluid Mechanics*, 71:481–495, 1975.

[23] D. Z. Zhang and A. Prosperetti. Momentum and energy equations for disperse two-phase flows and their closure for dilute suspensions. *International Journal of Multiphase Flow*, 23:425–453, 1997.

[24] S. M. Dinh and R. C. Armstrong. A rheological equation of state for semiconcentrated fiber suspensions. *Journal of Rheology*, 28:207–227, 1984.

[25] W. R. Blakeney. The viscosity of suspensions of straight rigid rods. *J. colloid Interface Science*, 22:324–330, 1966.

[26] R. O. Machmeyer and C. T. Hill. *Trans. Soc. Rheol.*, 21:183–195, 1977.

[27] J. N. Miles, N. K. Murty, and G. F. Molden. *Polym. Eng. Sci.*, 18:271–, 1981.

[28] T. Loimer, A. Nir, and R. Semiat. Shear-induced corrugation of free interfaces in concentrated suspensions. *Journal of Non-Newtonian Fluid Mechanics*, 102:115–134, 2002.

[29] G. K. Batchelor. The stress generated in a non-dilute suspension of elongated particles by pure straining motion. *Journal of Fluid Mechanics*, 46:813–829, 1971.

[30] J. D. Goddard. Tensile behavior of power-law fluids containing oriented slender fibers. *Journal of Rheology*, 22:615–622, 1975.

[31] A. G. Gibson and S. Toll. Mechanicsl of the squeeze flow of planar fiber suspensions. *Journal of Non-Newtonian Fluid Mechanics*, 82:1–24, 1999.

[32] H. Ramkissoon and St. Augustine. Slip flow past an approximate spheroid. *Acta Mechanica*, 123:227–233, 1997.

[33] S. Deo and S. Datta. Slip flow past a prolate spheroid. *Indian Journal of Pure Applied Mathematics*, 33:903–909, 2002.

[34] E. Bonaccurso, M. Kappl, and H.-J. Butt. Hydrodynamic force measurements: Boundary slip of water on hydrophilic surfaces and electrokinetic effects. *Phys. Rev. Lett.*, 88:076103, 2002.

[35] V. S. J. Craig, C. Neto, and D. R. M. Williams. Shear-dependent boundary slip in an aqueous newtonian liquid. *Phys. Rev. Lett.*, 87:054504, 2001.

[36] R. Pit, H. Hervet, and L. Léger. Direct experimental evidence of slip at hexadecane/solid interfaces. *Physical Review Letters*, 85:980, 2000.

[37] P.G. de Gennes. On fluid/wall slippage. *Langmuir*, 18:3413–3414, 2002.

[38] S. Lichter, A.Roxin, and S. Mandre. Mechanisms for liquid slip at solid surfaces. *Physical Review Letters*, 93:086001-1–086001-4, 2004.

[39] M. Vincent, E. Devilers, and J. F. Agassant. Fiber orientation in injection moulding of reinforced thermoplastics. *J. Non-Newtonian Fluid Mech.*, 73:317–326, 1997.

[40] P. A. Thompson and S.M. Troian. A general boundary condition for liquid flowat solid surfaces. *Nature (London)*, 389:360–362, 1997.

[41] S. Granick, Y. Zhu, and H. Lee. Slippery questions about complex fluids flowing past solids. *Nature Mater*, 2:221, 2003.

[42] J. R. A. Pearson and C. J. S. Petrie. *Polymer Systems: Deformation and Flow*. Macmillian, London, 1968.

[43] S. Richardson. On the no-slip boundary condition. *J. Fluid Mech.*, 59:707–719, 1973.

[44] L. M. Denn. Issues in viscoelastic fluid mechanics. *Annu. Rev. Fluid Mech.*, 22:13–34, 1990.

[45] N. V. Priezjev, A. A. Darhuber, and S. M. Troian. Slip behavior in liquid films on surfaces of patterned wettability: Comparison between continuum and molecular dynamics simulations. *PHYSICAL REVIEW E*, 71:0416081–041608–11, 2005.

[46] P. Ball. How to keep dry of water. *Nature (London)*, 423:25, 2003.

[47] A. Karlsson. Molecular engineering: Networks of nanotubes and containers. *Nature (London)*, 409:150, 2001.

[48] E. Schnell. Slippage of water over nonwettable surfaces. *J. Appl. Phys.*, 27:1149, 1956.

[49] O. I. Vinogradova. Slippage of water over hydrophobic surfaces. *Int. J. Min. Process*, 56:31, 1999.

[50] K. Watanabe, Y. Udagawa, and H. Udagawa. Drag reduction of newtonian fluid in a circular pipe with a highly water-repellent wall. *J. Fluid Mech.*, 381:225–238, 1999.

[51] C. Cottin-Bizonne, J. L. Barrat, L. Bocquet, and E. Charlaix. Low-friction flows of liquid at nanopatterned interfaces. *Nat. Mater.*, 2:237–240, 2003.

[52] S. Richardson. On the no-slip boundary condition. *J. Fluid Mech.*, 59:707–719, 1973.

[53] L. M. Hocking. A moving fluid interface on a rough surface. *J. Fluid Mech.*, 76:801–817, 1976.

[54] K. M. Jansons. Determination of the macroscopic (partial) slip boundary condition for a viscous flow over a randomly rough surface with a perfect slip microscopic boundary condition. *Phys. Fluids*, 31:15, 1988.

[55] D. Einzel, P. Panzer, and M. Liu. Boundary condition for fluid flow: Curved or rough surfaces. *Phys. Rev. Lett.*, 64:2269, 1990.

[56] M. J. Miksis and S. H. Davis. Slip over rough and coated surfaces. *J. Fluid Mech*, 273:125, 1994.

[57] L. Bocquet and J. L. Barrat. Hydrodynamic boundary conditions, correlation functions and kubo. relations for confined fluids. *Phys. Rev. E*, 49:3079, 1994.

[58] H. A. Barnes. A review of the slip (wall depletion) of polymer solutions,emulsions and particle suspensions in viscometers. *J. Non-Newtonian Fluid Mech.*, 56:221–251, 1995.

[59] D. Andrienko, B. Dnweg, and O. I. Vinogradova. slip as a result of a prewetting transition. *J. Chem. Phys.*, 119:13106–13112, 2003.

[60] M. M. Denn. Extrusion instabilities and. wall slip. *Annu. Rev. Fluid Mech.*, 33:265–287, 2001.

[61] K. B. Migler, H. Hervet, and L. Leger. Slip transition of a polymer melt under shear-stress. *Phys. Rev. Lett.*, 70:287–290, 1993.

[62] V. Mhetar and L. A. Archer. Slip in entangled polymer melts. 1. general. features. *Macromolecules*, 31:8607–8616, 1998.

[63] C. H. Choi, K. J. A. Westin, and K. S. Breuer. Apparent slip flow in hydrophilic and hydrophobic. microchannels. *Phys. Fluids*, 15:2897, 2003.

[64] P. A. Thompson and S. M. Troian. A general boundary condition for liquid flow at solid surfaces. *Nature (Londond)*, 389:360–362, 1997.

[65] N. V. Priezjev and S. M. Troian. Molecular origin and dynamic behaviour of slip in sheared. polymer films. *Phys. Rev. Lett.*, 92:018302, 2004.

[66] R. G. Horn, O. I. Vinogradova, M. E. Mackay, and N. Phan-Thien. Hydrodynamic slippage inferred from thin film drainage measurements in a solution of nonadsorbing polymer. *J. Chem. Phys.*, 112:6424–6433, 2000.

[67] Y. Zhu and S. Granick. Rate-dependent slip of newtonian fluids at smooth surfaces. *Phys. Rev. Lett.*, 87:096105, 2001.

[68] O. I. Vinogradova, N. F. Bunkin, N. V. Churaev, O. A. Kiseleva, A. V. Lobeyev, and B. W. Ninham. Submicrocavity structure of water between hydrophobic and hydrophilic walls as revealed by optical cavitation. *J. Colloid Interface Sci.*, 173:443–447, 1995.

[69] H. Brenner. The stokes resistance of an arbitrary particle ii an extension. *Chem. Engng. Sci.*, 19:599–629, 1964a.

[70] H. Brenner. The stokes resistance of an arbitrary particle iii shear fields. *Chem. Engng. Sci.*, 19:631–651, 1964b.

[71] H. Brenner. Coupling between the translational and rotational brownian motions of rigid particles of arbitrary shape: Ii general theory. *J. Colloid Interface Sci.*, 28:407–436, 1967.

[72] I. L. Claeys and J.F. Brady. Suspensions of prolage spheroids in stokes flow. part 1. dynamics of a finite number of particles in an unbounded fluid. *J. Fluid Mech.*, 251:411–442, 1993.

[73] S. G. Advani and C. L. Tucker III. The use of tensors to describe and predict fiber orientatioin in short fiber composites. *Journal of Rheology*, 31:751–784, 1987.

[74] T.M. Macrobert. *Spherical Harmonics*. Dover, New York, 1947.

[75] A.B Basset. *A Treatise on Hydrodynamics*. Dover, New York, 1961.

[76] G. G. II Lipscomb and M. M. Denn. The flow of the fiber suspensions in complex geometries. *Journal of Non-Newtonian Fluid Mechanics*, 26:297–325, 1988.

[77] R. B. Bird, R. C. Armstrong, and O. Hassager. *Dynamics of polymeric liquids, Volume 2, Fluid Mechanics*. John Wiley and Sons, 1987.

[78] P. K. Kundu. *Fluid mechanics*. Academic Press, Inc, 1990.

[79] T. E. Garstang. The flow of viscous liquid past spinning bodies. *Proceeedings of the Royal Society of London, Series A, Containing Papers of a Mathematical and Physical Character*, 142:491–508, 1933.

[80] S. Goldstein. On the two-dimmensional steady flwo of a viscous fluid behind a solid body ii. *Proceeedings of the Royal Society of London, A*, 142:563–537, 1933.

[81] L. Bairstow, B. M. Cave, and E. D. Lang. The resistance of a cylinder moving in a viscous fluid. *Philosophical Transactions of the Royal Society of London. Series A*, 223:383–432, 1923.

[82] P. V. Southwell and H. B. Squire. A modification of oseen's approximate equation for the motion in two dimensions of a viscous incompressible fluid. *Philosophical Transactions of the Royal Society of London. Series A*, 232:27–64, 1933.

[83] P. A. Davies, D. L. Boyer, H. J. S. Fernando, and X. Zhang. On the periodic motion of a circular cylinder through a linearly stratified fluid. *Philosophical Transactions: Physical Sciences and Engineering*, 346:353–386, 1994.

[84] A. Berry and L. M. Swain. On the steady motion of a cylinder through infinite viscous fluid. *Proceeedings of the Royal Society of London, A*, 102:766–, 1923.

[85] D. Meksyn. Solution of oseen's equations for an inclined elliptic cylinder in a viscous fluid. *Proceeedings of the Royal Society of London, A*, 162:232–251, 1937.

[86] G. J. Richards. On the motion of elliptic cylinder through a viscous fluid. *Phyilosiphical Transaction of the Royal Society of London, A*, 233:279–301, 1934.

[87] N. Piercy and H. F. Winny. The skin friction of flat plates to oseen's approximation. *Proceeedings of the Royal Society of London, A*, 140:543–561, 1933.

[88] K. K. Kabanemi, J. F. Hetu, and A. G. Rejon. A 3-d coupled solution for the flow and fiber orientation in injection molding fo fiber-filled systems. *Rheology and Fluid Mechanics of Nonlinear Materials*, 217:207–227, 1996.

[89] R. S. Bay and C. L. Tucker III. Fiber orientation in simple injection moldings, part 1: Theory and numerical methods. *Polymer Composites*, 13:317–321, 1992.

[90] R. S. Bay and C. L. Tucker III. Fiber orientation in simple injection moldings, part 2: Experimental results. *Polymer Composites*, 13:322–342, 1992.

[91] H. H. de Frahan, V. Verleye, F. Dupret, and M. J. Crochet. Numerical prediction of fiber orientation in injection molding. *Polym. Eng. Sci.*, 32:254–266, 1992.

[92] M. Gupta and K. K. Wang. Fiber orientation and mechanical properties of shor-fiber-reinforced injection-molded composites: simulated and experimentatl results. *Polymer Composites*, 147:367–382, 1993.

[93] E. J. Hinch and L. G. Leal. Time-dependent shear flows of a suspension of particles with weak brownian rotations. *Journal of Fluid Mechanics*, 57:753–797, 1973.

[94] J. Ko and J. R. Youn. Prediction of fiber orientation in the thickness plane during flow molding of short fiber composites. *Ploym. Compos.*, 16:114–124, 1995.

[95] F. Folgar and C. L. Tucker III. Orientation behavior of fibers in concentrated suspensions. *J. Reinf. Plast. Compos.*, 3:1095–1122, 1995.

[96] A. C. Papanastasiou and A. N. Alexandrou. Isothermal extrusion of non-dilute fiber suspensions. *J. Non-Newtonian Fluid Mech.*, 25:313–328, 1987.

[97] G. Ausias, J. F. Agassant, and M. Vincent. Flow and fiber orientation calculations in reinforced therplastic extruded tubes. *Int. Polymer Processing*, 9:51–59, 1994.

[98] E. J. Hinch and L. G. Leal. Constitutive equations in suspension mechanics, part 2. approximate forms for a suspension of rigid particles affected by borwnian rotations. *Journal of Fluid Mechanics*, 76:187–208, 1976.

[99] G. L. Hand. A theory of anisotropic fluids. *Journal of Fluid Mechanics*, 13:33–46, 1962.

[100] S. G. Advani and G. L. Tucker. Closure apporximations for three-dimensional structure tensors. *Journal of Rheology*, 34:367–386, 1990.

[101] J. S. Cintra and C. L. Tucker. Orthotropic closure approximation for flow-induced fiber orientation. *Journal of Rheology*, 39:6–, 1995.

[102] S. M. Parks and C. A. Petty. *Prediction of Low-Order Orientation Statistics for Flow-Induced Alignment of Fibers and Platelets.* paper presentation, Fundamental Research in Fluid Mechanics: Particulate and Multiphase Flow I, AIChE Annual Meeting, Dallas, TX, October 31- November 5, 1999a.

[103] S. M. Parks, C. A. Petty, and M. Shafer. *Flow-Induced Alignment of Fibers in the Absence of Fiber-Fiber Interactions*. paper presentation, Symposium on Suspensions, APS/DFD, New Orleans, LA, November 21-23, 1999.

[104] A. Acrivos and C. Taylor. The stokes flow past an arbitrary particle. *Chem. Engng. Sci.*, 19:445, 1964.

[105] H. J. Workman. Concerning the orientation distribution function of rigid particles in a suspension which is undergoing simple shear flow. *J. Colloid and Interface Science*, 29:664–669, 1969.

[106] J. M. Rallison. The effect of brownian rotations in a dilute suspension of rigid particles of arbitrary shape. *J. Fluid Mech.*, 84:237–263, 1978.

[107] R. G. Larson. *Consititutive equations for polymer melts and solutions*. Butterworth, 1988.

[108] W. C. Jackson, A. D. Advani, and C. L. Tucker III. Predicting the orientation of short fibers in thin compression moldings. *Journal of Composite Materials*, 20:539–557, 1986.

[109] M. C. Altan, S. G. Advani, S. I. Guceri, and R. B. Pipes. On the description of the orientation states for fiber suspensions in homogenous flows. *Journal of Rheology*, 33:1129–1155, 1989.

[110] J. Betten. Integrity basis for a second-order and a fourth-order tensor. *Internat. J. Math.*, 5:87–96, 1982.

[111] Y. Kim, C. T. Nguyen, S. M. Parks, D. Mandal, A. Bnard, and C. A. Petty. *Microstructure of Liquid Crystalline Polymers Induced by Simple Shear*. Symposium on Manipulation of Nanophases by External Fields,Annual AIChE Meeting, Indianapolis Convention Center, Indianapolis, 2002, November 3 - 8.

[112] Y-C Kim, H. Kini, D. Mandal, A. Bnard, and C. Petty. *Microstructure of Liquid Crystalline Polymers Induced by Simple Shear*. Symposium on Suspensions, 56th Annual Meeting, American Physical Society: Division of Fluid Dynamics,East Rutherford, NJ, 2003, November 23-25.

[113] D. Leighton and A. Acrivos. The shear-induced migration of particles in concentrated suspensions. *Journal of Fluid Mechanics*, 181:415–439, 1987.

[114] J. F. Brady and G. Bossis. The rheology of concentrated suspensions of spheres in simple shear flow by numerical simulation. *Journal of Fluid Mechanics*, 155:105–129, 1985.

[115] J. F. Brady and G. Bossis. Stokesian dynamics. *Annual Review of Fluid Mechanics*, 20:111–157, 1988.

[116] D. Chen and M. Doi. Simulation of aggregating colloids in shear flow. *Journal of Chemical Physics*, 91:2656–2663, 1995.

[117] N. Phan-Thien and S. Kim. *Microstructures in Elastic Media: Principles and Computational Methods*. Oxford, New York, 1994.

[118] M. S. Ingber, A. A. Mammoli, and L. A. Mondy. A parallel obundary elitent formulation for determining effective properties of heterogeneous media. *J. Numer. Meth. Eng.*, 37:3905–3919, 1994.

[119] G. Segre and A. Silberberg. Radial poiseuille flow of suspension. *Nature*, 189:209, 1961.

[120] G. Segre and A. Silberberg. Behavior of macroscopic rigid spheres in poiseuille flow. part 1. *Journal of Fluid Mechanics*, 14:385–413, 1962.

[121] J. H. Aubert and M. Tirrell. Macromolecules in nonhomogeneous velocity gradient fields. *J. Chem. Phys.*, 72:2694–2701, 1980a.

[122] J. H. Aubert, S. Prager, and M. Tirrell. Macromolecules in non-homogenous. velocity gradient field. part ii. *J. Chem. Phys.*, 73:4103–4112, 1980.

[123] R. C. Armstrong G. Sekhon and M. S. Jhon. The origin of polymer migration in a nonhomogeneous flow field. *Journal of Polymer Science: Polymer Physics Edition*, 20:947–952, 1982.

[124] C. Crowe, M. Sommerfeld, and Y. Tsuji. *Multiphase flows with droplets and particles*. CRC Press, Boca Raton, FL, 1998.

[125] S. S. Sadhal, P. S. Ayyaswamy, and J. N. Chung. *Transport phenomena with drops and bubbles*. Springer, New York, 1997.

[126] J. F. Davidson, R. Clift, and D. Harrison. *Fluidization*. Academic Press, Orlando, 1985.

[127] L. S. Fan and C. Zhu. *Principles of gas-solid flows*. Cambridge University Press, Cambridge, 1998.

[128] R. D. Marcus, L. S. Leung, G. E. Klinzing, and F. Rizk. *Pneumatic conveying of solids*. Chapman and Hall, London, 1990.

[129] M. Ungarish. *Hydrodynamics of suspensions*. Springer, New York, 1993.

[130] M. Massoudi. Constitutive relations for the interaction force in multicomponent particulate flows. *International Journal of Non-Linear Mechanics*, 38:313–336, 2003.

[131] T. B. Anderson and R. Jackson. Fluid mechanicsl description of fluidized beds. *Ind. Engng. Chem. Fundam.*, 6:527, 1967.

[132] R. Jackson. Locally averaged equations of motion for a mixture of identical spherical particles and a newtonian fluid. *Chemical Engineering Science*, 52:2457–2469, 1997.

[133] D. Drew. Mathematical modeling fo two-phase flow. *Annual Review of Fluid Mechanics*, 15:261–291, 1983.

[134] D. D. Joseph and T. S. Lundgren. Ensemble averaged and mixture theory equations for incompressible fluid-particle suspensions. *International Journal of Multiphase flow*, 1:35–42, 1990.

[135] D. A. Drew and S. L. Passman. *Theory of multicomponent fluids*. Apringer-Verlag, New York, 1998.

[136] M. Ishii. *Thermo-fluid dynamic theroy fo two-phase flow*. Eyrolles, Paris, France, 1975.

[137] D. Lakehal and C. Narayanan. Numerical analysis of the continum formulation for the initial evoluiton of mixing layers with particles. *International Journal of Multiphase Flow*, 29:927–941, 2003.

[138] D. Z. Zhang and A. Prosperetti. Average euqations for inviscid disperse two-phase flow. *Journal of Fluid Mechanics*, 267:185–219, 1994.

[139] T. Lendgren. Slow flow through stationalry random beds and suspensions fo sheres. *Journal of Fluid Mechanics*, 51:273–299, 1972.

[140] D. A. Drew. A turbulent dispersion model for particles or bubbles. *Journal of Engineering Mathematics*, 41:259–274, 2001.

[141] G. J. Hwang and H. H. Shen. Modeling the solid phase stress in a fluid-solid mixture. *Int. J. Multiphase Flow*, 15:257–268, 1989.

[142] G. J. Hwang and H. H. Shen. Modeling the phase interaction in the momentum equations fo a fluid-solid mixture. *Int. J. Multiphase Flow*, 1:45–57, 1991.

[143] G. K. Batchelor and J. T. Green. The determination of the bulk stress in a suspension of spherical particle to order c^2. *Journal of Fluid Mechanics*, 56:401–472, 1972.

[144] P. G. Saffman. The lift on a small sphere in a slow shear flow. *Journal of Fluid Mechanics*, 22:385–400, 1965.

[145] D. K. Mandal. *Similation of flow-induced fiber orientation with a new closure model using the finite element method.* PH.D dissertation, Michigan State University, 2004.

[146] J. N. Reddy and D. K. Gartling. *The finite element method in heat transfer and fluid dynamics.* CRC press, 2001.

[147] F. Brezzi and K. J. Bathe. A discourse on the stability conditions for mixed finite element formulations. *Computer Methods in Applied mechanics and Engineering*, 82, 1990.

MICHIGAN STATE UNIVERSITY LIBRARIES
3 1293 02845 9166